THE ASTROPHYSICAL JOURNAL, 245:416–453, 1981 April 15

THE HALO GLOBULAR CLUSTERS OF THE GIANT ELLIPTICAL GALAXY MESSIER 87

S. E. STROM
Kitt Peak National Observatory[1]
J. C. FORTE[2]
Observatorio Astronomico, Universidad Nacional de la Plata, Argentina
W. E. HARRIS[3]
Department of Physics, McMaster University
K. M. STROM AND D. C. WELLS
Kitt Peak National Observatory[1]
AND
MALCOLM G. SMITH[4]
Anglo-Australian Observatory, Australia
Received 1980 July 25; accepted 1980 September 25

ABSTRACT

New photographic *UBR* photometry of approximately 1700 stellar images surrounding the Virgo giant elliptical M87 is presented. The survey covers the radial region 1.'5–9.'0 to B(limiting)$\approx$23.5. Comparisons with two adjacent background fields indicate that 70% of our sample consists of globular clusters belonging to M87, enabling several statistical studies of the M87 halo to be made.

Our summarized conclusions are: (a) over the measured radial range, the M87 clusters become systematically bluer (more metal-poor) with increasing galactocentric distance; (b) the color gradient in the cluster system has the same slope as that for the M87 integrated halo *light*, but the clusters are bluer by $\Delta(U-R)\approx 0.5$ at all radii; (c) the cluster luminosities are not correlated with color; and (d) the cluster luminosity function that we derive is similar to that observed previously by Hanes and appears similar in all radial regions. The various characteristics of the radial color gradient, the cluster/halo color difference, and the luminosity function are all virtually identical with the same features of our own Milky Way halo clusters once the galactocentric distances are normalized by using the scale-free radial measure r/r_e where r_e is the de Vaucouleurs radius.

We argue from these results that galaxies were not likely to have been formed by accumulation of globular-cluster-sized masses or by mergers of separate smaller galaxies. Instead, the halos and globular cluster systems in widely different major galaxies (M87, the Milky Way) have remarkable similarities in their early stages. The intriguing differences between the cluster system itself and the underlying halo suggest that the enrichment and dynamical histories of these two subsystems are more distinct than previously believed: Globular clusters may be the first luminous tracers to appear during galaxy formation.

Subject headings: clusters: globular — galaxies: evolution — galaxies: individual — galaxies: photometry — galaxies: stellar content

I. INTRODUCTION

The utility of globular clusters in investigating the structure, dynamics, and evolution of the Milky Way halo has motivated a number of astronomers to attempt comparable studies of globular cluster systems surrounding external galaxies. (A recent review of progress in this field has been given by Harris and Racine 1979, hereafter HR.) These attempts have been made more feasible by the recent dramatic improvements in detectors and data analysis systems.

In this contribution, we report the results of a survey of the globular cluster system surrounding M87, the giant elliptical galaxy in the Virgo cluster. Harris and Smith (1976) and HR have estimated that the M87

[1]Operated by the Association of Universities for Research in Astronomy, Inc., under contract with the National Science Foundation.

[2]Member of the Carrera del Investigador Cientifico del Consejo Nacional de Investigaciones Cientificas y Técnicas, Republica Argentina.

[3]Visiting Astronomer, Cerro Tololo Inter-American Observatory.

[4]Presently at The Royal Observatory, Edinburgh, Scotland.

system contains as many as 10^4 clusters with $V<24.5$ mag. This uniquely large population provides, in principle, the best-known basis for a number of statistical studies. For example, because the brighter end of the luminosity function for clusters is more completely populated in M87 than in any other known galaxy, M87 is especially well suited to the study of systematic variations of cluster properties with luminosity. (In even the largest Local Group galaxies, the total number of clusters is nearly 2 orders of magnitude smaller.)

Most important for our present discussion, it should be possible to examine the distributions of cluster brightnesses and colors, as well as any variations of these distributions with galactocentric distance r. If integrated colors reflect overall metal-to-hydrogen ratios, it would be instructive to compare the radial dependence of the cluster colors with the integrated colors of the underlying galactic halo. This would then permit us to discuss whether or not the chemical enrichment histories of the cluster and halo population are identical and, conceivably, to decide whether there might be more than one distinct population in the halo.

We would also hope to learn from the observed color distributions whether or not M87 was most likely formed from the merger of many smaller systems. If the merger hypothesis is correct, then the M87 globular cluster system should contain a considerable range of high- and low-metallicity clusters at all radii; this is because any initial metallicity gradients in the constituent systems would be smeared out in the merger process. If, however, the spread in metallicity at a given radius in the present M87 halo were small and the metallicity gradient large, then a multiple-merger origin for M87 would be difficult to defend.

II. OBSERVATIONAL APPROACH

To sample a large fraction of the cluster system in a reasonable time, we decided that a multicolor, photographic survey of the M87 region was the only practical method available. Sky-limited (sky densities between 0.6 and 1.0) plates in U, B, and R were therefore obtained with the Mayall and CTIO 4 m telescopes as listed in Table 1.

Our choice of a *UBR* color system was dictated by the following considerations:

TABLE 1

4 m PLATE MATERIAL USED IN THIS SURVEY

Sequence No.	Emulsion	Filter	Exp. Time (min)
MPF 1905.....	IIIa-J	UG-2	134
MPF 2049.....	IIIa-J	UG-2	135
MPF 2046.....	IIIa-J	GG-385	50
CPF 635	IIIa-J	GG-385	50
MPF 1901.....	098-04	RG-610	55

TABLE 2

HALE SCHMIDT MATERIAL USED IN THIS INVESTIGATION

Plate Sequence No.	Emulsion	Filter	Exp. Time (min)
PS 22648	1032-0	UG-1	80
PS 22646	098-04	RG-1	55

1. The B plates provide the highest signal-to-noise ratio for the detection of globular clusters and enable us to study the luminosity function to $B \sim 23.5$ mag in M87.

2. The color index $(U-R)$ has been shown to provide a sensitive measure of the metal-to-hydrogen ratio both for external galaxies and for globular clusters (see, for example, Strom and Strom 1978; Strom *et al.* 1978). For globular clusters in our Galaxy, the range in observed $(U-R)$ exceeds 1.0 mag. By comparison, $(B-V)$ varies over a range only one-third as great.

Finally, to measure the halo colors of M87 we required areal coverage which exceeds the 50′ field of the Mayall and CTIO 4 m telescopes, since the halo of M87 exceeds 1° in diameter. Consequently, we obtained a U and R plate pair, using the 1.2 m Schmidt telescope at the Hale Observatories. The relevant data for this plate material are summarized in Table 2.

III. DATA ANALYSIS

a) Identification of Sources and Reduction to Instrumental Magnitude

Identifying an appropriate sample of globular clusters and accurately measuring their brightness and colors represents a formidable challenge because (1) the clusters are faint ($B>20$); (2) they are observed against the strong background halo light of the galaxy; and (3) the crowding of cluster images is severe, at least in the inner regions of the galaxy. These difficulties are well illustrated in Figure 1 (Plate 4), in which we reproduce a B plate of the M87 region. A new series of reduction procedures was, therefore, developed specifically to carry out accurate photometry of stellar images in crowded, background-dominated fields. The steps we followed to obtain our final list of cluster brightnesses and colors are outlined below; more detailed expositions of the routines used in the photographic reduction are available from the authors upon request.

1. The plates were traced with the Kitt Peak National Observatory (KPNO) PDS microdensitometer. The adopted slit size was 20×20 μm, and each chosen area was sampled at 15 μm intervals. For a 4 m prime-focus plate scale of 18″.5 mm^{-1}, 15 μm corresponds to 0″.27. This sampling size was comfortably smaller than the seeing disks on our plates, typically 1″.5–2″.0.

2. The resulting density-position rasters were converted to intensity-position matrices, using a function of the form

$$\mathrm{Log}\, I = a_0 + a_1 D + a_2 \log(1 - 10^{-D}) + 10^{a_3(D-a_4)},$$

which relates density D to intensity I. The routines incorporated in the DTOI package (Strom *et al.* 1977) at the KPNO Interactive Picture Processing System (IPPS) were used to achieve the conversion.

3. The intensity-position rasters (originally 3000 pixels square) were filtered by convolving them with a 3×3 matrix of weights of the form

0.086	0.121	0.086
0.121	0.172	0.121
0.086	0.121	0.086.

This operation attenuated the granulation noise at the highest spatial frequencies without appreciably degrading resolution (the convolving kernel was only 0".81 wide). The operation of forming the weighted sum of pixel values also reduced the quantization of the signal due to the original analog-to-digital converter in the PDS microdensitometer. Next, a new 300-square image was formed by taking every 10th pixel from the 3000-square filtered image. This smaller image was filtered with a 15-square median window filter. In this operation, at each pixel of the 300-square image the 225 surrounding pixels were extracted, sorted, and the middle value in the sorted list (the median) was delivered as the output pixel value at that location. This nonlinear lowpass filter ignored all objects in the scene whose diameters were less than about 100 pixels (or 28") in the original 3000-square image. Its output was, therefore, effectively a smoothed image of the envelope of M87, containing none of the smaller star images. Residual noise in the median estimate was suppressed by convolving the 300-square image with a 7-square kernel whose weights were chosen by a digital filter design program. This last operation suppressed spatial frequencies less than 0.2 in normalized units (i.e., periods less than 50 pixels in the 3000-square image).

4. The 300-square filtered image was enlarged by a factor of 10, using bi-cubic interpolation (4 pixels in each direction), and subtracted from the 3000-square image which had been computed by the initial 3×3 convolution. Figure 2 (Plate 5) illustrates the appearance of the images before and after subtraction. For $r \gtrsim 1'.5$, this technique effectively eliminated the contribution of the background galaxy.

5. We then used an automatic "peak-finding" routine to locate candidate stellar images. An image was considered a valid candidate if it contained more than five contiguous pixels with intensities above 2.5 times the standard deviation of the local background noise fluctuations. We then matched the candidate lists from plates MPF 2049 (U) and MPF 2046 (B) to obtain a master list suitable for deriving $U-B$ colors. Similarly, a merged list was derived from plates MPF 2046 and MPF 1901 from which $B-R$ colors were obtained. Finally, we compared the candidate lists from the B plates MPF 2046 and CPF 635. This merged list, based on the two plates yielding the highest signal-to-noise ratio, provided the basis for a discussion of the cluster luminosity function. Obvious extended (nonstellar) images ($d \gtrsim 3''$) were identified by visual inspection and removed from all lists.

6. The brightness for each image on the master list was sampled by placing a 2".22 radius (8 pixels) (numerical) circular aperture around its center and computing the total intensity within the aperture. An outer annulus of inner radius 4".45 and outer radius 5".84 (16 and 21 pixels) was used to sample the sky around each image.

For isolated objects, the distribution of pixel intensities within the local sky annulus should be approximately Gaussian. However, when other images contaminate the sky annulus, the distribution of sky intensities is biased or "skewed" toward higher intensities. Consequently, we adopted the *mode* of the sky intensities (Wells 1979) rather than the mean in order to improve the estimate of the true sky value in crowded regions. The effectiveness of this approach is illustrated in Figure 3, where a histogram of intensity values for a typical sky annulus is illustrated. A Gaussian distribution centered on the mode is presented as a visual aid to understanding the utility of the procedure. The "skew" of the distribution toward higher intensities, computed

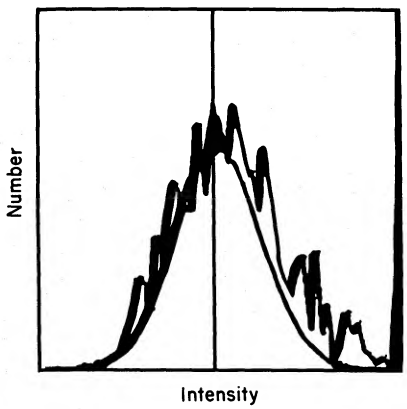

FIG. 3.—In this figure we plot the frequency distribution of intensities measured within a sky annulus. Superposed on the plot is a Gaussian centered on the mean of the distribution. Note the "skew" of the intensity distribution toward higher intensities caused by the presence, within the sky annulus, of a number of nearby sources. The mode of the intensity distribution represents a better estimate of the true sky (see text).

as

$$\text{skew} = \frac{[\text{mean} - \text{mode}]}{\sigma_{\text{sky}}},$$

was stored for each image so that we could later examine errors in the derived magnitudes as a function of skew level.

7. A table (Table 3) of position and brightness was assembled from photometry of all sources on the master lists. In Table 3 it will be noted that the number of sources actually measured for U and R are smaller than the number of sources resulting from comparison of the two B plates, since the U and R material had lower signal-to-noise. The column headings in this table are self-explanatory, except to say that the x and y coordinates were measured from the southeast corner of the scanned square area (13.′95 on a side), and that the coordinates of the galaxy center are $x=423.''5$, $y=426.''1$.

b) *Calibration*

Our original instrumental magnitudes (u, b, r) were measured as described above. To transform these into true U, B, and R values, we compared our measured brightnesses for 38 objects identified on the five plates in common with Hanes' (1971) list. Because Hanes did not measure R magnitudes, we were forced to use his measured U, B, and V colors to predict R. This prediction was made by using the observed color-color relations published by Johnson (1966). R values were computed only over that range in $B-V$ color where differences in luminosity class have negligible effects on the color-color relations.

In Table 4 we list the Hanes standards, his observed magnitudes, the R magnitudes estimated from the observed colors, and our instrumental magnitudes. The coordinate system is identical to that of Table 3. From a comparison of the instrumental and observed magnitudes in Table 4, we adopted the following transformations:

$$U' = u + 3.76,$$

$$B' = 1.11b + 2.67,$$

$$R' = r + 2.70.$$

The zero points for the U' and B' magnitudes correspond to plates MPF 1905 and MPF 2046. Instrumental magnitudes measured on plates MPF 2049 and CPF 635 were reduced to the system of the former plates. The quantities listed in the table are averages from these two plate pairs. An assessment of the quality of the transformation can be made from examination of Figure 4 in which the instrumental and "true" system measurements are compared. The estimated errors in the transformation are listed in Table 5. Although the data presented in Table 4 and Figure 4 suggest that our instrumental measurements could be transformed into *UBR* with high internal precision, the systematic accuracy of our zero points plainly depends heavily on Hanes' system (which was calibrated through secondary-image extensions of a photoelectric sequence in the field). A more direct check on our zero points would be highly desirable.

To take account of the color term in B resulting from use of the IIIa-J+GG-385 filter (J magnitude), we corrected our colors according to the following prescriptions:

$$(U-B) = (U'-B') - 0.22\,[(U'-B') - 0.08],$$

$$(B-R) = (B'-R') + 0.19\,[(B'-R') - 1.31],$$

if $B_I \propto J_I + 0.3\ (B-V)$ (Schweizer 1976; Harris and Smith 1981).

Note that where we did not have any measured colors, a standard globular cluster color of $(B-V)=0.65$ [$(U-B)=+0.08$, $(B-R)=1.31$] was adopted in deriving the B' transformation listed above.

An independent check on our color zero points was obtained from surface photometry of the M87 halo. De Vaucouleurs (1969) has published measurements of $U-B$ and $B-V$ colors from analysis of photoelectric scans of the halo. In addition, FAST-SCAN photometry (Strom *et al.* 1977) in the U and R bands taken through a 16″ aperture could be used to provide the run of $(U-R)$ against galactocentric distance for $r<120''$ along the east-to-west axis of the galaxy. These measurements were compared with suitable numerical aperture photometry carried out on the U, B, and R plate material listed in Table 1. From these data, we derive the following transformations:

$$(U-R) = (U-R)_I + 1.06,$$

$$(U-B) = (U-B)_I - 0.83,$$

$$(B-R) = (B-R)_I + 1.87.$$

Note that the subscript I signifies our "instrumental" system. By comparison, for a globular cluster of typical brightness $B=22.0$, we derive from the calibration based on Hanes' photometry $c_{U-R}=+1.07$, $c_{U-B}=-0.83$, and $c_{B-R}=+1.95$. To within 0.08 mag, the values agree with those obtained from the U and R FAST-SCAN photometry. It should also be noted that the color transformation obtained from surface photometry of the halo permits accurate differential comparison of the halo and globular cluster colors.

As a final check on the color zero points, we compared (Fig. 5) the locus of our observed colors in the $(U-B)$,$(U-R)$ and $(U-B)$,$(B-R)$ planes with the

TABLE 3

BASIC DATA FOR THE GLOBULAR CLUSTERS IN OUR SAMPLE

I.D. No.	x (arcsec)	y (arcsec)	r (arcsec)	B (mag)	(U–B) (mag)	(U–R) (mag)	(B–R) (mag)	I.D. No.	x (arcsec)	y (arcsec)	r (arcsec)	B (mag)	(U–B) (mag)	(U–R) (mag)	(B–R) (mag)
1.....	379.6	3.0	425.2	23.10	...	...	...	41.....	131.5	38.7	486.1	21.45	0.25	1.58	1.28
2.....	391.1	3.1	423.9	23.16	...	...	...	42.....	342.0	40.8	393.8	21.69	-0.62	...	...
3.....	570.7	4.0	446.0	21.58	0.53	3.25	2.83	43.....	784.9	40.9	526.4	21.54	0.47	2.03	1.48
4.....	275.7	4.2	447.3	21.68	-0.08	...	...	44.....	682.8	42.3	461.6	21.44	0.27	1.73	1.42
5.....	753.5	6.9	531.8	22.46	-1.02	...	...	45.....	536.9	42.4	399.1	22.61	...	...	...
6.....	659.0	8.6	477.9	22.76	-1.00	...	...	46.....	583.6	44.6	412.5	22.60	-1.11	...	...
7.....	576.0	9.3	442.7	23.63	...	...	...	47.....	287.1	45.0	405.1	22.86	-0.16	...	...
8.....	471.8	10.6	417.6	22.75	...	...	...	48.....	200.5	45.8	441.5	18.11	0.37	1.70	1.23
9.....	430.2	10.7	415.0	21.18	0.63	2.25	1.50	49.....	509.9	45.8	389.0	22.68	-0.41	1.26	1.90
10.....	770.0	10.9	539.1	23.36	...	...	...	50.....	813.5	46.9	542.1	23.18	...	...	...
11.....	403.4	11.7	414.6	23.49	...	...	...	51.....	467.4	47.3	380.7	23.06	...	...	...
12.....	745.8	12.6	522.6	22.77	-0.44	...	...	52.....	237.1	48.4	421.7	23.57	...	...	...
13.....	308.1	13.0	429.0	23.76	...	...	...	53.....	411.9	48.6	377.3	23.53	...	...	...
14.....	346.6	13.1	420.0	22.58	0.00	...	...	54.....	340.6	49.8	385.4	22.54	0.23	...	...
15.....	523.4	14.0	423.1	21.90	...	...	...	55.....	426.7	50.0	375.7	23.06	...	...	...
16.....	89.7	15.2	530.4	22.24	0.12	...	...	56.....	252.8	50.5	413.1	22.71	-0.87	...	...
17.....	185.8	15.6	475.1	23.72	...	...	...	57.....	121.6	50.6	482.8	23.39	...	...	...
18.....	555.7	15.8	430.0	23.13	...	...	...	58.....	577.1	52.4	402.8	21.93	0.01	1.62	1.69
19.....	787.6	16.2	546.5	23.07	...	...	...	59.....	439.8	53.3	372.6	19.63	0.54	2.12	1.47
20.....	270.4	16.7	437.4	23.40	...	...	...	60.....	504.4	53.5	380.4	22.88	...	...	...
21.....	368.6	16.9	412.8	22.94	...	...	...	61.....	603.9	53.7	412.5	22.90	...	...	...
22.....	589.9	17.3	440.2	23.68	...	...	...	62.....	558.3	54.2	394.4	22.68	...	...	...
23.....	795.9	17.3	551.2	23.42	...	...	...	63.....	39.2	54.7	535.7	23.77	...	...	...
24.....	222.2	18.0	455.6	22.91	...	...	...	64.....	109.2	55.0	487.3	22.82	...	...	...
25.....	672.8	19.7	475.2	18.40	1.33	3.98	2.49	65.....	32.0	56.5	539.7	21.84	0.15	...	...
26.....	287.2	21.4	427.3	22.41	...	...	...	66.....	62.9	57.7	516.7	21.39	0.17	0.85	0.53
27.....	307.3	22.0	420.6	22.51	...	...	...	67.....	280.6	60.6	392.8	23.20	...	...	...
28.....	140.7	22.7	493.5	20.72	0.25	1.56	1.25	68.....	390.1	60.7	366.6	22.00	-0.20	1.44	1.79
29.....	291.4	27.7	420.0	23.67	...	...	...	69.....	456.3	61.0	365.9	22.04	0.16	1.77	1.64
30.....	71.4	28.3	532.3	23.53	...	...	...	70.....	349.5	61.6	371.9	22.89	-0.37	...	...
31.....	462.8	28.9	398.5	23.41	...	...	...	71.....	216.9	62.1	419.3	23.25	...	...	...
32.....	179.5	28.9	466.9	22.78	...	...	...	72.....	665.0	62.2	435.2	23.05	...	...	...
33.....	88.3	29.0	520.7	23.13	...	...	...	73.....	226.5	62.7	414.0	23.15	...	...	...
34.....	391.0	29.6	397.6	23.22	...	...	...	74.....	783.4	62.9	509.5	23.59	...	...	...
35.....	439.5	29.9	396.0	23.24	...	...	...	75.....	330.0	63.8	374.2	23.19	...	...	...
36.....	166.4	30.8	472.4	23.34	...	...	...	76.....	382.2	64.5	363.7	22.38	...	...	...
37.....	701.8	33.2	479.8	19.33	0.22	1.35	1.04	77.....	311.9	65.4	377.8	20.83	0.19	1.30	1.04
38.....	416.9	33.4	392.3	21.81	...	...	...	78.....	533.3	65.8	375.6	23.31	...	...	...
39.....	71.8	37.7	525.1	23.68	...	...	...	79.....	761.3	67.1	491.1	20.42	-0.22	0.52	0.74
40.....	498.6	38.7	393.8	23.27	...	...	...	80.....	304.9	68.6	376.9	22.81	-0.44	...	...

TABLE 3—*Continued*

I.D. No.	x (arcsec)	y (arcsec)	r (arcsec)	B (mag)	(U-B) (mag)	(U-R) (mag)	(B-R) (mag)
81.....	217.3	69.4	412.7	21.95	-0.18	1.47	1.81
82.....	259.8	70.1	392.3	23.57	...	...	...
83.....	773.7	71.0	496.9	22.89	...	...	...
84.....	786.4	71.9	505.2	23.27	...	...	...
85.....	544.2	72.2	372.8	19.54	-0.12	0.79	0.90
86.....	342.0	73.1	362.4	22.86	...	...	...
87.....	22.9	73.1	535.3	20.98	1.23	3.87	2.51
88.....	403.8	73.4	352.9	21.95	...	...	...
89.....	621.4	74.1	402.4	23.41	...	...	...
90.....	467.0	74.3	353.7	21.70	0.14	1.38	1.21
91.....	425.6	74.3	351.3	21.91	-0.13	0.68	0.79
92.....	481.8	74.8	355.3	23.06	...	...	...
93.....	76.6	74.9	494.8	18.61	0.09	1.13	0.99
94.....	244.1	77.6	392.5	21.79	0.30	1.66	1.30
95.....	320.7	77.8	363.3	22.55	0.13	1.95	1.90
96.....	663.0	80.8	418.7	22.52	-0.48	0.74	1.40
97.....	791.0	81.0	502.2	22.35	0.15	1.83	1.72
98.....	636.7	83.0	402.4	23.84	...	...	...
99.....	363.6	83.1	348.2	23.72	...	...	...
100.....	74.8	83.3	490.2	23.60	...	...	...
101.....	453.1	83.6	343.2	22.14	0.10	1.46	1.37
102.....	410.1	83.7	342.3	22.83	...	...	...
103.....	271.0	83.8	375.2	22.46	...	...	...
104.....	577.1	84.5	373.3	23.81	...	...	...
105.....	114.9	88.4	458.6	23.54	...	...	...
106.....	417.0	88.9	336.9	22.14	...	...	...
107.....	422.8	89.1	336.6	21.48	0.32	1.57	1.17
108.....	355.3	89.2	343.7	23.23	...	...	...
109.....	345.0	90.4	344.8	23.31	...	...	...
110.....	155.7	91.3	429.8	23.39	...	...	...
111.....	115.1	91.4	456.3	23.64	...	...	...
112.....	493.1	92.0	340.4	23.72	...	...	...
113.....	817.4	92.2	514.5	22.16	0.10	...	...
114.....	453.0	92.3	334.5	21.22	0.15	1.52	1.35
115.....	614.4	92.4	383.0	23.02	...	...	...
116.....	510.0	93.2	343.0	23.01	...	...	...
117.....	729.8	93.9	450.1	22.73	...	...	...
118.....	800.5	94.4	500.2	23.21	...	...	...
119.....	677.3	94.8	415.7	20.96	-0.07	0.46	0.43
120.....	770.8	95.5	477.6	23.60	...	...	...
121.....	808.4	96.0	505.1	21.25	0.23	1.41	1.10
122.....	594.1	96.0	370.2	22.24	-0.63	...	...
123.....	44.1	96.8	503.7	22.53	...	...	...
124.....	316.4	96.8	346.5	21.92	-0.12	1.29	1.49
125.....	327.8	96.8	343.1	23.18	...	...	...
126.....	750.0	96.9	461.9	23.15	...	...	...
127.....	606.6	99.2	373.3	22.91	...	...	...
128.....	341.1	101.0	335.4	22.52	0.33	...	...
129.....	488.9	101.5	330.2	22.88	...	...	...
130.....	760.9	102.8	465.4	23.07	...	...	...
131.....	632.4	103.4	382.9	23.72	...	...	...
132.....	531.3	103.5	339.0	23.57	...	...	...
133.....	601.7	104.1	366.6	23.36	...	...	...
134.....	536.0	104.7	339.4	22.90	-0.68	...	...
135.....	432.6	104.7	321.0	23.14	...	...	...
136.....	44.2	104.9	498.4	23.39	...	...	...
137.....	237.9	105.6	371.1	20.65	0.06	1.17	1.07
138.....	198.0	106.6	391.9	23.64	...	...	...
139.....	642.0	107.1	385.1	23.13	...	...	...
140.....	702.5	107.8	421.5	23.18	...	...	...
141.....	383.2	109.1	319.4	21.38	0.29	1.72	1.37
142.....	418.7	109.6	316.1	23.26	...	...	...
143.....	140.2	109.6	425.8	22.10	-0.18	1.85	2.25
144.....	406.9	109.9	316.3	22.82	-0.08	...	...
145.....	271.8	110.1	351.0	21.98	-0.31	...	...
146.....	327.4	110.8	329.8	22.86	...	...	...
147.....	120.2	111.1	438.5	21.04	-0.03	1.12	1.15
148.....	150.4	111.7	417.5	22.86	-0.49	...	...
149.....	657.2	112.7	389.3	23.28	...	...	...
150.....	265.1	113.0	351.5	22.13	-0.67	...	...
151.....	513.3	113.7	324.0	19.64	-0.15	0.62	0.74
152.....	607.9	114.8	360.4	23.24	...	...	...
153.....	249.8	115.3	356.7	21.49	-0.14	1.21	1.44
154.....	750.1	115.4	448.9	22.45	...	...	...
155.....	826.4	115.4	506.8	23.34	...	...	...
156.....	631.4	117.0	370.9	23.01	...	...	...
157.....	296.2	117.7	334.1	23.05	...	...	...
158.....	221.8	117.8	369.2	22.34	-0.53	...	...
159.....	397.7	118.4	308.5	22.86	...	...	...
160.....	455.1	119.1	307.9	21.27	0.49	2.58	2.10
161.....	173.1	119.3	397.0	23.16	...	...	...
162.....	441.0	120.7	305.4	23.51	...	...	...
163.....	650.7	121.2	378.6	21.67	-0.32	...	...
164.....	713.0	121.5	418.4	23.76	...	...	...
165.....	159.7	121.6	403.9	23.50	...	...	...
166.....	667.9	123.5	387.2	23.34	...	...	...
167.....	371.7	123.6	306.8	19.63	0.23	1.44	1.15
168.....	334.8	123.7	315.3	22.81	-0.23	...	...
169.....	92.6	125.1	448.6	23.43	...	...	...
170.....	62.9	126.2	470.3	19.49	-0.15	0.53	0.64

TABLE 3—*Continued*

I.D. No.	x (arcsec)	y (arcsec)	r (arcsec)	B (mag)	(U-B) (mag)	(U-R) (mag)	(B-R) (mag)	I.D. No.	x (arcsec)	y (arcsec)	r (arcsec)	B (mag)	(U-B) (mag)	(U-R) (mag)	(B-R) (mag)
171.....	490.8	126.3	306.4	21.31	0.71	3.05	2.33	216.....	449.8	151.1	275.6	23.20	...	...	...
172.....	831.0	126.5	503.8	23.53	...	...	...	217.....	564.6	152.2	306.8	23.07	...	...	...
173.....	784.0	127.2	466.4	23.40	...	...	...	218.....	764.6	153.0	435.0	20.81	1.18	3.79	2.49
174.....	72.0	127.5	462.5	23.33	...	...	...	219.....	296.7	153.0	301.5	22.35	...	...	...
175.....	152.0	127.8	404.5	23.47	...	...	...	220.....	372.7	153.7	277.0	22.86	...	...	...
176.....	21.3	128.1	502.0	21.63	0.26	1.44	1.10	221.....	221.2	154.6	339.5	22.01	0.70	3.16	2.47
177.....	48.8	129.9	479.1	21.55	0.35	1.31	0.81	222.....	113.4	155.0	413.2	22.99	...	...	...
178.....	472.7	130.8	298.5	22.27	-1.15	...	...	223.....	287.4	155.4	303.6	23.25	...	...	...
179.....	753.0	131.5	440.1	23.59	...	...	...	224.....	294.4	157.0	299.0	23.69	...	...	...
180.....	344.9	132.5	304.0	22.80	...	...	...	225.....	666.4	157.1	360.7	23.96	...	...	...
181.....	279.0	133.1	327.3	22.91	...	...	...	226.....	357.7	157.8	276.4	22.38	0.22	1.79	1.57
182.....	712.4	133.4	409.4	23.63	...	...	...	227.....	503.3	158.5	278.2	22.52	0.09	1.84	1.83
183.....	238.0	133.9	346.9	22.89	-0.97	...	...	228.....	171.0	159.1	368.6	23.30	...	...	...
184.....	246.1	134.0	342.5	22.89	-0.88	...	...	229.....	354.1	159.1	276.0	23.44	...	...	...
185.....	436.2	134.2	291.7	23.71	...	...	...	230.....	770.2	159.3	435.4	23.66	...	...	...
186.....	523.1	134.6	306.9	22.17	-0.05	1.50	1.64	231.....	717.0	159.4	394.7	22.27	...	...	...
187.....	610.1	135.2	344.1	23.25	...	...	...	232.....	764.8	159.7	431.0	22.44	...	...	...
188.....	603.2	135.6	340.1	22.14	-0.38	...	...	233.....	244.8	160.2	321.2	22.73	...	...	...
189.....	285.5	136.2	321.6	23.63	...	...	...	234.....	267.9	161.3	307.8	21.30	0.14	1.95	1.89
190.....	822.4	136.5	490.9	23.24	...	...	...	235.....	537.2	162.2	286.1	21.39	-0.07	0.93	1.00
191.....	369.9	136.6	294.4	21.92	0.08	1.49	1.43	236.....	738.9	162.3	409.2	19.35	-0.06	0.36	0.31
192.....	724.3	136.7	415.5	23.28	...	...	...	237.....	363.7	162.4	270.4	22.77	-0.08	1.55	1.75
193.....	383.3	137.0	291.7	22.67	...	...	...	238.....	304.5	162.6	289.7	22.81	...	...	...
194.....	431.1	137.2	288.5	23.07	...	...	...	239.....	251.0	163.5	315.0	23.68	...	...	...
195.....	635.8	137.8	356.4	23.67	...	...	...	240.....	506.1	163.9	273.8	23.24	...	...	...
196.....	40.5	139.1	480.1	22.20	-0.05	1.05	1.11	241.....	360.7	164.1	269.5	23.87	...	...	...
197.....	87.6	139.6	442.8	23.60	...	...	...	242.....	804.7	164.2	460.5	23.71	...	...	...
198.....	185.4	140.7	372.7	23.44	...	...	...	243.....	475.0	164.7	265.6	23.45	...	...	...
199.....	387.4	140.8	287.4	22.36	...	...	...	244.....	179.7	164.7	358.6	22.50	...	...	...
200.....	254.7	141.3	331.7	22.15	0.08	1.91	1.93	245.....	778.9	165.3	438.9	22.51	...	...	...
201.....	22.8	141.9	492.8	22.77	...	...	...	246.....	554.1	165.7	290.0	22.35	...	...	...
202.....	48.4	142.1	472.0	22.77	...	...	...	247.....	747.8	165.9	413.8	23.30	...	...	...
203.....	233.1	142.2	342.6	23.83	...	...	...	248.....	464.0	166.7	261.7	21.12	0.42	...	...
204.....	51.8	142.7	468.9	23.06	...	...	...	249.....	346.9	167.0	270.3	23.32	...	...	...
205.....	726.0	143.5	412.1	23.56	...	...	...	250.....	9.8	167.7	489.4	23.32	...	...	...
206.....	798.0	143.7	467.0	20.86	0.12	1.45	1.33	251.....	697.5	169.1	373.8	22.46	...	...	...
207.....	817.2	145.3	481.6	20.12	0.04	0.86	0.73	252.....	592.2	169.2	305.8	22.23	-0.36	...	...
208.....	292.2	146.0	309.9	23.41	...	...	...	253.....	163.9	169.2	366.4	23.31	...	...	...
209.....	294.4	147.0	308.0	23.78	...	...	...	254.....	278.5	169.3	295.6	23.31	...	...	...
210.....	564.6	147.6	310.8	22.49	...	...	...	255.....	770.5	170.0	429.3	23.59	...	...	...
211.....	542.6	148.4	300.9	22.43	-0.04	1.87	2.07	256.....	686.9	170.4	365.2	23.17	...	...	...
212.....	579.2	148.6	316.8	23.36	...	...	...	257.....	519.9	171.3	271.3	22.64	...	...	...
213.....	626.1	149.5	341.2	22.45	-0.08	...	...	258.....	547.1	171.3	281.9	23.78	...	...	...
214.....	692.2	150.1	383.4	23.66	...	...	...	259.....	505.9	171.4	266.7	22.80	...	...	...
215.....	718.0	150.5	401.5	23.75	...	...	...	260.....	79.5	171.5	429.4	22.27	...	...	...

TABLE 3—*Continued*

I.D. No.	x (arcsec)	y (arcsec)	r (arcsec)	B (mag)	(U-B) (mag)	(U-R) (mag)	(B-R) (mag)	I.D. No.	x (arcsec)	y (arcsec)	r (arcsec)	B (mag)	(U-B) (mag)	(U-R) (mag)	(B-R) (mag)
261.....	184.0	171.7	350.5	22.54	...	...	...	306.....	719.4	197.1	372.2	23.18	...	...	...
262.....	208.5	172.1	333.8	23.45	...	...	...	307.....	130.8	198.3	372.4	21.14	0.27	1.61	1.29
263.....	45.7	173.3	456.1	22.80	...	...	...	308.....	412.5	199.3	226.7	21.93	0.10	1.56	1.48
264.....	441.7	173.8	252.3	23.21	...	...	...	309.....	759.1	199.8	402.7	21.18	-0.21	-0.05	0.04
265.....	33.1	174.0	466.3	23.43	...	...	...	310.....	457.4	199.9	227.9	22.43	...	...	...
266.....	167.9	174.7	359.7	23.64	...	...	...	311.....	444.0	200.3	226.1	21.98	...	...	...
267.....	313.6	175.0	274.5	23.37	...	...	...	312.....	159.9	200.6	348.2	22.22	...	...	...
268.....	458.3	175.2	252.6	23.12	...	...	...	313.....	147.9	200.9	357.2	22.03	0.36	1.74	1.30
269.....	185.6	175.9	346.4	23.35	...	...	...	314.....	213.7	201.0	308.8	20.90	0.49	1.90	1.30
270.....	22.2	176.0	474.4	19.64	0.76	2.49	1.58	315.....	767.4	202.5	408.2	23.80	...	...	...
271.....	321.8	177.4	269.1	21.82	0.09	1.41	1.32	316.....	16.3	202.5	466.2	22.30	...	...	...
272.....	88.0	177.7	418.9	22.79	...	...	...	317.....	126.7	202.9	372.8	22.34	...	...	...
273.....	270.5	177.8	292.4	22.34	0.01	1.07	1.04	318.....	381.2	204.9	225.2	23.25	...	...	...
274.....	286.6	178.2	283.9	21.90	...	...	...	319.....	307.0	205.0	250.6	22.91	-0.22	...	...
275.....	307.1	178.9	273.7	22.79	...	...	...	320.....	586.6	205.6	272.7	20.88	0.11	1.92	1.89
276.....	244.5	179.3	305.7	23.15	...	...	...	321.....	615.1	206.0	290.0	20.96	0.08	1.16	1.03
277.....	681.5	180.2	354.5	22.44	0.04	1.68	1.71	322.....	325.7	206.5	240.9	22.07	0.29	...	...
278.....	158.2	181.0	362.4	22.92	...	...	...	323.....	411.2	206.6	219.5	21.09	0.09	1.17	1.04
279.....	609.8	181.7	305.7	21.05	0.26	1.65	1.35	324.....	98.7	206.6	393.6	21.85	0.33	...	...
280.....	214.4	182.8	321.9	21.45	0.34	2.09	1.74	325.....	22.2	207.4	458.7	23.78	...	...	...
281.....	713.9	183.9	376.2	23.72	...	...	...	326.....	515.4	207.8	235.6	21.85	0.16	1.20	0.96
282.....	289.7	184.6	276.8	22.15	0.15	1.53	1.37	327.....	810.6	208.3	442.1	19.49	1.10	3.43	2.19
283.....	828.5	184.8	469.3	23.09	...	...	...	328.....	372.4	210.1	222.0	23.87	...	...	...
284.....	586.5	185.0	289.4	22.66	...	...	...	329.....	162.0	211.3	339.7	23.24	...	...	...
285.....	330.0	185.2	258.7	20.99	0.29	1.52	1.15	330.....	620.2	211.4	289.4	22.31	0.34	...	...
286.....	192.2	185.3	335.1	20.78	-0.01	0.82	0.77	331.....	313.5	211.8	241.5	22.86	...	...	...
287.....	662.0	185.7	336.8	23.06	...	...	...	332.....	89.4	212.0	398.4	22.43	0.30	...	...
288.....	42.2	186.3	452.0	23.57	...	...	...	333.....	675.5	212.0	328.7	22.23	0.22	...	...
289.....	241.6	186.8	301.5	23.23	...	...	...	334.....	749.2	212.2	387.6	23.06	...	...	...
290.....	234.8	187.5	305.1	22.04	0.40	2.23	1.83	335.....	217.2	213.5	297.4	23.47	...	...	...
291.....	432.5	188.3	237.5	22.33	0.24	1.25	0.90	336.....	260.6	215.3	267.4	22.96	...	...	...
292.....	505.0	189.5	249.1	22.15	0.06	1.28	1.22	337.....	656.3	215.7	312.0	21.93	0.22	1.85	1.64
293.....	738.2	190.2	391.3	19.75	...	...	...	338.....	464.2	216.3	212.9	23.29	...	...	...
294.....	415.2	191.0	234.9	22.40	...	...	...	339.....	424.5	217.1	208.6	22.69	...	...	...
295.....	426.6	193.3	232.4	21.14	-0.20	0.36	0.52	340.....	608.2	219.1	275.7	23.16	...	...	...
296.....	710.4	193.6	367.3	21.96	...	...	...	341.....	179.5	219.4	321.1	23.84	...	...	...
297.....	207.5	194.4	317.9	22.61	-1.10	...	...	342.....	409.5	219.9	206.4	22.11	0.17	1.47	1.26
298.....	451.9	194.8	232.3	23.47	...	...	...	343.....	576.8	220.2	255.1	23.51	...	...	...
299.....	180.3	195.2	336.7	22.94	...	...	...	344.....	117.9	220.2	370.0	23.39	...	...	...
300.....	32.6	196.2	455.2	21.72	0.13	...	...	345.....	134.9	220.4	355.9	22.51	0.40	...	...
301.....	63.6	196.2	428.6	21.65	...	...	...	346.....	259.5	220.8	263.8	23.52	...	...	...
302.....	371.5	196.5	235.4	23.05	...	...	...	347.....	552.6	221.3	240.5	23.42	...	...	...
303.....	87.9	196.5	408.1	23.51	...	...	...	348.....	396.5	222.2	205.5	20.25	0.27	1.58	1.26
304.....	222.3	196.7	306.3	23.03	...	...	...	349.....	349.0	222.4	217.2	23.37	...	...	...
305.....	703.2	197.0	359.6	23.83	...	...	...	350.....	640.8	222.9	295.6	21.97	0.13	1.35	1.18

TABLE 3—*Continued*

I.D. No.	x (arcsec)	y (arcsec)	r (arcsec)	B (mag)	(U-B) (mag)	(U-R) (mag)	(B-R) (mag)
351.....	391.2	223.2	205.3	23.51	...	...	...
352.....	511.3	223.3	219.7	21.53	0.07	1.49	1.45
353.....	241.1	223.5	273.7	23.78	...	...	...
354.....	86.3	224.3	394.5	20.76	0.74	2.96	2.17
355.....	263.8	224.4	258.3	22.51	-0.38	...	...
356.....	559.8	224.7	241.6	21.90	...	...	...
357.....	659.0	224.9	307.8	22.23	-0.25	0.38	0.62
358.....	764.1	227.2	392.4	20.40	0.49	2.54	2.05
359.....	399.8	227.8	199.5	23.47	...	...	...
360.....	37.5	228.5	435.3	23.68	...	...	...
361.....	437.8	228.9	197.1	22.26	...	...	...
362.....	682.2	229.1	323.2	22.87	...	...	...
363.....	18.7	229.8	451.6	23.67	...	...	...
364.....	493.1	230.2	206.8	21.90	0.34	1.83	1.44
365.....	181.8	230.2	312.5	22.24	0.28	1.73	1.42
366.....	122.8	230.4	360.3	21.75	...	...	...
367.....	505.0	230.8	210.4	22.83	...	...	...
368.....	236.1	231.1	271.6	22.40	-0.26	...	...
369.....	564.4	231.2	238.9	23.66	...	...	...
370.....	690.3	231.6	328.2	22.80	...	...	...
371.....	8.1	232.0	460.2	23.87	...	...	...
372.....	601.2	232.2	261.2	23.42	...	...	...
373.....	191.7	233.0	303.1	22.81	...	...	...
374.....	430.4	233.4	192.4	22.65	...	...	...
375.....	363.6	233.4	202.0	22.56	-0.23	1.32	1.70
376.....	680.0	233.6	318.7	21.02	0.08	1.27	1.17
377.....	171.9	233.6	318.2	21.85	0.13	...	...
378.....	417.5	233.7	192.1	21.51	0.06	0.85	0.69
379.....	60.0	234.8	412.5	21.22	0.14	1.16	0.95
380.....	96.0	234.9	380.8	23.81	...	...	...
381.....	517.8	235.6	211.2	23.67	...	...	...
382.....	294.3	235.7	230.9	22.75	-0.76	...	...
383.....	454.2	236.1	191.7	22.60	0.11	...	...
384.....	746.9	237.7	372.2	21.71	0.07	1.28	1.19
385.....	165.1	237.8	321.2	21.03	-0.11	1.48	1.71
386.....	357.7	238.3	199.3	22.40	-1.27	...	...
387.....	575.8	238.7	239.8	22.57	-0.11	0.51	0.55
388.....	173.9	238.7	313.6	23.05	...	...	...
389.....	462.4	238.9	190.3	22.55	...	...	...
390.....	211.2	239.0	284.3	23.79	...	...	...
391.....	339.6	239.8	204.8	23.88	...	...	...
392.....	386.0	240.3	189.5	22.36	...	...	...
393.....	430.4	240.6	185.1	23.29	...	...	...
394.....	777.0	241.3	396.8	23.51	...	...	...
395.....	404.3	243.0	183.9	22.20	0.28	...	...
396.....	77.8	244.5	392.2	19.81	-0.09	0.51	0.51
397.....	244.3	244.6	256.3	22.82	...	...	...
398.....	486.6	245.2	190.5	22.93	...	...	...
399.....	521.7	245.7	204.0	23.47	...	...	...
400.....	559.6	246.8	223.5	23.79	...	...	...
401.....	289.7	246.9	224.6	23.55	...	...	...
402.....	113.5	247.5	359.5	22.25	...	...	...
403.....	181.5	247.6	302.2	22.89	...	...	...
404.....	684.5	247.7	314.1	22.46	-1.08	...	...
405.....	289.9	249.8	222.2	23.12	...	...	...
406.....	171.7	249.9	308.8	22.61	-0.27	...	...
407.....	753.2	250.1	371.6	21.24	0.66	2.89	2.20
408.....	215.4	250.4	273.7	21.54	...	...	...
409.....	412.9	250.9	175.2	22.76	...	...	...
410.....	646.7	251.3	281.5	22.17	...	...	...
411.....	508.4	252.6	191.8	22.28	0.17	...	...
412.....	387.2	252.8	177.0	21.96	-0.07	...	...
413.....	802.1	253.5	413.9	18.18	1.27	3.89	2.47
414.....	357.5	254.1	184.6	23.28	...	...	...
415.....	63.1	254.1	401.1	21.99	0.69	...	...
416.....	512.1	254.8	191.5	23.02	...	...	...
417.....	176.2	255.4	302.0	20.06	0.43	1.78	1.24
418.....	268.0	256.3	231.4	21.80	-0.09	1.32	1.50
419.....	622.7	256.8	259.5	23.14	...	...	...
420.....	725.4	256.8	344.0	20.86	-0.10	0.52	0.54
421.....	498.0	257.0	183.5	21.13	0.33	1.93	1.57
422.....	450.8	257.6	169.9	23.74	...	...	...
423.....	226.4	258.7	260.0	22.43	...	...	...
424.....	794.5	259.4	404.6	19.90	1.30	3.97	2.52
425.....	365.7	259.5	176.7	23.51	...	...	...
426.....	23.3	259.9	435.2	23.47	...	...	...
427.....	429.8	260.2	165.5	23.70	...	...	...
428.....	327.6	260.8	191.9	22.27	0.08	1.32	1.22
429.....	75.2	261.4	387.1	23.01	...	...	...
430.....	262.5	261.5	231.4	23.37	...	...	...
431.....	293.1	262.0	210.6	23.80	...	...	...
432.....	512.7	262.4	185.0	20.93	0.19	1.27	0.99
433.....	754.3	262.6	366.9	23.78	...	...	...
434.....	443.0	262.8	163.7	23.56	...	...	...
435.....	337.4	263.1	185.0	21.37	0.09	1.36	1.27
436.....	117.0	263.2	348.8	23.82	...	...	...
437.....	414.8	263.6	162.4	23.44	...	...	...
438.....	469.0	264.6	166.8	22.94	...	...	...
439.....	575.0	264.7	219.6	23.76	...	...	...
440.....	301.3	265.6	202.7	23.21	...	...	...

TABLE 3—*Continued*

I.D. No.	x (arcsec)	y (arcsec)	r (arcsec)	B (mag)	(U–B) (mag)	(U–R) (mag)	(B–R) (mag)	I.D. No.	x (arcsec)	y (arcsec)	r (arcsec)	B (mag)	(U–B) (mag)	(U–R) (mag)	(B–R) (mag)
441.....	510.6	266.7	180.2	22.83	-0.15	...	...	486.....	195.5	282.4	271.1	23.40	...	...	...
442.....	729.2	266.7	342.7	21.16	0.16	1.36	1.16	487.....	321.9	282.4	176.9	23.35	...	...	...
443.....	227.7	267.3	253.5	23.27	...	...	...	488.....	562.1	283.0	197.4	22.95	...	...	...
444.....	329.1	267.3	185.5	20.73	-0.14	1.04	1.24	489.....	187.3	283.5	277.5	22.83	...	...	...
445.....	128.8	267.5	336.3	23.48	...	...	...	490.....	295.3	283.6	192.8	21.08	0.80	2.61	1.66
446.....	318.5	268.4	190.3	23.51	...	...	...	491.....	284.4	283.8	200.2	21.79	-0.04	1.21	1.28
447.....	149.5	268.5	317.8	22.82	-0.29	1.31	1.78	492.....	462.2	284.0	146.2	22.24	0.14	1.03	0.79
448.....	165.7	268.5	303.7	22.96	...	...	...	493.....	5.9	285.2	442.6	23.18	...	...	...
449.....	774.9	268.8	382.8	22.07	0.20	1.92	1.75	494.....	689.5	285.2	298.9	22.76	...	...	...
450.....	611.4	269.2	242.9	22.50	...	...	...	495.....	75.6	285.2	377.2	23.64	...	...	...
451.....	207.3	269.4	268.5	23.69	...	...	...	496.....	391.4	285.7	144.1	23.66	...	...	...
452.....	310.4	269.8	193.9	22.98	...	...	...	497.....	18.9	286.0	430.0	22.94	...	...	...
453.....	426.3	270.8	154.9	21.92	0.27	...	...	498.....	722.1	286.6	327.4	22.93	...	...	...
454.....	446.8	271.0	156.1	23.10	...	...	...	499.....	694.5	286.8	302.6	22.83	...	...	...
455.....	729.4	271.4	340.7	23.17	...	...	...	500.....	328.4	287.5	169.0	23.45	...	...	...
456.....	193.2	271.5	278.9	23.56	...	...	...	501.....	596.4	287.7	219.5	20.91	0.20	1.51	1.27
457.....	801.7	271.5	406.4	23.91	...	...	...	502.....	392.8	288.4	141.1	22.87	...	...	...
458.....	652.2	272.1	273.7	22.88	...	...	...	503.....	349.1	289.0	156.6	21.28	-0.02	0.61	0.53
459.....	396.8	272.6	155.8	22.22	0.09	0.91	0.73	504.....	223.2	289.0	244.2	21.92	...	...	...
460.....	343.0	272.9	173.6	22.64	-0.30	...	...	505.....	273.1	289.4	204.6	21.94	-0.11	0.76	0.85
461.....	712.6	273.4	324.8	22.80	...	...	...	506.....	625.9	290.7	241.5	22.28	-0.50	1.14	1.90
462.....	317.4	274.1	186.2	21.66	0.20	1.51	1.28	507.....	277.0	290.9	200.6	23.45	...	...	...
463.....	401.0	274.3	153.4	22.88	...	...	...	508.....	591.0	291.1	213.2	21.91	...	...	...
464.....	203.7	274.3	268.6	23.53	...	...	...	509.....	488.3	291.2	148.3	22.73	...	...	...
465.....	443.2	274.9	151.8	22.31	0.54	...	...	510.....	352.4	291.8	152.6	22.98	...	...	...
466.....	583.4	274.9	218.2	23.53	...	...	...	511.....	344.0	291.9	156.7	23.15	...	...	...
467.....	280.0	275.2	209.4	22.31	...	...	...	512.....	217.2	292.7	247.2	23.58	...	...	...
468.....	614.9	275.3	241.7	21.57	0.46	2.27	1.78	513.....	351.4	293.1	151.9	23.26	...	...	...
469.....	359.1	276.3	163.5	23.52	...	...	...	514.....	35.0	293.7	412.3	22.30	0.25	...	...
470.....	504.5	276.7	168.6	22.50	...	...	...	515.....	436.6	293.7	132.4	22.90	...	...	...
471.....	202.8	276.9	267.9	23.36	...	...	...	516.....	777.9	294.8	375.8	22.57	-0.05	0.75	0.75
472.....	288.0	277.7	202.1	23.38	...	...	...	517.....	810.1	295.0	406.0	23.64	...	...	...
473.....	452.2	278.2	149.9	23.19	...	...	...	518.....	758.0	296.7	356.5	21.48	-0.16	0.25	0.32
474.....	122.1	278.2	337.5	22.16	-0.04	...	...	519.....	255.3	296.9	213.5	22.12	0.43	...	...
475.....	629.1	278.5	251.1	22.44	...	...	...	520.....	288.4	297.4	187.9	23.33	...	...	...
476.....	300.5	279.1	192.7	22.40	0.20	1.86	1.69	521.....	266.6	297.5	204.3	22.58	-0.28	0.47	0.76
477.....	93.2	280.3	362.8	20.35	0.16	1.17	0.92	522.....	373.6	297.5	138.3	19.05	0.60	2.28	1.59
478.....	207.5	280.8	261.9	22.70	...	...	...	523.....	176.3	297.5	280.4	22.80	...	...	...
479.....	232.3	281.2	241.4	23.24	...	...	...	524.....	513.0	298.6	154.2	22.40	...	...	...
480.....	670.8	281.5	284.4	22.54	-0.23	...	...	525.....	625.5	300.1	236.0	22.76	0.26	...	...
481.....	251.0	281.9	226.2	22.10	-0.52	0.37	1.00	526.....	478.8	300.2	136.3	21.49	0.42	1.92	1.42
482.....	751.8	282.2	356.3	22.82	...	...	...	527.....	259.0	301.0	208.1	23.34	...	...	...
483.....	684.0	282.2	295.5	23.19	...	...	...	528.....	506.6	301.2	148.5	22.82	...	...	...
484.....	499.3	282.3	161.2	22.79	...	...	...	529.....	186.4	301.8	269.4	22.75	...	...	...
485.....	612.4	282.3	235.4	23.12	...	...	...	530.....	574.4	301.8	193.6	23.73	...	...	...

TABLE 3—*Continued*

I.D. No.	x (arcsec)	y (arcsec)	r (arcsec)	B (mag)	(U-B) (mag)	(U-R) (mag)	(B-R) (mag)	I.D. No.	x (arcsec)	y (arcsec)	r (arcsec)	B (mag)	(U-B) (mag)	(U-R) (mag)	(B-R) (mag)
531.....	277.4	302.6	192.7	23.17	...	...	...	576.....	241.4	315.2	214.8	23.70	...	...	...
532.....	623.3	302.8	232.7	23.07	...	...	...	577.....	390.0	315.3	116.0	23.03	...	...	...
533.....	583.7	303.3	199.9	21.82	...	...	...	578.....	655.1	315.4	254.6	23.43	...	...	...
534.....	408.3	303.4	123.5	22.18	0.48	2.48	2.00	579.....	280.2	315.5	182.5	21.56	0.05	1.21	1.14
535.....	353.2	303.5	142.1	23.77	...	...	...	580.....	423.7	316.4	109.3	21.94	...	...	...
536.....	372.7	303.6	133.0	23.18	...	...	...	581.....	330.3	316.8	144.8	21.75	0.29	...	...
537.....	232.9	303.7	228.1	21.76	0.16	1.21	0.97	582.....	603.4	317.4	208.2	20.97	0.18	1.38	1.15
538.....	266.5	304.1	200.3	22.58	-0.38	1.35	1.97	583.....	411.6	317.4	109.1	23.07	...	...	...
539.....	203.7	304.1	253.1	23.35	...	...	...	584.....	726.7	317.7	319.8	21.90	-0.44	...	...
540.....	296.9	304.7	176.6	22.63	-0.14	...	...	585.....	377.3	318.5	117.5	23.04	...	...	...
541.....	786.9	304.9	380.9	23.68	...	...	...	586.....	273.5	319.4	185.6	22.47	0.10	1.07	0.90
542.....	438.6	305.0	121.4	23.54	...	...	...	587.....	312.8	320.8	154.1	23.56	...	...	...
543.....	329.0	305.0	154.6	23.08	...	...	...	588.....	280.8	321.1	178.6	21.07	0.19	1.42	1.17
544.....	399.8	305.1	123.3	22.41	...	...	...	589.....	500.4	321.4	128.3	20.34	0.48	2.07	1.51
545.....	420.7	305.1	120.6	22.62	0.00	1.66	1.75	590.....	392.0	321.6	109.4	22.67	...	...	...
546.....	76.2	306.1	369.3	23.19	...	...	...	591.....	382.5	321.7	112.6	22.26	0.35	2.35	2.04
547.....	556.6	306.2	177.3	19.21	0.68	2.31	1.49	592.....	302.4	321.8	161.1	22.52	...	...	...
548.....	249.0	306.5	213.1	23.57	...	...	...	593.....	400.7	322.2	106.5	22.74	...	...	...
549.....	612.9	306.8	221.8	21.15	0.41	2.42	2.03	594.....	487.3	323.1	119.6	21.95	0.03	1.57	1.61
550.....	274.7	307.3	191.8	23.39	...	...	...	595.....	478.0	323.3	115.0	22.86	...	...	...
551.....	382.8	307.5	125.7	22.49	...	...	...	596.....	598.2	324.5	200.0	22.64	-0.35	...	...
552.....	627.6	307.5	234.0	23.77	...	...	...	597.....	156.3	324.6	287.7	22.60	-0.98	...	...
553.....	560.6	308.0	179.0	23.05	...	...	...	598.....	616.4	325.0	215.7	23.07	...	...	...
554.....	75.3	308.2	369.6	23.49	...	...	...	599.....	128.7	325.3	313.4	23.08	...	...	...
555.....	400.0	309.1	119.3	23.01	...	...	...	600.....	34.3	325.6	403.9	22.67	-0.14	...	...
556.....	500.0	310.3	137.2	21.42	-0.94	...	...	601.....	366.7	326.5	115.4	20.79	0.13	1.42	1.27
557.....	590.4	310.4	201.1	22.45	...	...	...	602.....	424.0	327.2	98.5	20.82	0.30	1.86	1.53
558.....	524.2	310.9	151.3	22.10	...	...	...	603.....	40.9	327.2	397.1	21.54	-0.47	...	...
559.....	817.8	310.9	408.5	22.99	...	...	...	604.....	472.4	327.3	108.9	23.72	...	...	...
560.....	519.1	311.0	147.9	22.30	0.06	...	...	605.....	493.3	327.3	119.3	23.68	...	...	...
561.....	321.7	311.0	154.8	22.60	...	...	...	606.....	194.2	327.3	251.4	22.80	...	...	...
562.....	384.5	311.2	121.7	22.87	...	...	...	607.....	180.8	327.7	263.7	21.71	0.08	1.35	1.26
563.....	512.7	311.5	143.6	21.82	0.12	1.83	1.77	608.....	290.5	328.1	166.6	23.38	...	...	...
564.....	31.5	311.5	410.4	23.33	...	...	...	609.....	723.1	328.5	312.9	23.09	...	...	...
565.....	288.3	311.6	178.6	22.26	...	...	...	610.....	484.1	328.6	113.2	21.76	0.22	1.97	1.79
566.....	227.4	311.7	228.6	23.61	...	...	...	611.....	627.1	328.9	223.5	21.97	0.09	1.52	1.45
567.....	397.7	311.8	117.3	22.36	...	...	...	612.....	444.2	328.9	98.5	21.26	0.30	1.96	1.64
568.....	786.0	312.0	377.9	23.40	...	...	...	613.....	250.5	329.2	199.9	23.38	...	...	...
569.....	478.1	312.6	124.7	22.92	...	...	...	614.....	749.1	329.2	337.5	22.31	0.09	1.08	0.92
570.....	454.0	312.6	116.6	22.37	0.01	1.71	1.80	615.....	505.2	329.7	124.6	23.62	...	...	...
571.....	412.0	312.6	113.8	21.96	0.22	1.91	1.73	616.....	435.9	329.9	96.3	23.52	...	...	...
572.....	292.4	313.2	174.4	22.13	...	...	...	617.....	560.8	330.0	165.6	23.24	...	...	...
573.....	432.4	313.6	112.3	22.64	...	...	...	618.....	568.7	331.1	171.5	22.35	0.34	...	...
574.....	419.6	313.6	112.2	22.78	...	...	...	619.....	27.3	331.1	409.4	23.42	...	...	...
575.....	576.1	314.0	187.3	23.15	...	...	...	620.....	52.9	331.5	384.5	22.80	-0.12	1.47	1.72

TABLE 3—*Continued*

I.D. No.	x (arcsec)	y (arcsec)	r (arcsec)	B (mag)	(U-B) (mag)	(U-R) (mag)	(B-R) (mag)	I.D. No.	x (arcsec)	y (arcsec)	r (arcsec)	B (mag)	(U-B) (mag)	(U-R) (mag)	(B-R) (mag)
621.....	421.8	332.9	92.8	23.12	...	...	...	666.....	404.8	349.3	79.2	22.84	...	...	...
622.....	414.8	333.0	93.3	21.98	0.12	...	...	667.....	516.4	349.3	118.6	21.77	0.13	...	...
623.....	476.2	333.1	105.5	23.45	...	...	...	668.....	577.6	349.7	169.9	21.53	0.29	1.76	1.42
624.....	520.5	333.2	132.5	23.11	...	...	...	669.....	356.5	350.0	102.5	21.93	...	...	...
625.....	537.2	334.2	144.2	23.12	...	...	...	670.....	537.5	350.1	135.0	20.91	1.09	3.72	2.54
626.....	678.3	334.4	268.6	23.29	...	...	...	671.....	271.3	350.4	171.8	22.39	0.40	2.29	1.90
627.....	432.1	334.5	91.4	22.57	...	...	...	672.....	312.3	350.9	135.7	21.24	0.04	1.22	1.18
628.....	79.8	334.9	357.6	23.15	...	...	...	673.....	298.4	351.8	147.1	23.44	...	...	...
629.....	539.4	334.9	145.4	23.00	...	...	...	674.....	735.5	352.2	318.5	23.58	...	...	...
630.....	483.6	335.9	106.8	22.69	...	...	...	675.....	324.3	352.4	125.1	22.83	...	...	...
631.....	98.1	336.5	339.4	22.75	...	...	...	676.....	396.2	352.8	78.6	22.62	...	...	...
632.....	260.2	337.1	187.7	23.56	...	...	...	677.....	532.2	353.0	128.9	22.80	...	...	...
633.....	436.1	337.4	88.9	22.84	...	...	...	678.....	108.9	353.5	324.9	21.93	-0.17	0.46	0.59
634.....	469.4	337.7	98.2	22.60	...	...	...	679.....	780.4	353.5	362.0	22.10	0.31	2.03	1.71
635.....	493.0	337.8	110.7	21.45	0.16	1.82	1.70	680.....	494.3	353.6	99.5	21.86	0.14	1.58	1.44
636.....	574.6	338.2	172.7	22.41	0.09	...	...	681.....	668.1	353.6	252.9	21.89	...	...	...
637.....	407.4	338.2	89.3	22.73	...	...	...	682.....	236.6	353.7	202.3	21.65	-0.02	...	...
638.....	218.2	338.3	225.1	23.23	...	...	...	683.....	480.3	353.9	90.2	21.99	0.13	1.51	1.37
639.....	304.5	338.3	149.3	22.87	...	...	...	684.....	608.7	353.9	196.6	21.29	0.15	1.25	1.04
640.....	384.8	339.1	95.8	22.14	0.03	...	...	685.....	598.2	354.4	186.7	22.39	-0.15	2.04	2.43
641.....	390.0	339.7	93.0	23.14	...	...	...	686.....	711.8	354.7	294.9	20.97	0.18	1.51	1.31
642.....	341.0	339.7	120.6	23.32	...	...	...	687.....	48.9	354.7	383.4	23.61	...	...	...
643.....	429.1	341.9	83.8	21.88	0.31	1.90	1.57	688.....	402.5	355.6	73.8	22.79	...	...	...
644.....	108.8	342.3	327.7	23.59	...	...	...	689.....	562.8	355.8	154.0	23.17	...	...	...
645.....	369.3	342.5	100.4	20.77	0.41	1.75	1.24	690.....	231.6	355.8	206.2	23.38	...	...	...
646.....	456.4	342.6	88.6	22.36	0.15	...	...	691.....	445.2	356.1	72.2	23.31	...	...	...
647.....	524.5	342.7	129.1	21.04	0.22	1.71	1.49	692.....	589.5	356.1	178.0	23.10	...	...	...
648.....	398.5	342.7	87.3	23.68	...	...	...	693.....	460.6	356.3	77.6	23.18	...	...	...
649.....	412.1	343.3	83.5	20.89	0.19	1.59	1.38	694.....	349.2	356.7	103.0	23.62	...	...	...
650.....	535.2	343.9	136.7	22.24	-0.04	...	...	695.....	376.3	357.1	84.5	21.74	0.11	1.80	1.76
651.....	267.9	344.1	177.6	22.18	0.00	1.51	1.57	696.....	508.1	357.1	107.2	23.70	...	...	...
652.....	475.4	344.9	94.8	22.47	...	...	...	697.....	388.8	358.1	77.0	21.42	...	...	...
653.....	214.0	345.7	226.2	23.21	...	...	...	698.....	368.0	358.9	88.2	23.81	...	...	...
654.....	465.5	346.3	88.8	21.17	0.22	1.75	1.52	699.....	253.8	359.4	184.2	23.10	...	...	...
655.....	187.1	346.4	251.4	22.47	0.01	...	...	700.....	689.1	359.5	271.6	22.09	...	...	...
656.....	683.1	346.5	269.3	23.12	...	...	...	701.....	211.1	359.7	224.5	23.79	...	...	...
657.....	599.2	346.7	190.7	22.31	0.24	2.04	1.84	702.....	354.8	359.8	96.7	22.98	...	...	...
658.....	204.0	346.9	235.3	22.55	...	...	...	703.....	527.5	360.8	120.7	21.80	0.14	1.63	1.50
659.....	223.9	346.9	216.6	22.23	...	...	...	704.....	146.6	361.2	286.4	22.60	...	...	...
660.....	128.6	346.9	307.3	23.01	...	...	...	705.....	500.4	361.4	98.5	22.78	...	...	...
661.....	486.7	347.2	99.4	22.09	0.13	1.79	1.71	706.....	518.8	361.4	113.1	23.45	...	...	...
662.....	445.2	348.3	79.8	22.79	...	...	...	707.....	470.1	361.7	77.9	22.56	...	...	...
663.....	254.3	348.6	187.8	19.60	0.04	1.09	1.02	708.....	589.3	362.4	175.5	22.35	-0.08	1.50	1.69
664.....	341.1	348.6	114.4	22.34	0.15	1.72	1.59	709.....	639.2	362.6	222.7	22.80	0.09	2.10	2.14
665.....	280.1	348.9	164.5	23.29	...	...	...	710.....	511.8	362.7	106.7	23.36	...	...	...

TABLE 3—*Continued*

I.D. No.	x (arcsec)	y (arcsec)	r (arcsec)	B (mag)	(U–B) (mag)	(U–R) (mag)	(B–R) (mag)
711.....	545.6	362.9	135.4	22.90	-0.49	...	...
712.....	241.8	363.0	194.3	22.52	...	...	...
713.....	534.6	363.0	125.6	23.30	...	...	...
714.....	366.6	363.5	85.8	21.43	0.07	1.71	1.71
715.....	255.5	363.8	181.1	22.02	0.47	2.08	1.54
716.....	186.1	364.0	247.4	23.16	...	...	...
717.....	414.8	364.6	62.0	22.59	...	...	...
718.....	655.2	365.1	237.4	22.92	...	...	...
719.....	71.2	365.4	359.5	23.14	...	...	...
720.....	561.2	365.4	148.3	21.23	0.81	3.16	2.30
721.....	167.7	365.8	264.8	23.18	...	...	...
722.....	31.1	366.2	399.0	22.58	-0.19	...	...
723.....	235.9	367.1	198.6	21.96	0.19	...	...
724.....	680.7	367.2	261.7	22.43	...	...	...
725.....	811.9	367.3	390.6	23.79	...	...	...
726.....	323.5	367.7	117.5	23.09	...	...	...
727.....	227.0	368.4	206.7	22.49	-0.02	...	...
728.....	630.8	368.4	212.9	23.35	...	...	...
729.....	117.9	368.9	313.0	23.31	...	...	...
730.....	125.2	369.1	305.8	23.11	...	...	...
731.....	46.8	369.5	383.0	21.39	0.27	1.49	1.14
732.....	170.8	369.9	260.9	23.59	...	...	...
733.....	32.8	370.1	396.8	22.69	-0.75	...	...
734.....	505.9	370.7	97.3	23.11	...	...	...
735.....	698.9	370.9	278.7	23.44	...	...	...
736.....	561.2	370.9	146.2	22.24	...	...	...
737.....	661.5	371.5	242.0	22.55	-0.08	...	...
738.....	602.8	372.2	185.1	23.63	...	...	...
739.....	637.8	372.4	218.7	23.12	...	...	...
740.....	568.5	372.6	152.4	21.60	0.14	1.40	1.22
741.....	266.6	374.0	167.3	21.78	0.51	2.50	1.98
742.....	498.8	374.1	89.5	21.94	-0.10	1.10	1.23
743.....	255.3	374.2	177.9	23.24	...	...	...
744.....	516.3	375.3	103.7	23.13	...	...	...
745.....	142.4	375.4	287.7	23.15	...	...	...
746.....	476.9	375.7	71.6	20.72	...	...	...
747.....	369.6	376.2	74.7	23.62	...	...	...
748.....	575.3	376.4	157.6	22.71	...	...	...
749.....	181.9	376.7	248.7	23.20	...	...	...
750.....	361.3	376.7	80.8	21.40	...	...	...
751.....	235.9	376.8	195.9	22.19	-0.08	...	...
752.....	638.7	377.1	218.5	23.78	...	...	...
753.....	310.2	377.3	125.2	22.43	0.19	1.70	1.51
754.....	132.1	377.4	297.5	23.18	...	...	...
755.....	73.1	379.0	355.7	23.63	...	...	...
756.....	136.5	379.3	292.9	22.58	...	...	...
757.....	635.9	379.4	215.2	23.10	...	...	...
758.....	316.0	379.6	119.0	22.06	0.31	1.81	1.45
759.....	526.3	379.7	110.6	23.43	...	...	...
760.....	68.4	379.7	360.2	23.12	...	...	...
761.....	233.2	382.1	197.3	22.99	...	...	...
762.....	683.2	382.6	261.2	23.10	...	...	...
763.....	353.4	382.7	84.1	21.68	...	...	...
764.....	339.4	382.9	96.3	22.49	-0.54	...	...
765.....	242.7	383.6	187.7	23.18	...	...	...
766.....	819.7	384.0	396.3	21.78	0.21	...	...
767.....	285.8	384.2	145.9	22.69	...	...	...
768.....	604.8	384.8	183.8	23.64	...	...	...
769.....	195.2	384.9	234.0	23.19	...	...	...
770.....	504.8	385.1	88.9	21.78	...	...	...
771.....	119.4	386.4	308.8	22.12	...	...	...
772.....	485.1	388.3	70.2	20.41	...	...	...
773.....	163.4	388.7	264.8	23.34	...	...	...
774.....	525.5	389.0	106.4	23.08	...	...	...
775.....	576.0	389.2	154.7	22.26	0.07	...	...
776.....	752.4	389.3	328.8	19.00	1.07	3.54	2.35
777.....	182.4	389.3	246.0	23.43	...	...	...
778.....	346.1	389.5	87.4	22.61	...	...	...
779.....	6.5	389.7	420.6	23.33	...	...	...
780.....	586.8	389.8	165.1	21.60	0.07	1.25	1.16
781.....	772.6	390.2	348.8	22.92	-0.75	...	...
782.....	204.5	390.2	224.0	21.25	0.95	3.31	2.27
783.....	822.9	390.4	398.8	23.11	...	...	...
784.....	621.9	391.3	199.3	20.60	0.28	1.62	1.29
785.....	134.5	391.7	293.2	22.73	...	...	...
786.....	140.6	392.2	287.0	23.66	...	...	...
787.....	193.1	392.8	234.9	22.04	0.16	1.89	1.78
788.....	209.0	393.5	219.1	23.06	...	...	...
789.....	524.5	393.6	103.9	21.54	0.18	1.05	0.76
790.....	301.1	393.9	128.6	23.62	...	...	...
791.....	502.7	394.4	83.2	23.25	...	...	...
792.....	148.2	394.4	279.2	22.79	-0.15	...	...
793.....	225.4	394.6	202.7	22.46	0.15	...	...
794.....	632.6	394.8	209.2	21.84	-1.15	...	...
795.....	656.3	395.1	232.6	23.81	...	...	...
796.....	268.3	395.5	160.3	21.28	0.03	1.48	1.46
797.....	601.2	395.6	178.1	21.24	-0.10	1.21	1.37
798.....	242.2	395.9	185.9	21.51	0.08	...	...
799.....	559.1	396.0	136.7	22.06	-0.02	1.67	1.80
800.....	537.9	396.2	116.1	21.44	0.19	1.74	1.56

TABLE 3—*Continued*

I.D. No.	x (arcsec)	y (arcsec)	r (arcsec)	B (mag)	(U–B) (mag)	(U–R) (mag)	(B–R) (mag)	I.D. No.	x (arcsec)	y (arcsec)	r (arcsec)	B (mag)	(U–B) (mag)	(U–R) (mag)	(B–R) (mag)
801.....	766.8	396.4	342.4	20.56	1.22	3.65	2.26	846.....	319.1	415.9	107.0	21.43	-0.01	...	...
802.....	127.1	397.4	299.9	23.44	...	...	...	847.....	303.4	415.9	122.6	22.87	...	...	...
803.....	675.6	397.5	251.6	23.43	...	...	...	848.....	229.5	416.1	196.3	23.14	...	...	...
804.....	586.2	397.8	162.9	20.05	0.40	1.77	1.27	849.....	166.3	416.4	259.6	21.95	0.34	1.73	1.31
805.....	218.0	398.4	209.4	23.73	...	...	...	850.....	23.0	416.5	402.7	22.76	-0.59	...	...
806.....	54.5	398.6	372.1	23.42	...	...	...	851.....	527.5	416.7	102.2	22.45	0.18	...	...
807.....	527.1	399.1	104.9	21.80	0.24	1.17	0.80	852.....	87.2	417.8	338.5	22.54	...	...	...
808.....	42.9	399.9	383.6	22.61	0.31	...	...	853.....	524.3	419.9	98.8	21.98	0.09	0.57	0.32
809.....	182.7	400.1	244.3	21.21	0.18	1.40	1.16	854.....	682.7	420.9	257.1	21.11	-0.09	0.93	1.02
810.....	252.9	400.8	174.5	22.98	...	...	...	855.....	28.3	421.2	397.4	22.94	...	...	...
811.....	321.0	401.0	107.5	21.24	-0.05	0.97	1.02	856.....	110.5	421.3	315.2	22.96	0.19	...	...
812.....	95.8	401.1	330.8	23.51	...	...	...	857.....	483.8	421.3	58.3	22.17	0.21	...	...
813.....	492.2	401.6	70.8	23.01	...	...	...	858.....	503.8	421.9	78.2	22.93	-0.37	...	...
814.....	721.2	401.6	296.5	22.33	0.20	...	...	859.....	673.1	422.1	247.5	22.28	0.32	...	...
815.....	202.9	402.0	224.0	22.75	...	...	...	860.....	265.7	422.7	160.0	23.28	...	...	...
816.....	356.9	402.1	72.6	22.31	0.41	...	...	861.....	348.2	422.9	77.5	23.82	...	...	...
817.....	563.2	402.5	139.4	22.90	...	...	...	862.....	569.7	423.0	144.1	23.67	...	...	...
818.....	25.6	402.6	400.7	23.64	...	...	...	863.....	89.1	423.5	336.6	23.59	...	...	...
819.....	615.6	402.7	191.4	23.51	...	...	...	864.....	517.3	424.4	91.7	22.89	...	...	...
820.....	231.8	403.5	195.1	23.50	...	...	...	865.....	314.2	426.9	111.4	22.07	...	...	...
821.....	600.4	404.0	176.1	23.22	...	...	...	866.....	304.8	427.4	120.9	22.19	0.15	1.05	0.80
822.....	222.7	405.0	204.0	23.24	...	...	...	867.....	25.8	427.7	399.8	21.62	0.10	1.97	1.96
823.....	100.9	405.2	325.4	23.47	...	...	...	868.....	320.5	427.7	105.2	21.63	0.11	1.45	1.33
824.....	341.5	405.3	86.6	21.56	0.15	1.70	1.57	869.....	526.3	428.2	100.7	19.57	0.52	2.24	1.64
825.....	294.6	405.4	132.6	22.13	-0.06	1.46	1.62	870.....	169.7	428.3	256.0	23.31	...	...	...
826.....	583.0	406.5	158.6	23.16	...	...	...	871.....	227.2	428.3	198.5	22.03	...	...	...
827.....	489.8	407.4	66.7	22.09	...	...	...	872.....	629.2	429.0	203.6	23.87	...	...	...
828.....	320.3	407.9	106.8	21.53	0.15	...	...	873.....	99.6	429.5	326.1	23.33	...	...	...
829.....	543.7	408.5	119.3	21.67	0.00	1.54	1.62	874.....	70.1	430.2	355.6	18.31	0.56	1.98	1.28
830.....	137.7	409.2	288.4	23.17	...	...	...	875.....	729.5	430.3	303.8	22.68	...	...	...
831.....	660.7	409.9	235.6	21.27	0.17	1.60	1.42	876.....	491.3	430.7	65.9	22.15	...	...	...
832.....	578.0	410.0	153.1	22.44	...	...	...	877.....	514.7	430.8	89.2	23.27	...	...	...
833.....	169.9	410.8	256.2	22.90	-0.06	...	...	878.....	29.0	431.3	396.7	21.93	0.43	1.91	1.40
834.....	617.7	411.0	192.6	22.71	-0.03	...	...	879.....	346.3	431.5	79.6	22.36	...	...	...
835.....	638.1	411.5	212.9	21.69	...	...	...	880.....	544.8	432.4	119.3	23.13	...	...	...
836.....	508.0	411.7	83.5	22.59	-0.20	...	...	881.....	796.0	433.1	370.4	21.94	0.19	1.40	1.16
837.....	533.2	411.9	108.4	22.29	0.15	...	...	882.....	610.0	433.1	184.5	22.53	...	...	...
838.....	571.6	412.0	146.6	21.42	0.16	1.06	0.80	883.....	604.6	433.6	179.1	21.44	0.09	1.47	1.39
839.....	596.2	412.4	171.1	23.13	...	...	...	884.....	296.8	434.1	129.1	23.51	...	...	...
840.....	674.5	412.4	249.2	23.58	...	...	...	885.....	663.4	434.3	237.9	22.76	-0.09	...	...
841.....	704.9	412.5	279.5	22.36	...	...	...	886.....	249.0	434.6	176.9	22.65	...	...	...
842.....	199.6	412.6	226.5	23.79	...	...	...	887.....	331.4	435.1	94.7	21.66	0.17	1.69	1.54
843.....	306.1	413.0	120.3	21.78	0.46	...	...	888.....	502.5	435.6	77.4	23.32	...	...	...
844.....	347.9	413.3	78.7	23.39	...	...	...	889.....	676.3	435.8	250.8	23.06	...	...	...
845.....	580.2	415.2	154.9	22.85	...	...	...	890.....	525.9	436.5	100.8	23.18	...	...	...

TABLE 3—*Continued*

I.D. No.	x (arcsec)	y (arcsec)	r (arcsec)	B (mag)	(U–B) (mag)	(U–R) (mag)	(B–R) (mag)
891.....	547.3	436.6	122.1	21.03	0.13	1.38	1.22
892.....	363.7	437.2	63.1	21.81	...	...	...
893.....	237.1	437.6	188.9	22.56	...	...	...
894.....	481.5	437.7	57.1	22.01	-0.04	...	...
895.....	341.8	438.6	84.8	23.78	...	...	...
896.....	569.2	439.1	144.1	22.46	...	...	...
897.....	735.4	439.4	310.1	22.97	...	...	...
898.....	158.9	439.6	267.1	23.34	...	...	...
899.....	181.6	439.7	244.4	23.40	...	...	...
900.....	58.1	439.8	367.8	23.01	...	...	...
901.....	511.3	439.9	86.9	23.08	...	...	...
902.....	494.3	439.9	70.1	22.00	...	...	...
903.....	605.2	440.1	180.1	22.32	0.51	...	...
904.....	726.8	440.4	301.5	21.98	...	...	...
905.....	555.6	440.4	130.8	22.91	...	...	...
906.....	85.2	440.5	340.7	22.05	0.10	0.86	0.66
907.....	7.5	444.0	418.6	23.53	...	...	...
908.....	267.6	444.2	159.1	23.54	...	...	...
909.....	93.2	444.6	333.0	23.01	...	...	...
910.....	590.9	444.8	166.4	21.24	0.19	1.24	0.96
911.....	755.7	444.9	330.6	22.57	0.20	...	...
912.....	551.1	445.2	127.0	21.44	...	...	...
913.....	516.1	445.4	92.6	21.91	-0.07	1.49	1.65
914.....	697.9	445.7	273.0	21.70	-0.24	0.72	1.00
915.....	181.6	445.7	244.9	22.60	-0.51	...	...
916.....	601.2	445.8	176.7	22.95	...	...	...
917.....	89.7	446.2	336.6	22.30	0.40	...	...
918.....	361.8	446.6	67.2	23.49	...	...	...
919.....	25.6	446.8	400.6	22.84	...	...	...
920.....	351.9	446.9	76.8	22.22	...	...	...
921.....	644.4	446.9	219.8	22.61	0.15	1.56	1.41
922.....	764.2	447.1	339.3	22.38	-0.25	...	...
923.....	208.5	447.3	218.3	22.52	0.00	...	...
924.....	187.2	447.9	239.5	23.50	...	...	...
925.....	580.7	448.8	156.8	22.33	0.12	0.56	0.25
926.....	710.9	449.2	286.2	23.46	...	...	...
927.....	739.9	449.2	315.1	22.87	...	...	...
928.....	485.8	449.3	64.6	20.16	...	...	...
929.....	252.4	450.8	175.1	23.05	...	...	...
930.....	600.3	450.8	176.4	22.66	...	...	...
931.....	260.7	451.1	166.9	22.43	-0.70	...	...
932.....	697.4	451.1	272.9	21.50	0.45	2.03	1.50
933.....	537.8	451.3	115.1	22.91	...	...	...
934.....	68.8	451.4	357.8	22.66	-0.67	...	...
935.....	527.1	451.6	104.7	23.44	...	...	...
936.....	533.2	451.8	110.7	22.08	0.25	1.88	1.63
937.....	659.3	452.1	235.1	21.86	0.07	1.54	1.50
938.....	85.2	452.2	341.5	23.46	...	...	...
939.....	513.5	452.5	91.8	20.88	-0.12	0.98	1.14
940.....	357.2	452.7	73.6	23.09	...	...	...
941.....	674.7	453.1	250.6	21.24	0.10	1.45	1.36
942.....	266.2	453.7	161.9	21.43	0.22	1.54	1.28
943.....	216.7	455.1	211.0	21.65	0.55	3.02	2.53
944.....	201.3	455.1	226.2	21.71	...	...	...
945.....	508.9	455.1	88.3	22.73	...	...	...
946.....	524.2	455.1	102.9	22.00	0.51	1.79	1.13
947.....	66.4	455.9	360.5	22.27	...	...	...
948.....	354.0	456.6	78.0	22.97	...	...	...
949.....	699.1	457.3	275.3	22.72	...	...	...
950.....	324.5	457.8	106.2	18.60	1.21	3.65	2.27
951.....	814.4	458.1	390.1	22.36	-0.38	1.03	1.58
952.....	14.6	458.3	412.4	21.88	0.10	1.36	1.24
953.....	226.6	458.4	201.7	22.70	...	...	...
954.....	822.3	458.6	398.0	22.42	...	...	...
955.....	259.5	458.9	169.5	23.47	...	...	...
956.....	574.3	459.3	152.4	23.51	...	...	...
957.....	159.8	459.7	268.1	23.29	...	...	...
958.....	588.0	460.7	166.1	22.97	...	...	...
959.....	283.2	461.5	146.9	22.98	...	...	...
960.....	159.9	461.7	268.2	23.20	...	...	...
961.....	188.8	462.2	239.7	23.08	...	...	...
962.....	333.7	463.4	99.4	23.09	...	...	...
963.....	831.4	464.1	407.5	21.42	0.20	1.63	1.41
964.....	503.1	464.5	86.7	23.30	...	...	...
965.....	179.7	465.2	249.1	21.36	0.32	1.72	1.34
966.....	172.6	465.6	256.2	23.54	...	...	...
967.....	594.2	465.6	173.3	23.54	...	...	...
968.....	287.0	466.2	144.5	22.23	0.49	...	...
969.....	275.1	466.8	156.0	21.65	0.41	...	...
970.....	538.0	466.9	119.7	21.37	0.20	1.65	1.45
971.....	92.0	467.1	336.2	22.15	-0.36	0.82	1.31
972.....	572.7	467.2	152.8	23.45	...	...	...
973.....	255.3	468.0	175.5	21.38	-0.17	0.57	0.72
974.....	519.5	468.1	103.0	22.40	...	...	...
975.....	671.2	468.2	249.2	23.23	...	...	...
976.....	74.2	468.3	354.0	22.68	-0.31	...	...
977.....	637.4	468.4	216.0	23.38	...	...	...
978.....	478.5	468.7	68.2	21.66	...	...	...
979.....	222.6	468.8	207.5	22.72	...	...	...
980.....	350.7	469.0	86.6	23.18	...	...	...

TABLE 3—*Continued*

I.D. No.	x (arcsec)	y (arcsec)	r (arcsec)	B (mag)	(U-B) (mag)	(U-R) (mag)	(B-R) (mag)	I.D. No.	x (arcsec)	y (arcsec)	r (arcsec)	B (mag)	(U-B) (mag)	(U-R) (mag)	(B-R) (mag)
981.....	733.0	469.6	310.4	23.63	...	...	...	1026.....	644.0	483.9	225.9	23.17	...	...	...
982.....	108.8	470.0	319.9	20.81	0.02	1.03	0.97	1027.....	398.8	484.3	64.5	23.64	...	...	...
983.....	268.3	470.3	163.6	22.40	-0.53	0.67	1.38	1028.....	761.8	484.5	341.3	22.85	-0.68	...	...
984.....	557.0	470.7	138.9	22.97	...	...	...	1029.....	466.4	484.7	71.8	21.91	-0.15	...	...
985.....	542.8	471.1	125.6	22.36	0.08	...	...	1030.....	617.9	485.1	201.2	23.83	...	...	...
986.....	491.3	471.2	79.9	22.16	...	...	...	1031.....	244.0	485.5	191.3	23.17	...	...	...
987.....	210.0	471.4	220.4	21.70	...	...	...	1032.....	482.0	485.6	82.2	21.53	...	...	...
988.....	290.0	472.4	143.5	22.94	...	...	...	1033.....	56.7	486.6	373.9	20.07	0.85	3.30	2.40
989.....	176.7	472.7	253.4	23.55	...	...	...	1034.....	171.1	487.0	261.8	21.71	0.31	1.52	1.12
990.....	381.5	472.9	64.7	23.47	...	...	...	1035.....	393.0	487.1	69.6	23.48	...	...	...
991.....	234.6	473.1	196.8	21.20	0.03	1.18	1.14	1036.....	84.9	487.3	346.2	22.35	-0.23	...	...
992.....	681.2	473.6	260.0	22.14	0.01	1.18	1.17	1037.....	629.6	487.6	213.2	23.56	...	...	...
993.....	262.4	473.7	170.2	21.84	-0.34	...	...	1038.....	811.9	488.0	391.3	23.40	...	...	...
994.....	764.4	473.9	342.2	22.70	...	...	...	1039.....	531.8	488.6	123.4	21.61	0.15	1.50	1.34
995.....	173.7	474.4	256.6	22.74	-0.42	...	...	1040.....	273.1	488.7	165.1	22.61	0.06	...	...
996.....	504.8	474.4	93.0	20.95	1.21	3.88	2.55	1041.....	521.5	488.8	114.8	23.30	...	...	...
997.....	535.9	474.7	120.6	22.78	...	...	...	1042.....	383.9	489.2	76.1	21.69	0.06	...	...
998.....	551.9	474.7	135.4	22.23	...	...	...	1043.....	181.9	489.7	252.1	20.95	-0.47	...	...
999.....	518.5	474.7	105.0	20.77	0.11	1.49	1.38	1044.....	250.7	489.7	186.3	21.05	0.10	1.34	1.23
1000.....	146.4	475.3	283.7	22.76	...	...	...	1045.....	672.3	489.8	254.9	23.66	...	...	...
1001.....	250.5	475.8	182.2	22.60	-0.03	...	...	1046.....	440.5	489.8	65.8	22.00	0.10	...	...
1002.....	713.3	476.3	292.0	22.72	-0.18	...	...	1047.....	582.0	490.2	169.2	23.67	...	...	...
1003.....	194.5	476.5	236.7	23.74	...	...	...	1048.....	402.9	490.6	68.8	23.23	...	...	...
1004.....	359.4	476.7	83.6	23.17	...	...	...	1049.....	261.7	490.9	176.4	22.09	0.17	1.38	1.16
1005.....	705.1	477.8	284.2	22.77	-0.04	1.94	2.15	1050.....	598.1	490.9	184.4	23.47	...	...	...
1006.....	568.0	478.1	151.7	23.19	...	...	...	1051.....	358.7	491.1	93.6	23.24	...	...	...
1007.....	59.7	478.8	369.8	20.83	0.48	1.87	1.27	1052.....	761.6	491.8	342.4	23.15	...	...	...
1008.....	316.8	478.8	121.1	23.11	...	...	...	1053.....	769.0	491.9	349.7	22.96	...	...	...
1009.....	324.5	479.3	114.5	22.93	...	...	...	1054.....	706.7	492.0	288.7	23.07	...	...	...
1010.....	302.5	479.6	134.5	21.51	0.48	2.18	1.63	1055.....	674.1	492.8	257.4	21.85	0.16	1.97	1.88
1011.....	321.4	479.7	117.4	22.60	...	...	...	1056.....	303.3	493.1	139.7	23.04	...	...	...
1012.....	642.9	479.9	223.9	23.14	...	...	...	1057.....	290.6	493.2	151.0	23.28	...	...	...
1013.....	475.6	480.5	74.1	21.16	...	...	...	1058.....	481.0	493.5	87.6	22.89	...	...	...
1014.....	541.4	480.7	128.2	21.53	0.23	...	...	1059.....	369.5	493.6	88.2	22.41	0.09	...	...
1015.....	535.5	480.8	122.9	21.50	0.10	1.20	1.05	1060.....	514.2	493.6	111.6	22.12	0.18	1.30	1.06
1016.....	311.4	481.3	127.1	21.58	0.70	2.43	1.60	1061.....	103.2	494.2	329.7	21.89	-0.17	1.22	1.48
1017.....	264.8	481.8	170.3	22.94	...	...	...	1062.....	219.4	494.2	217.3	22.73	-0.48	...	...
1018.....	39.4	481.8	390.3	22.89	...	...	...	1063.....	336.7	494.4	112.4	17.69	0.69	2.41	1.59
1019.....	697.7	482.5	277.9	20.48	0.24	1.56	1.27	1064.....	507.9	494.6	107.3	21.91	0.11	...	...
1020.....	9.3	482.9	420.3	23.48	...	...	...	1065.....	545.7	495.1	138.7	21.94	...	...	...
1021.....	349.0	483.1	95.8	21.38	0.56	2.34	1.71	1066.....	399.8	495.2	74.2	22.35	...	...	...
1022.....	359.9	483.2	87.4	23.19	...	...	...	1067.....	425.9	495.3	69.6	21.57	...	...	...
1023.....	549.9	483.2	136.9	21.66	...	...	...	1068.....	438.4	495.6	71.1	22.24	...	...	...
1024.....	404.8	483.4	61.4	22.08	...	...	...	1069.....	532.3	495.7	127.6	22.40	0.20	1.33	1.06
1025.....	435.4	483.9	59.0	23.25	...	...	...	1070.....	800.6	495.9	381.5	22.04	0.01	1.71	1.79

TABLE 3—*Continued*

I.D. No.	x (arcsec)	y (arcsec)	r (arcsec)	B (mag)	(U-B) (mag)	(U-R) (mag)	(B-R) (mag)
1071.....	462.8	496.4	79.9	23.17	...	...	...
1072.....	391.1	496.6	78.9	22.18	0.21	...	...
1073.....	577.7	496.7	167.8	22.21	...	...	...
1074.....	17.2	496.8	414.6	22.07	...	...	...
1075.....	491.8	499.2	98.9	23.77	...	...	...
1076.....	275.4	500.0	167.6	23.15	...	...	...
1077.....	379.7	500.1	87.5	23.30	...	...	...
1078.....	83.5	500.3	350.1	23.22	...	...	...
1079.....	308.0	500.3	139.4	21.93	0.04	1.08	1.00
1080.....	366.6	501.9	96.5	22.66	...	...	...
1081.....	317.2	502.5	132.9	21.35	-0.14	...	...
1082.....	643.4	502.8	231.0	23.67	...	...	...
1083.....	557.9	504.2	153.8	23.30	...	...	...
1084.....	498.1	504.4	106.9	22.41	-0.22	...	...
1085.....	223.5	504.8	217.1	21.96	0.06	0.84	0.69
1086.....	636.5	505.1	225.3	20.74	1.09	3.65	2.45
1087.....	238.4	505.4	203.6	22.48	0.24	1.41	1.09
1088.....	509.1	506.1	115.9	23.05	...	...	...
1089.....	523.3	506.4	126.7	21.86	...	...	...
1090.....	158.5	506.5	279.1	23.26	...	...	...
1091.....	444.6	506.7	83.2	21.54	...	...	...
1092.....	105.1	506.9	330.7	23.66	...	...	...
1093.....	700.3	507.4	286.5	20.44	0.40	1.67	1.15
1094.....	687.8	507.4	274.6	23.55	...	...	...
1095.....	684.0	507.4	271.0	23.24	...	...	...
1096.....	625.0	507.7	215.5	23.46	...	...	...
1097.....	387.8	507.8	90.4	23.50	...	...	...
1098.....	414.5	507.9	83.0	22.75	...	...	...
1099.....	588.4	508.1	182.4	23.06	...	...	...
1100.....	450.2	508.1	86.0	22.59	...	...	...
1101.....	486.5	508.2	102.5	21.99	...	...	...
1102.....	269.3	509.2	177.2	23.82	...	...	...
1103.....	528.3	509.2	132.3	21.89	-0.08	0.73	0.78
1104.....	423.3	509.3	83.7	22.18	...	...	...
1105.....	312.4	509.6	140.9	23.08	...	...	...
1106.....	705.0	509.9	291.8	23.18	...	...	...
1107.....	193.9	510.3	246.7	23.41	...	...	...
1108.....	200.6	510.7	240.6	21.38	0.16	1.83	1.71
1109.....	534.7	511.1	138.5	19.50	0.38	1.82	1.36
1110.....	237.4	511.2	206.7	22.13	...	...	...
1111.....	458.1	511.6	91.8	23.25	...	...	...
1112.....	444.3	512.0	88.4	22.02	0.44	2.00	1.48
1113.....	468.9	512.2	96.8	21.61	0.11	...	...
1114.....	480.0	512.5	102.4	22.31	...	...	...
1115.....	394.8	512.7	92.4	22.27	0.18	0.90	0.57
1116.....	499.3	513.3	114.5	21.68	0.38	1.88	1.44
1117.....	811.2	513.3	395.4	22.18	0.29	...	...
1118.....	79.5	513.8	357.2	23.23	...	...	...
1119.....	733.0	513.9	319.8	22.30	0.23	...	...
1120.....	609.2	514.1	203.8	22.15	0.13	1.38	1.21
1121.....	472.1	514.5	100.2	22.62	0.25	...	...
1122.....	21.1	514.7	414.3	23.15	...	...	...
1123.....	415.0	515.0	90.0	23.14	...	...	...
1124.....	633.5	515.0	226.3	21.54	0.15	1.61	1.47
1125.....	385.6	515.0	97.9	23.13	...	...	...
1126.....	31.5	515.4	404.3	23.44	...	...	...
1127.....	520.0	515.9	130.6	22.66	...	...	...
1128.....	24.8	516.6	411.0	22.44	-0.14	...	...
1129.....	542.4	516.6	148.0	23.63	...	...	...
1130.....	391.9	517.1	97.5	23.34	...	...	...
1131.....	350.0	517.7	119.1	21.60	0.15	1.42	1.24
1132.....	613.7	517.7	209.4	23.39	...	...	...
1133.....	12.4	518.1	423.5	22.65	-1.07	...	...
1134.....	440.1	518.1	93.6	21.70	...	...	...
1135.....	453.3	518.4	96.8	22.54	...	...	...
1136.....	31.8	518.4	404.7	23.94	...	...	...
1137.....	43.0	519.0	393.9	21.65	-0.21	1.24	1.57
1138.....	375.1	519.8	106.8	23.47	...	...	...
1139.....	423.7	519.9	94.2	23.45	-0.23	...	...
1140.....	382.3	519.9	103.7	22.46	-0.29	...	...
1141.....	159.2	519.9	282.7	22.78	...	...	...
1142.....	518.8	520.2	132.8	21.67	0.04	1.26	1.22
1143.....	659.7	520.3	252.5	21.76	0.41	2.36	1.97
1144.....	763.0	520.5	350.5	22.27	0.33	...	...
1145.....	360.6	520.5	115.0	23.59	...	...	...
1146.....	511.7	520.7	128.2	23.48	...	...	...
1147.....	474.0	521.5	107.4	21.63	0.19	1.63	1.42
1148.....	533.5	521.5	144.3	22.62	0.06	1.81	1.85
1149.....	341.7	521.7	127.6	23.73	...	...	...
1150.....	652.4	521.8	246.3	22.71	-1.04	...	...
1151.....	100.2	522.1	339.4	21.67	0.36	1.84	1.41
1152.....	460.0	522.3	102.6	23.17	...	...	...
1153.....	496.5	522.4	120.0	23.22	...	...	...
1154.....	229.4	523.2	219.2	22.37	...	...	...
1155.....	561.6	523.3	167.3	21.34	0.59	2.18	1.47
1156.....	191.5	523.6	253.8	22.66	...	...	...
1157.....	422.0	523.8	98.2	20.45	0.20	1.51	1.26
1158.....	403.9	523.9	100.6	21.58	0.14	1.54	1.40
1159.....	707.4	523.9	298.4	22.62	...	...	...
1160.....	611.7	524.2	210.5	22.44	-0.38	...	...

TABLE 3—*Continued*

I.D. No.	x (arcsec)	y (arcsec)	r (arcsec)	B (mag)	(U–B) (mag)	(U–R) (mag)	(B–R) (mag)
1161.....	457.3	524.8	104.1	22.83	...	...	...
1162.....	342.9	525.1	129.4	23.59	...	...	...
1163.....	134.8	525.5	307.5	22.85	...	...	...
1164.....	140.7	525.6	302.0	23.57	...	...	...
1165.....	597.9	525.8	199.3	21.43	0.28	1.08	0.65
1166.....	266.5	525.9	188.1	23.38	...	...	...
1167.....	723.1	526.1	314.0	22.06	-0.10	0.99	1.11
1168.....	43.8	526.2	394.8	23.47	...	...	...
1169.....	312.7	527.3	151.9	17.95	0.92	2.96	1.89
1170.....	10.7	527.4	427.2	23.66	...	...	...
1171.....	603.7	528.5	205.6	22.91	...	...	...
1172.....	418.1	529.1	103.7	22.89	...	...	...
1173.....	361.9	529.2	121.6	21.75	0.68	2.31	1.48
1174.....	479.0	529.5	116.8	23.32	...	...	...
1175.....	506.7	529.9	132.1	22.58	...	...	...
1176.....	348.5	530.0	129.8	22.67	...	...	...
1177.....	685.3	530.5	280.0	23.05	...	...	...
1178.....	520.5	530.8	141.6	22.66	...	...	...
1179.....	407.7	530.8	106.7	22.43	...	...	...
1180.....	775.6	531.1	365.5	21.21	...	...	...
1181.....	756.0	531.5	346.9	22.17	0.16	1.64	1.48
1182.....	334.1	532.0	140.3	22.14	...	...	...
1183.....	511.6	532.5	137.1	23.54	...	...	...
1184.....	738.2	532.5	330.3	23.24	...	...	...
1185.....	70.7	532.7	370.8	22.90	...	...	...
1186.....	592.7	532.7	198.4	22.30	-0.22	...	...
1187.....	397.1	532.7	110.8	22.74	...	...	...
1188.....	426.3	532.8	107.1	22.83	...	...	...
1189.....	444.7	533.0	109.0	23.45	...	...	...
1190.....	204.9	533.7	245.8	23.09	...	...	...
1191.....	277.8	534.4	183.5	21.31	0.17	1.24	0.99
1192.....	84.3	534.5	358.2	23.80	...	...	...
1193.....	351.7	534.6	131.7	22.42	-0.41	0.98	1.56
1194.....	356.7	535.0	129.3	22.50	...	...	...
1195.....	577.8	535.4	187.6	22.19	0.15	1.70	1.58
1196.....	177.9	535.7	271.1	21.23	0.10	1.08	0.91
1197.....	360.9	536.0	127.9	22.09	...	...	...
1198.....	497.8	536.4	132.1	22.12	0.20	1.63	1.40
1199.....	374.5	536.5	122.1	23.46	...	...	...
1200.....	471.2	536.6	119.9	21.12	0.26	1.65	1.35
1201.....	439.2	536.6	111.8	21.56	0.08	1.41	1.34
1202.....	460.3	537.0	116.7	22.96	...	...	...
1203.....	666.4	537.1	265.3	23.26	...	...	...
1204.....	26.8	537.1	414.1	23.12	...	...	...
1205.....	828.4	537.3	418.0	21.27	0.15	1.15	0.91
1206.....	235.0	537.7	221.1	21.48	-0.40	0.36	0.80
1207.....	679.3	538.9	277.8	23.62	...	...	...
1208.....	821.5	539.1	411.8	22.30	0.28	1.69	1.36
1209.....	778.7	539.1	370.8	23.62	0.34	1.69	1.36
1210.....	770.8	539.4	363.4	22.22	-0.11	1.76	2.04
1211.....	224.0	539.6	231.6	23.08	...	...	...
1212.....	458.3	540.0	118.9	22.81	-0.08	...	...
1213.....	278.8	540.3	186.4	23.51	...	...	...
1214.....	493.4	540.4	133.2	22.26	...	...	...
1215.....	23.8	540.5	418.0	23.67	...	...	...
1216.....	165.3	540.9	284.7	19.40	-0.09	0.75	0.80
1217.....	372.4	541.4	127.4	22.12	0.54	2.59	2.04
1218.....	263.3	541.4	199.4	22.80	0.02	1.32	1.32
1219.....	557.1	543.3	176.4	21.96	0.20	1.81	1.62
1220.....	498.7	544.4	139.4	21.59	0.18	1.44	1.22
1221.....	747.6	545.0	343.3	21.34	-0.14	1.19	1.41
1222.....	639.8	545.1	245.2	23.50	...	...	...
1223.....	48.3	545.4	395.9	22.53	...	...	...
1224.....	630.4	545.8	237.4	22.63	...	...	...
1225.....	448.7	546.1	122.6	22.09	...	...	...
1226.....	538.4	546.1	165.0	23.01	...	...	...
1227.....	139.5	546.9	310.8	22.80	-0.24	...	...
1228.....	96.4	546.9	350.8	22.53	-0.11	1.69	1.95
1229.....	534.9	546.9	163.2	23.42	...	...	...
1230.....	590.4	547.1	204.7	23.24	...	...	...
1231.....	324.6	547.5	158.3	23.37	...	...	...
1232.....	397.9	547.6	125.1	21.80	0.14	...	...
1233.....	229.4	547.9	231.2	23.07	...	...	...
1234.....	543.1	548.0	169.6	22.39	0.05	...	...
1235.....	653.5	548.1	258.7	23.56	...	...	...
1236.....	387.7	548.3	128.3	23.35	...	...	...
1237.....	4.0	548.8	439.3	22.86	-0.48	...	...
1238.....	433.7	548.8	123.4	21.87	0.14	1.63	1.50
1239.....	686.7	550.8	289.5	21.76	-0.15	0.83	0.99
1240.....	204.9	551.5	254.1	21.74	0.52	2.07	1.45
1241.....	382.5	551.7	133.2	22.22	0.48	2.17	1.63
1242.....	243.1	551.7	221.9	21.57	0.02	1.33	1.32
1243.....	484.4	552.5	139.8	22.93	...	...	...
1244.....	675.8	553.0	280.7	21.10	0.04	1.36	1.34
1245.....	98.5	553.1	351.1	23.49	...	...	...
1246.....	470.3	554.6	136.4	21.55	0.36	2.24	1.90
1247.....	134.7	554.8	318.3	21.47	0.32	1.74	1.37
1248.....	429.4	554.8	129.2	22.94	...	...	...
1249.....	387.5	555.9	135.7	22.69	...	...	...
1250.....	527.6	556.1	165.6	22.74	...	...	...

TABLE 3—*Continued*

I.D. No.	x (arcsec)	y (arcsec)	r (arcsec)	B (mag)	(U–B) (mag)	(U–R) (mag)	(B–R) (mag)	I.D. No.	x (arcsec)	y (arcsec)	r (arcsec)	B (mag)	(U–B) (mag)	(U–R) (mag)	(B–R) (mag)
1251.....	437.7	556.4	131.3	22.76	...	...	...	1296.....	564.3	576.4	204.8	23.24	...	...	...
1252.....	478.5	556.5	141.1	21.21	0.16	1.44	1.25	1297.....	436.8	576.5	151.2	23.57	...	...	...
1253.....	259.8	556.6	211.3	20.71	0.22	1.74	1.51	1298.....	634.5	576.6	257.7	20.75	0.01	1.24	1.24
1254.....	730.7	556.8	332.0	22.42	0.13	...	...	1299.....	429.2	577.6	152.0	22.78	-0.03	1.94	2.14
1255.....	384.3	557.0	137.7	23.18	...	...	...	1300.....	405.1	578.2	153.9	23.37	...	...	...
1256.....	221.2	557.6	243.3	19.95	0.07	1.39	1.32	1301.....	311.7	578.6	190.8	21.10	0.13	1.60	1.48
1257.....	494.6	558.0	149.2	23.04	...	...	...	1302.....	594.0	579.0	227.7	23.63	...	...	...
1258.....	397.2	558.0	135.4	23.13	...	...	...	1303.....	361.0	579.1	166.6	19.29	0.66	2.38	1.60
1259.....	320.5	558.1	169.1	22.45	0.01	...	...	1304.....	381.0	579.1	159.9	23.40	...	...	...
1260.....	241.0	558.2	227.2	22.96	...	...	...	1305.....	803.3	579.2	407.7	22.82	-0.81	1.35	2.62
1261.....	201.1	559.6	261.4	22.31	0.01	1.23	1.22	1306.....	502.3	579.7	172.1	23.05	...	...	...
1262.....	762.9	559.8	362.9	22.69	...	...	...	1307.....	419.6	580.2	154.7	22.12	...	...	...
1263.....	587.2	560.5	210.4	23.93	...	...	...	1308.....	570.4	581.0	212.3	22.94	...	...	...
1264.....	476.1	560.8	144.3	21.33	1.06	3.38	2.19	1309.....	448.7	581.3	157.4	21.01	0.35	1.83	1.41
1265.....	38.4	561.0	410.2	20.84	0.17	...	...	1310.....	426.5	581.8	156.2	21.33	...	...	...
1266.....	301.4	561.2	183.9	21.66	0.13	1.39	1.23	1311.....	505.6	581.9	175.5	22.62	...	...	...
1267.....	294.4	561.6	189.0	21.96	...	...	...	1312.....	474.4	582.2	164.0	22.77	...	...	...
1268.....	542.0	562.0	179.3	22.33	0.40	...	...	1313.....	688.8	583.1	306.7	22.09	0.02	1.26	1.25
1269.....	233.2	562.9	236.4	22.57	-0.02	1.87	2.03	1314.....	535.3	584.3	192.8	22.60	...	...	...
1270.....	405.5	562.9	138.7	23.37	...	...	...	1315.....	285.0	584.3	212.0	22.98	...	...	...
1271.....	328.2	563.1	168.5	22.55	0.03	1.94	2.04	1316.....	303.5	584.7	200.6	21.62	0.58	2.25	1.57
1272.....	753.7	563.1	355.7	23.52	...	...	...	1317.....	105.7	584.8	357.3	23.01	...	...	...
1273.....	700.3	563.8	307.4	22.89	...	...	...	1318.....	805.7	586.6	412.7	23.31	...	...	...
1274.....	814.2	563.9	412.4	23.50	...	...	...	1319.....	483.6	586.7	171.1	22.38	0.12	1.43	1.30
1275.....	426.8	564.7	139.1	23.10	...	...	...	1320.....	640.6	587.2	268.9	22.52	-0.10	...	...
1276.....	289.8	565.4	194.9	21.73	0.56	1.80	1.07	1321.....	163.6	587.3	307.9	22.50	-0.20	...	...
1277.....	305.6	566.3	184.9	22.62	...	...	...	1322.....	338.6	587.9	184.2	21.61	0.04	0.75	0.60
1278.....	197.3	566.3	268.2	23.46	...	...	...	1323.....	149.2	588.1	320.7	23.52	...	...	...
1279.....	716.5	566.8	323.2	23.14	...	...	...	1324.....	656.0	588.6	282.2	22.76	...	...	...
1280.....	65.9	567.5	386.7	20.33	0.15	1.21	0.99	1325.....	311.9	588.7	198.8	22.50	...	...	...
1281.....	342.7	568.0	164.7	22.76	...	...	...	1326.....	137.1	588.9	331.5	23.45	...	...	...
1282.....	484.1	568.0	153.9	22.89	-0.29	0.94	1.34	1327.....	614.1	588.9	249.3	23.61	...	...	...
1283.....	752.7	568.6	356.9	23.40	...	...	...	1328.....	441.8	590.0	165.2	21.95	0.23	1.84	1.62
1284.....	622.7	569.0	243.7	22.93	...	...	...	1329.....	331.0	590.2	189.8	22.05	...	...	...
1285.....	269.3	569.6	212.5	21.08	0.25	1.52	1.21	1330.....	479.1	590.3	173.1	23.03	...	...	...
1286.....	553.2	570.8	193.2	22.23	0.00	1.27	1.29	1331.....	303.9	590.4	204.9	22.64	-0.31	...	...
1287.....	581.8	571.0	213.3	23.39	...	...	...	1332.....	61.4	590.6	399.9	22.35	...	...	...
1288.....	86.3	571.8	369.5	22.64	-0.47	...	...	1333.....	752.3	590.8	366.0	23.59	...	...	...
1289.....	532.8	571.8	181.3	23.46	-0.38	...	...	1334.....	38.2	590.9	421.2	19.32	0.88	2.71	1.67
1290.....	249.0	572.2	229.5	22.21	0.18	1.47	1.25	1335.....	231.2	590.9	255.2	22.48	...	...	...
1291.....	167.0	573.2	297.8	21.02	0.62	2.37	1.66	1336.....	209.8	591.3	272.1	21.14	0.25	1.65	1.37
1292.....	667.7	573.5	283.6	23.46	...	...	...	1337.....	266.9	591.9	229.8	23.69	...	...	...
1293.....	712.4	574.7	323.2	21.41	0.44	1.87	1.33	1338.....	130.9	592.6	338.8	21.79	-0.31	0.97	1.41
1294.....	546.0	575.4	192.1	20.56	0.42	1.92	1.42	1339.....	744.7	592.8	360.2	23.59	...	...	...
1295.....	437.5	575.4	150.2	23.45	...	...	...	1340.....	794.8	592.8	405.2	21.98	...	...	...

TABLE 3—*Continued*

I.D. No.	x (arcsec)	y (arcsec)	r (arcsec)	B (mag)	(U-B) (mag)	(U-R) (mag)	(B-R) (mag)	I.D. No.	x (arcsec)	y (arcsec)	r (arcsec)	B (mag)	(U-B) (mag)	(U-R) (mag)	(B-R) (mag)
1341.....	523.8	592.9	193.9	21.09	0.82	3.03	2.12	1386.....	355.8	616.5	203.2	21.80	-0.03	1.38	1.46
1342.....	555.8	593.3	212.3	22.19	0.08	1.72	1.70	1387.....	523.2	616.6	214.4	22.78	...	...	...
1343.....	233.7	593.6	255.1	22.14	...	...	...	1388.....	332.7	616.7	212.5	20.92	0.23	1.36	1.04
1344.....	427.2	594.0	168.3	21.03	0.24	1.50	1.19	1389.....	499.0	616.9	204.9	22.56	...	...	...
1345.....	443.6	594.0	169.3	22.90	...	...	...	1390.....	588.1	617.6	251.5	22.39	...	...	...
1346.....	716.6	594.3	336.3	20.24	-0.12	0.44	0.48	1391.....	228.9	618.8	275.7	20.86	0.16	1.53	1.35
1347.....	686.1	594.3	310.3	23.44	...	...	...	1392.....	809.3	619.5	429.8	23.30	...	...	...
1348.....	395.7	595.7	172.7	23.68	...	...	...	1393.....	638.1	620.1	288.0	20.85	1.32	4.06	2.60
1349.....	805.8	596.4	416.7	20.13	0.01	0.97	0.91	1394.....	381.1	620.4	199.8	22.51	...	...	...
1350.....	72.3	596.4	392.5	22.05	...	...	...	1395.....	197.8	620.8	300.0	23.24	...	...	...
1351.....	60.4	597.3	403.6	21.11	0.38	1.56	1.05	1396.....	282.7	621.3	242.3	22.65	...	...	...
1352.....	633.3	597.5	269.5	22.30	0.21	...	...	1397.....	685.1	621.6	325.1	22.60	0.12	...	...
1353.....	226.3	597.6	263.3	21.71	0.02	1.19	1.16	1398.....	534.2	622.1	224.5	20.92	-0.11	1.11	1.27
1354.....	477.5	598.8	180.7	22.57	...	...	...	1399.....	486.7	622.3	206.0	22.71	-0.01	...	...
1355.....	354.2	599.0	187.5	22.93	...	...	...	1400.....	439.6	622.6	197.5	21.64	-0.04	...	...
1356.....	361.5	599.4	185.2	21.14	1.14	3.73	2.48	1401.....	341.8	622.8	214.2	21.16	-0.02	1.15	1.17
1357.....	637.1	599.9	274.0	23.08	...	...	...	1402.....	302.1	622.9	232.7	21.86	0.24	1.71	1.45
1358.....	325.2	601.2	202.3	23.10	...	...	...	1403.....	52.2	623.0	422.3	22.97	...	...	...
1359.....	769.2	601.9	386.1	23.02	...	...	...	1404.....	248.7	623.0	265.1	22.45	...	...	...
1360.....	690.2	602.4	318.2	22.83	...	...	...	1405.....	599.8	623.4	263.5	23.02	...	...	...
1361.....	493.9	602.5	189.5	22.06	-0.13	0.93	1.09	1406.....	326.6	623.4	221.1	22.65	...	...	...
1362.....	546.3	604.4	215.6	22.69	...	...	...	1407.....	579.1	623.6	250.4	23.59	...	...	...
1363.....	542.4	605.4	214.4	22.65	...	...	...	1408.....	422.9	624.8	199.2	22.91	...	...	...
1364.....	84.6	606.3	386.0	22.96	...	...	...	1409.....	668.0	625.8	314.3	21.31	0.27	1.65	1.33
1365.....	251.7	606.4	250.9	23.55	...	...	...	1410.....	408.1	627.9	203.0	22.17	-0.15	...	...
1366.....	656.8	606.7	293.6	23.45	...	...	...	1411.....	170.5	628.0	325.7	22.80	...	...	...
1367.....	584.9	606.8	241.2	21.77	0.15	1.44	1.27	1412.....	736.1	629.5	371.4	22.10	0.36	...	...
1368.....	259.1	606.9	246.1	23.72	...	...	...	1413.....	439.9	630.0	204.8	23.14	...	...	...
1369.....	296.3	607.0	222.7	23.18	...	...	...	1414.....	547.9	630.4	238.5	23.27	...	...	...
1370.....	177.9	607.4	307.3	20.47	0.42	1.88	1.38	1415.....	589.2	630.9	262.5	23.68	...	...	...
1371.....	426.3	607.6	181.9	23.85	...	...	...	1416.....	161.5	631.3	334.8	23.96	...	...	...
1372.....	593.4	608.2	247.9	22.19	-0.71	...	...	1417.....	247.5	631.4	272.2	23.17	...	...	...
1373.....	377.3	608.4	189.0	22.09	0.22	...	...	1418.....	526.8	632.5	230.3	23.36	...	...	...
1374.....	525.6	608.6	208.5	22.24	-0.21	1.24	1.58	1419.....	514.0	633.0	225.4	21.49	0.03	1.58	1.61
1375.....	220.1	608.9	275.4	23.05	...	...	...	1420.....	350.5	634.1	221.6	21.71	0.25	1.80	1.53
1376.....	476.3	609.4	190.6	23.39	...	...	...	1421.....	37.6	635.5	441.1	22.19	0.30	...	...
1377.....	398.0	610.9	187.3	22.68	...	...	...	1422.....	144.6	635.6	350.8	23.01	...	...	...
1378.....	89.9	611.0	383.5	23.39	...	...	...	1423.....	597.1	635.7	271.1	22.74	...	...	...
1379.....	341.4	611.1	203.6	22.92	...	...	...	1424.....	742.0	635.8	379.8	21.91	0.16	1.59	1.43
1380.....	764.9	612.7	387.4	22.50	0.06	...	...	1425.....	480.5	636.7	218.1	22.43	0.11	...	...
1381.....	540.7	613.1	219.9	23.26	...	...	...	1426.....	547.1	636.9	243.7	22.84	...	...	...
1382.....	417.3	613.9	188.4	21.67	-0.04	0.64	0.60	1427.....	216.3	637.8	298.1	19.68	0.22	1.81	1.59
1383.....	584.3	614.3	246.5	23.00	...	...	...	1428.....	731.9	638.3	372.8	22.80	-0.24	...	...
1384.....	253.5	615.0	255.9	21.00	0.32	1.83	1.47	1429.....	537.6	638.4	240.5	22.20	...	...	...
1385.....	552.3	615.3	228.0	22.59	0.32	...	...	1430.....	285.1	640.6	256.8	21.82	-0.01	0.96	0.93

TABLE 3—*Continued*

I.D. No.	x (arcsec)	y (arcsec)	r (arcsec)	B (mag)	(U-B) (mag)	(U-R) (mag)	(B-R) (mag)
1431.....	84.0	640.7	403.7	21.84	-0.19	1.10	1.37
1432.....	735.1	641.1	377.1	23.20	...	...	...
1433.....	119.7	642.1	374.8	20.85	0.33	1.57	1.14
1434.....	618.6	642.3	290.1	22.66	...	...	...
1435.....	327.1	642.9	238.6	23.68	...	...	...
1436.....	49.0	643.3	435.0	23.08	...	...	...
1437.....	768.8	643.4	406.4	22.74	...	...	...
1438.....	262.8	643.8	272.2	23.74	...	...	...
1439.....	510.4	644.9	235.1	23.40	...	...	...
1440.....	126.7	645.1	370.8	21.39	-0.01	1.47	1.54
1441.....	371.8	645.9	226.7	23.11	...	...	...
1442.....	99.7	647.6	394.4	23.09	...	...	...
1443.....	647.4	647.8	313.8	23.67	0.56	1.95	1.38
1444.....	221.8	647.8	301.5	21.97	0.46	1.95	1.40
1445.....	699.3	648.1	352.6	22.90	...	...	...
1446.....	73.5	649.7	417.4	22.92	-0.56	...	...
1447.....	214.6	649.9	307.9	22.84	...	...	...
1448.....	232.1	650.2	296.5	22.89	...	...	...
1449.....	387.3	650.4	228.0	21.81	-0.06	1.31	1.42
1450.....	815.1	650.5	449.7	19.49	0.26	1.48	1.14
1451.....	710.1	650.5	362.6	23.00	...	...	...
1452.....	457.2	650.8	227.4	22.69	-0.94	...	...
1453.....	277.4	650.8	269.6	23.59	...	...	...
1454.....	624.0	651.4	300.5	23.32	...	...	...
1455.....	773.0	651.5	414.3	22.10	-1.12	...	...
1456.....	819.4	651.8	454.1	23.47	...	...	...
1457.....	675.1	652.7	337.4	22.08	0.17	1.62	1.45
1458.....	306.6	653.5	257.1	22.47	...	...	...
1459.....	583.6	653.6	277.3	22.08	0.15	1.93	1.84
1460.....	290.5	653.8	265.2	23.29	...	...	...
1461.....	640.1	654.2	313.4	21.93	-0.03	1.24	1.30
1462.....	349.9	655.4	241.9	22.01	0.10	1.34	1.23
1463.....	83.6	655.5	412.1	21.68	-0.15	0.61	0.73
1464.....	337.1	655.6	246.5	22.37	0.00	...	...
1465.....	123.9	656.1	379.7	22.75	...	...	...
1466.....	615.6	656.4	298.9	22.30	-0.58	...	...
1467.....	369.6	657.5	238.5	22.45	0.03	1.35	1.35
1468.....	560.3	657.6	268.3	22.03	0.22	1.82	1.61
1469.....	721.7	658.1	376.4	22.19	...	...	...
1470.....	411.1	658.8	233.6	23.12	...	...	...
1471.....	548.7	659.1	263.9	22.85	...	...	...
1472.....	99.0	659.3	401.6	21.47	-0.08	0.82	0.88
1473.....	693.6	661.3	356.8	23.05	...	...	...
1474.....	592.3	661.8	289.0	22.44	-0.05	...	...
1475.....	498.3	662.7	247.9	23.50	...	...	...
1476.....	735.6	666.3	392.4	23.01	...	...	...
1477.....	599.0	667.5	297.5	21.21	-0.25	0.88	1.20
1478.....	388.2	668.2	245.4	23.03	...	...	...
1479.....	746.4	668.4	402.2	20.84	0.09	1.33	1.22
1480.....	717.8	670.0	380.8	23.04	...	...	...
1481.....	455.1	670.4	246.6	21.82	0.22	1.85	1.64
1482.....	338.8	672.4	261.6	22.55	...	...	...
1483.....	40.3	673.1	458.0	22.32	-0.01	...	...
1484.....	619.0	673.4	314.3	23.54	...	...	...
1485.....	264.4	673.8	296.0	23.52	...	...	...
1486.....	548.5	674.0	277.1	23.36	...	...	...
1487.....	742.1	674.7	402.7	21.62	0.09	1.31	1.19
1488.....	297.8	674.8	280.0	22.49	-0.55	0.97	1.78
1489.....	225.8	675.2	319.7	22.21	...	...	...
1490.....	638.5	675.6	328.3	22.10	...	...	...
1491.....	480.2	676.5	256.7	23.23	...	...	...
1492.....	508.7	676.6	264.3	23.13	...	...	...
1493.....	749.4	676.9	409.8	22.40	...	...	...
1494.....	218.2	677.3	326.1	23.41	...	...	...
1495.....	170.6	677.7	358.6	22.17	0.05	...	...
1496.....	707.7	677.9	378.4	23.24	...	...	...
1497.....	23.1	678.7	475.5	20.55	-0.16	0.65	0.79
1498.....	41.5	679.2	460.2	22.45	...	...	...
1499.....	325.3	679.4	272.9	21.02	...	...	...
1500.....	523.6	680.1	272.6	22.81	-0.24	...	...
1501.....	620.8	680.7	321.2	23.28	...	...	...
1502.....	409.0	681.0	255.9	20.96	0.28	1.70	1.38
1503.....	423.3	681.0	255.4	22.51	-0.06	...	...
1504.....	583.9	683.6	302.7	20.70	0.08	1.31	1.22
1505.....	503.6	684.2	270.0	23.04	...	...	...
1506.....	320.1	685.3	280.3	20.04	-0.03	0.89	0.88
1507.....	715.3	685.7	389.2	22.74	-0.55	...	...
1508.....	546.4	686.3	287.3	22.66	...	...	...
1509.....	483.1	686.3	266.9	23.47	...	...	...
1510.....	86.0	686.9	428.5	22.98	...	...	...
1511.....	535.3	687.4	283.8	20.78	0.03	1.02	0.95
1512.....	260.9	687.6	309.5	21.73	0.08	0.97	0.81
1513.....	678.5	688.2	364.5	22.33	...	...	...
1514.....	387.1	688.3	265.5	20.94	0.45	2.09	1.58
1515.....	283.3	688.4	298.9	23.28	...	...	...
1516.....	663.9	688.5	354.8	23.72	...	...	...
1517.....	300.2	688.8	291.6	23.38	...	...	...
1518.....	4.6	689.3	496.7	23.21	...	...	...
1519.....	409.2	689.6	264.4	23.48	...	...	...
1520.....	832.2	690.1	485.0	23.45	...	...	...

TABLE 3—*Continued*

I.D. No.	x (arcsec)	y (arcsec)	r (arcsec)	B (mag)	(U-B) (mag)	(U-R) (mag)	(B-R) (mag)	I.D. No.	x (arcsec)	y (arcsec)	r (arcsec)	B (mag)	(U-B) (mag)	(U-R) (mag)	(B-R) (mag)
1521.....	233.2	692.1	328.7	22.50	-0.68	...	...	1566.....	253.7	719.0	340.0	21.46	...	...	...
1522.....	451.2	692.1	267.6	22.39	-0.01	1.22	1.25	1567.....	200.7	719.7	370.2	23.42	...	...	...
1523.....	535.9	693.0	289.2	22.86	...	...	...	1568.....	746.4	723.2	437.5	21.93	-0.03	1.09	1.13
1524.....	611.1	693.4	325.7	21.11	-0.44	0.16	0.64	1569.....	479.1	723.2	302.3	22.26	0.12	...	...
1525.....	511.2	693.6	281.3	23.32	...	...	...	1570.....	588.1	723.4	339.2	22.89	...	...	...
1526.....	542.8	694.4	293.2	23.34	...	...	...	1571.....	570.6	723.9	331.6	23.27	...	...	...
1527.....	658.5	694.6	355.8	22.47	-0.24	1.30	1.69	1572.....	246.7	724.3	348.2	22.03	0.05	1.23	1.17
1528.....	581.5	694.7	310.9	23.30	...	...	...	1573.....	113.1	724.6	432.5	23.37	...	...	...
1529.....	621.3	694.9	332.8	22.48	...	...	...	1574.....	832.2	726.2	505.6	23.78	...	...	...
1530.....	676.5	695.2	368.2	21.80	-0.10	0.95	1.07	1575.....	500.2	726.3	309.8	21.50	0.20	1.35	1.08
1531.....	108.1	695.4	416.7	21.50	-0.15	0.40	0.47	1576.....	68.5	726.4	466.9	23.69	...	...	...
1532.....	145.3	696.8	390.1	20.86	0.04	1.09	1.01	1577.....	364.0	727.6	308.1	21.85	0.03	...	...
1533.....	721.5	697.0	401.5	22.45	...	...	...	1578.....	135.8	730.2	420.4	23.44	...	...	...
1534.....	718.2	699.4	400.6	23.48	...	...	...	1579.....	692.2	730.7	405.1	22.76	-0.40	...	...
1535.....	626.2	700.0	339.8	18.32	1.08	3.21	1.95	1580.....	795.0	731.8	479.7	21.80	0.50	1.72	1.05
1536.....	804.6	700.7	468.2	23.51	...	...	...	1581.....	676.8	731.9	396.1	22.56	0.31	...	...
1537.....	224.2	701.0	341.2	23.29	...	...	...	1582.....	731.3	732.1	432.8	23.65	...	...	...
1538.....	397.9	701.3	277.1	20.54	0.35	1.70	1.26	1583.....	188.1	733.0	388.5	23.31	...	...	...
1539.....	766.9	702.8	439.6	22.05	-0.61	0.65	1.48	1584.....	516.6	734.3	321.8	20.54	0.39	1.72	1.22
1540.....	698.4	703.1	389.0	21.46	0.34	1.99	1.61	1585.....	461.7	734.4	310.8	22.28	0.03	1.61	1.65
1541.....	609.5	703.7	333.3	22.67	...	...	...	1586.....	30.7	734.9	501.6	23.20	...	...	...
1542.....	758.6	703.7	433.8	21.94	0.13	1.10	0.89	1587.....	495.5	735.3	317.4	22.62	-1.33	...	...
1543.....	144.1	704.4	396.2	20.07	0.22	1.43	1.14	1588.....	715.2	735.7	424.2	22.83	-0.47	...	...
1544.....	500.7	705.1	289.3	23.47	...	...	...	1589.....	661.5	736.0	389.8	23.06	...	...	...
1545.....	278.4	705.3	316.0	22.79	0.03	...	...	1590.....	166.5	736.2	404.4	23.32	...	...	...
1546.....	497.2	706.1	289.5	22.64	...	...	...	1591.....	95.5	738.2	454.6	22.33	-0.62	1.26	2.22
1547.....	767.3	707.0	442.6	23.36	...	...	...	1592.....	89.6	738.3	459.0	23.61	...	...	...
1548.....	107.6	707.7	425.1	20.92	0.29	1.60	1.24	1593.....	412.2	738.7	313.4	23.54	...	...	...
1549.....	515.1	708.8	296.9	20.45	1.19	3.82	2.50	1594.....	423.7	740.5	314.9	21.98	0.21	1.60	1.37
1550.....	520.6	709.0	298.8	22.49	...	...	...	1595.....	563.1	742.0	344.9	22.88	...	...	...
1551.....	371.7	709.3	288.8	20.16	1.14	3.67	2.41	1596.....	772.1	742.6	469.6	21.64	0.26	1.62	1.30
1552.....	504.6	709.5	294.6	22.65	...	...	...	1597.....	577.6	742.7	351.6	23.26	...	...	...
1553.....	708.4	710.3	401.2	22.67	...	...	...	1598.....	716.4	743.2	430.6	22.75	...	...	...
1554.....	384.3	710.5	287.8	22.22	...	...	...	1599.....	630.7	744.6	379.2	22.48	...	...	...
1555.....	72.3	710.6	453.9	23.27	...	...	...	1600.....	124.2	744.6	438.9	22.54	...	...	...
1556.....	510.2	710.8	297.4	22.38	0.25	...	...	1601.....	787.3	745.9	483.0	23.09	...	...	...
1557.....	114.9	711.4	422.1	23.15	...	...	...	1602.....	66.3	748.0	482.7	22.42	0.42	3.13	2.86
1558.....	298.0	712.3	313.8	22.60	0.28	...	...	1603.....	354.1	748.1	330.3	22.88	...	...	...
1559.....	486.4	714.0	294.7	22.93	...	...	...	1604.....	324.0	748.5	338.5	23.46	...	...	...
1560.....	204.0	714.5	364.1	21.59	0.20	1.48	1.23	1605.....	395.7	748.7	324.4	22.53	...	...	...
1561.....	697.7	716.1	397.9	18.78	0.06	1.02	0.90	1606.....	270.1	748.9	358.7	22.78	...	...	...
1562.....	139.5	716.1	407.8	23.29	...	...	...	1607.....	719.2	750.6	437.9	23.40	...	...	...
1563.....	639.8	716.3	361.1	21.68	0.22	1.16	0.82	1608.....	568.4	751.3	355.6	20.33	1.09	3.57	2.37
1564.....	50.8	716.6	474.6	22.60	...	...	...	1609.....	500.4	751.4	334.3	23.25	...	...	...
1565.....	470.5	717.8	295.6	21.78	0.18	1.51	1.29	1610.....	612.1	752.6	376.4	20.24	1.08	3.45	2.23

TABLE 3—*Continued*

I.D. No.	x (arcsec)	y (arcsec)	r (arcsec)	B (mag)	(U-B) (mag)	(U-R) (mag)	(B-R) (mag)	I.D. No	x (arcsec)	y (arcsec)	r (arcsec)	B (mag)	(U-B) (mag)	(U-R) (mag)	(B-R) (mag)
1611.....	580.8	752.7	362.0	22.48	...	...	...	1656.....	455.1	783.2	358.7	19.33	1.20	3.80	2.47
1612.....	32.3	753.0	511.8	23.46	...	...	...	1657.....	700.5	783.7	451.4	21.95	0.05	1.32	1.27
1613.....	246.6	753.4	373.5	22.70	...	...	...	1658.....	279.6	784.3	387.2	21.53	0.64	2.64	1.93
1614.....	292.7	753.6	353.9	23.52	...	...	...	1659.....	371.9	784.7	363.0	22.91	...	...	...
1615.....	535.9	754.7	347.0	20.68	0.18	1.68	1.51	1660.....	7.7	784.8	551.0	23.00	...	...	...
1616.....	628.7	754.7	386.7	22.23	0.17	...	...	1661.....	461.7	785.5	361.6	23.43	...	...	...
1617.....	434.5	755.1	329.5	20.32	0.22	1.39	1.10	1662.....	290.5	785.8	384.7	23.64	...	...	...
1618.....	337.8	755.6	341.4	22.71	...	...	...	1663.....	721.5	786.2	466.4	23.41	...	...	...
1619.....	357.3	755.7	337.1	23.06	...	...	...	1664.....	520.0	786.3	372.8	20.78	0.32	1.73	1.35
1620.....	457.0	757.8	333.6	22.38	-0.10	0.74	0.81	1665.....	662.1	786.5	431.4	23.04	...	...	...
1621.....	295.0	757.8	356.9	21.57	-0.34	0.88	1.34	1666.....	496.1	787.3	368.5	22.21	0.05	...	...
1622.....	267.3	758.1	368.3	22.06	-0.14	1.72	2.04	1667.....	531.1	789.4	378.7	22.42	0.21	1.36	1.08
1623.....	483.6	759.5	338.8	23.28	...	...	...	1668.....	153.4	792.1	456.5	21.11	1.22	3.71	2.33
1624.....	56.8	760.1	497.9	22.07	-0.26	...	...	1669.....	674.1	792.4	442.9	23.23	...	...	...
1625.....	358.8	760.1	341.1	22.97	...	...	...	1670.....	636.3	794.0	424.3	22.31	-1.25	...	...
1626.....	552.2	760.7	358.2	22.81	-0.15	...	...	1671.....	621.0	794.1	417.1	21.91	0.16	1.64	1.49
1627.....	533.0	762.5	353.5	22.84	...	...	...	1672.....	677.3	794.5	446.5	22.35	-0.06	1.30	1.41
1628.....	135.7	763.0	444.9	21.85	-0.31	1.35	1.86	1673.....	348.1	794.5	376.9	21.39	-0.28	1.58	2.08
1629.....	268.4	764.2	373.3	20.80	0.14	1.49	1.34	1674.....	116.4	796.8	483.1	22.38	...	...	...
1630.....	127.3	767.1	453.4	22.43	-0.25	...	...	1675.....	818.7	797.2	540.8	23.09	...	...	...
1631.....	604.7	767.8	386.1	20.92	0.14	1.24	1.03	1676.....	603.7	797.8	412.6	21.73	0.03	1.23	1.20
1632.....	495.5	768.2	349.6	22.13	-0.07	1.25	1.37	1677.....	30.5	798.1	543.0	23.90	...	...	...
1633.....	295.5	768.2	366.5	23.55	...	...	...	1678.....	465.5	799.5	376.0	21.95	0.59	...	...
1634.....	479.1	769.2	347.7	21.73	0.39	1.91	1.46	1679.....	640.5	799.9	431.6	21.71	-0.78	...	...
1635.....	631.5	769.3	400.6	23.52	...	...	...	1680.....	734.2	801.8	486.5	22.65	-0.25	...	...
1636.....	240.9	769.3	390.1	22.34	-0.42	...	...	1681.....	701.5	802.3	466.9	22.71	...	...	...
1637.....	562.9	769.4	370.2	22.82	-1.01	...	...	1682.....	812.4	802.6	540.1	22.12	-0.71	-0.02	0.84
1638.....	85.7	770.3	484.0	23.25	...	...	...	1683.....	607.3	802.9	418.7	22.93	...	...	...
1639.....	302.6	770.6	366.2	21.35	0.44	1.92	1.40	1684.....	662.4	803.5	445.9	23.29	...	...	...
1640.....	537.1	771.1	363.0	22.65	-0.28	...	...	1685.....	311.0	803.5	394.9	23.67	...	...	...
1641.....	523.9	771.3	359.4	23.36	...	...	...	1686.....	152.7	803.8	466.4	23.56	...	...	...
1642.....	431.7	772.3	346.7	22.81	-0.19	1.38	1.72	1687.....	274.2	803.8	407.3	22.40	-0.47	...	...
1643.....	69.6	772.9	497.4	22.50	0.12	...	...	1688.....	43.5	804.2	538.0	23.88	...	...	...
1644.....	594.3	773.8	386.8	22.76	...	...	...	1689.....	41.6	807.0	541.2	23.73	...	...	...
1645.....	605.0	774.3	392.1	21.99	0.12	1.29	1.12	1690.....	284.3	807.0	406.7	21.60	-0.08	0.73	0.76
1646.....	812.4	778.2	523.3	21.98	-0.23	1.15	1.50	1691.....	408.2	807.1	381.8	22.68	-1.26	...	...
1647.....	163.4	778.7	439.8	22.22	...	...	...	1692.....	6.7	807.6	567.0	22.99	...	...	...
1648.....	181.8	778.9	429.2	23.36	...	...	...	1693.....	455.1	809.3	384.7	22.83	...	...	...
1649.....	302.3	781.1	376.3	22.30	-1.08	...	...	1694.....	211.3	809.3	439.4	23.85	...	...	...
1650.....	88.6	781.3	490.0	23.48	...	...	...	1695.....	674.0	809.5	457.2	20.85	0.45	2.01	1.49
1651.....	319.5	781.4	371.2	22.01	-0.41	1.17	1.79	1696.....	265.9	809.6	415.8	22.83	-1.11	...	...
1652.....	402.2	781.8	356.9	22.98	...	...	...	1697.....	712.0	810.0	479.3	23.26	...	...	...
1653.....	488.3	782.2	362.0	23.49	...	...	...	1698.....	403.6	810.2	385.1	23.42	...	...	...
1654.....	694.8	782.8	447.3	22.97	...	...	...	1699.....	665.6	811.8	454.7	21.78	0.86	3.20	2.27
1655.....	791.3	782.9	511.2	21.90	0.25	1.94	1.71	1700.....	321.7	813.3	401.3	22.80	...	...	...

TABLE 3—*Continued*

I.D. No.	x (arcsec)	y (arcsec)	r (arcsec)	B (mag)	(U-B) (mag)	(U-R) (mag)	(B-R) (mag)	I.D. No.	x (arcsec)	y (arcsec)	r (arcsec)	B (mag)	(U-B) (mag)	(U-R) (mag)	(B-R) (mag)
1701.....	393.2	813.9	389.6	22.16	0.32	1.79	1.42	1715.....	329.2	826.6	412.4	22.49	-0.43	0.83	1.43
1702.....	531.0	814.5	402.9	22.77	-0.42	1.54	2.24	1716.....	488.8	827.7	407.0	22.16	...	...	...
1703.....	410.1	814.7	389.4	23.20	...	...	...	1717.....	829.2	828.2	570.0	23.34	...	...	...
1704.....	73.0	815.8	525.9	19.94	0.92	2.93	1.86	1718.....	467.6	828.7	405.2	20.35	0.40	1.81	1.32
1705.....	718.0	821.7	492.3	21.53	0.04	1.23	1.18	1719.....	496.7	829.5	410.1	23.10	...	...	...
1706.....	566.9	821.7	420.5	23.31	...	...	...	1720.....	400.0	829.7	404.8	22.05	-0.56	...	...
1707.....	498.0	822.7	403.6	23.09	...	...	...	1721.....	503.4	830.4	412.2	23.50	...	...	...
1708.....	10.5	823.7	575.2	19.69	-0.10	0.44	0.46	1722.....	428.1	830.5	404.8	23.80	...	...	...
1709.....	578.9	823.7	426.6	21.87	0.12	1.59	1.49	1723.....	88.8	830.5	526.7	22.35	...	...	...
1710.....	42.3	824.4	553.2	21.66	...	...	...	1724.....	378.3	830.7	407.8	22.40	...	...	...
1711.....	609.0	824.6	439.0	22.81	-0.19	...	...	1725.....	169.7	830.8	479.3	22.22	...	...	...
1712.....	779.7	825.4	534.0	23.58	...	...	...	1726.....	338.4	830.9	414.6	23.35	...	...	...
1713.....	700.2	825.8	485.3	23.29	...	...	...	1727.....	112.4	831.9	513.0	23.02	...	...	...
1714.....	646.9	826.5	457.9	21.50	0.35	2.10	1.74	1728.....	451.5	831.9	407.1	23.24	...	...	...

TABLE 4

POSITIONS, INSTRUMENTAL AND STANDARD MAGNITUDES FOR CALIBRATION STARS

Hanes No.	I.D. No.	x (arcsec)	y (arcsec)	u(MPF 2049) (mag)	b(MPF 2046) (mag)	r(MPF 1901) (mag)	Hanes Magnitudes U	B	R
I-40.....	348	396.5	222.2	16.76	15.82	16.28	20.51	20.30	18.83
I-50.....	444	329.1	267.3	16.68	16.25	16.79	21.01	21.23	19.03
I-76.....	588	280.8	321.1	17.51	16.59	17.18	21.25	21.21	19.70
I-84.....	663	254.3	348.6	15.89	15.25	15.84	19.72	19.65	18.55
I-98.....	809	182.7	400.1	17.64	16.70	17.32	21.35	21.29	19.72
I-130.....		214.7	251.9	17.71	16.90	17.56	21.50	21.46	20.26
II-40.....	1398	341.8	622.8	17.40	16.65	17.23	21.33	21.29	20.12
II-41.....	1385	332.7	616.7	17.50	16.47	17.15	21.12	21.06	19.78
II-93.....	1214	165.3	540.9	15.53	15.07	15.82	19.45	19.42	18.38
II-106....	1334	209.8	591.3	17.66	16.64	17.08	21.39	21.30	19.93
II-111....	1388	228.9	618.8	17.32	16.38	16.81	21.02	20.94	19.62
II-128....	1541	371.7	709.3	17.85	15.78	15.22	21.50	20.38	17.81
II-134....	1535	397.9	701.3	17.28	16.09	16.57	21.07	20.64	19.09
II-179....	1540	144.1	704.4	16.61	15.67	16.20	20.46	20.10	18.43
II-180....	1529	145.3	696.8	17.26	16.38	17.09	21.19	20.89	19.87
II-183....	1437	126.7	645.1	17.83	16.86	17.16	21.44	21.81	---
II-184....	1430	119.7	642.1	17.56	16.38	16.99	21.03	20.89	19.64
II-189....	1278	65.9	567.5	16.77	15.92	16.60	20.63	20.56	19.39
II-196....	1263	37.8	561.3	17.27	16.36	17.02	20.94	21.07	19.80
III-45....	908	590.9	444.8	17.66	16.72	17.53	21.25	21.34	20.17
III-46....	882	604.6	433.6	17.72	16.94	17.35	21.40	21.50	20.16
III-70....	1153	561.6	523.3	18.30	16.81	17.19	21.64	21.44	19.86
III-72....	1217	557.1	543.3	18.37	17.44	17.70	22.19	21.76	20.54
III-97....	1307	448.7	581.3	17.65	16.53	16.92	21.33	21.18	19.71
III-119...	1572	500.2	726.3	18.11	17.01	17.67	21.23	21.46	20.21
III-122...	1581	516.6	734.3	17.28	16.12	16.61	20.75	20.56	19.09
III-137...	1501	583.9	683.6	17.00	16.25	16.77	20.88	20.79	19.52
III-226...		586.3	798.0	18.06	17.19	17.82	21.85	21.78	20.51
III-239...	1653	455.1	783.2	17.16	15.02	---	20.62	19.65	---
IV-67.....	547	556.6	306.2	16.29	---	---	20.11	---	---
IV-90.....	804	586.2	397.8	16.77	15.66	16.07	20.47	20.15	18.33
IV-93.....	797	601.2	395.6	17.68	16.71	17.18	21.64	21.56	20.52
IV-116....	321	617.4	206.1	17.21	16.47	17.19	21.01	21.01	19.91
IV-133....	151	513.3	113.7	15.67	15.27	16.11	19.59	19.58	18.91

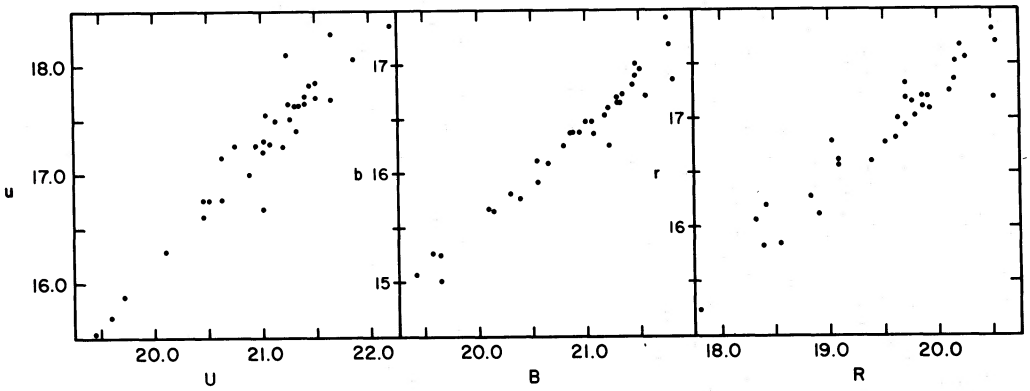

FIG. 4.—A comparison of our instrumental magnitudes and the standard magnitudes of Hanes.

TABLE 5

ESTIMATED MEAN ERRORS IN TRANSFORMATION

σ_B (mag)	σ_{U-B} (mag)	σ_{U-R} (mag)	σ_{B-R} (mag)
0.02	0.03	0.04	0.04

main-sequence and giant branch color-color relations derived by Johnson (1966). In this comparison, we selected only those stellar objects with $B<20.5$ mag. If the distance modulus to M87 is $(m-M)=31.5$ ($d=20$ Mpc), we should, by restricting our sample to this magnitude range, include very few M87 clusters, since globular clusters with $M_B<-10$ are likely to be rare or absent. Note first that the *shapes* of the observed and standard color-color relations are virtually identical, suggesting the absence of any significant color terms that might have been overlooked. Second, the Johnson relations were shifted by $\Delta(U-B)=-0.10$ mag and $\Delta(B-R)=\Delta(U-R)=-0.20$ mag in order to effect the illustrated match. Hence, we must make our observed $(U-B)$, $(U-R)$, and $(B-R)$ values redder by these amounts. We suspect that the required $(U-R)$ and $(B-R)$ shifts result in part from adopting $(U-R)$ and $(B-R)$ colors appropriate to main-sequence stars in

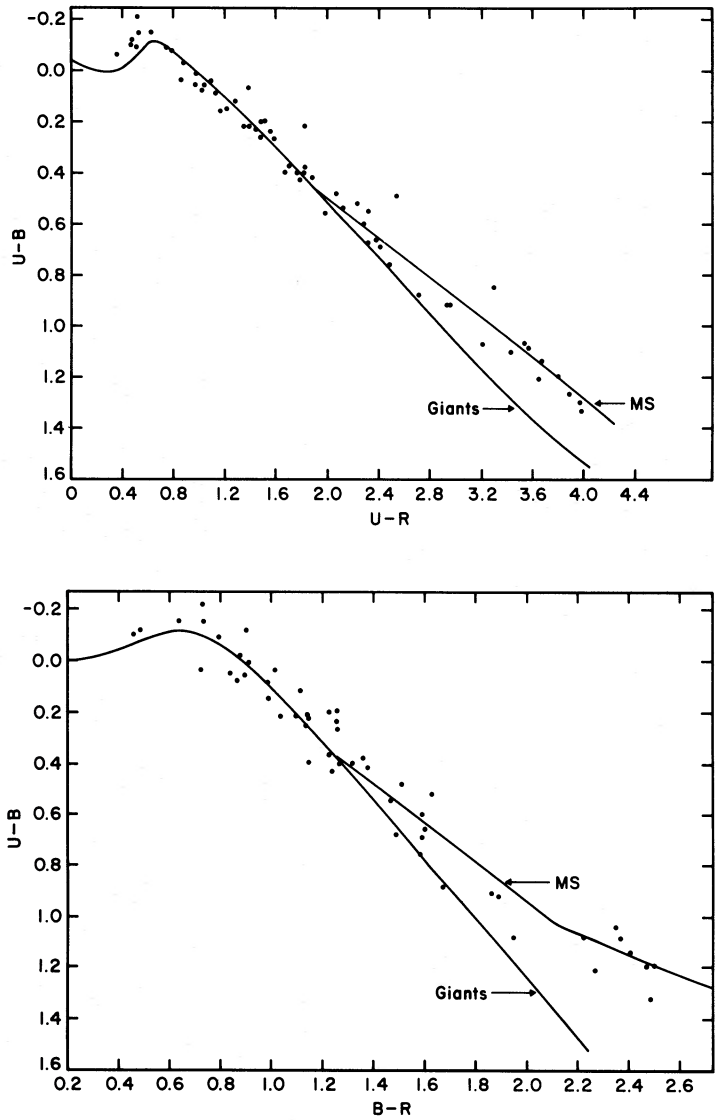

FIG. 5.—*Bottom*: A plot of our observed $(U-B)$, $(B-R)$ relations for objects with $B<20.5$ mag. Superposed on this plot are the Johnson (1966) color-color relations for main-sequence and giant branch stars. Note that the Johnson sequence has been shifted blueward by 0.10 mag in $(U-B)$ and by 0.20 mag in $(B-R)$. *Top*: Same as bottom, except for $(U-B)$ and $(U-R)$. Note that the Johnson sequences have been shifted blueward by 0.10 mag in $(U-B)$ and by 0.20 mag in $(U-R)$.

predicting the R magnitudes for the Hanes standards. In fact, most of the Hanes standards used to effect our R predictions may be M87 globular clusters rather than main-sequence stars. Examination of the colors of galactic globular clusters suggests that they lie redder than the Johnson main sequence by $\sim$0.20 mag in the $(U-B),(B-R)$ and $(U-B),(B-R)$ planes, thereby accounting for the zero-point shift. We also note that Hanes (1971) suspected a possible zero-point error of 0.20 mag in $(U-B)$ in the same direction as deduced here.

We cannot, without additional observations, provide a better estimate of the color zero points, and have chosen to publish magnitudes and colors based on the Hanes standards. Reobservation of the Hanes standards along with the magnitudes reproduced here (Table 4) should permit future observers to place our magnitudes on a more secure absolute system. However, we believe that our additional checks suggest zero-point uncertainties of no more than 0.10 mag in $(U-B)$ and 0.20 mag in $(U-R)$ and $(B-R)$.

Note that for $r<1'.4$ no clusters are included. The galaxy background and crowding problems in this region are too severe to permit accurate photometric measurements. Analysis of the cluster population in this inner region must await application of linear detectors located at foci of large telescopes at which large plate scales can be achieved.

c) *Error Analysis*

1. From a comparison of the two B plates, we were able to derive an estimate of the standard error per single measurement $\sigma(B)$ as a function of B magnitude. In Figure 6 we plot the instrumental blue magnitudes obtained from plate MPF 2046 against those derived from plate CPF 635, and in Table 6 we list $\sigma(B)$ as a function of B at 1.0 mag intervals.

2. A similar comparison for the two U plates, MPF 1905 and MPF 2049, is illustrated in Figure 7; the resulting values of $\sigma(U)$ are given in Table 6.

3. Unfortunately, we were unable to effect a similar direct comparison for R, since only one plate was available.[5] However, from the U and B plate pairs, we noted that a good estimate of σ was given by $\sigma(\text{sky})/2.7$. Here $\sigma^2(\text{sky})$ is the variance of the intensities measured within the sky annulus. The corresponding $\sigma(R)$ values are listed in Table 6.

4. We list in Table 7 the estimated standard errors in color, $\sigma(U-R)$, $\sigma(U-B)$, and $\sigma(B-R)$ as a function of B magnitudes.

[5]Subsequent to the completion of this paper, we were fortunate to obtain from Dr. T. D. Kinman an additional R plate (127-04 emulsion plus RG-610 filter) of M87. Comparison of the instrumental magnitudes derived from Dr. Kinman's plate and our own enabled us to confirm the integrity of the R-magnitude scale. The results of the comparison are similar to those obtained for the U and B material.

5. Because the contribution of the background light of the galaxy and the crowding of cluster images both vary with galactocentric distance r, we also computed errors as a function of r. In Table 8 we list the error estimates for the indicated ranges in r.

6. We finally examined the errors as a function of the skew parameter defined in § III*a*. There was no evidence of a significant increase in the measured σ values as a function of skew. We therefore conclude that the mode estimator has been fairly successful in predicting sky values.

d) *"Background" Corrections*

Not all images included in the master list are true members of the M87 globular cluster system; some are faint stars in the halo of our Galaxy, and some are very distant galaxies, so small and faint as to appear stellar. In order to estimate this field contamination, we sampled two fields (1000 pixels square) located in the "corners" of our 4 m plates (see Fig. 8, Plate 6). The mean galactocentric distance of these fields is 18'.7. We selected images from these fields by using the procedures outlined in § III*a* and reduced them, using the prescription described above.

From these measurements, we derived the number of stars as a function of magnitude and color. A crude check on the background counts was effected by comparing the run with radius of cluster surface density to the R band surface brightness counts. If the two relations are normalized at $r=2'.5$, we note that at $r=18'.7$ we expect that clusters will contribute at a level less than 10% of the background counts. The resulting background counts and colors are listed in Table 9.

e) *Completeness of the Survey*

In Figure 9 we plot for five radial zones the frequency distribution of the images identified from (a) the B plate match and (b) the subset of objects (crosshatched area) that could be measured in all three colors: U, B, and R. From this figure, we deduce that for $B<22.5$ the color sample is about 65% complete. We should note that the decrease in the number of matches between the U and B pair for $B>22.0$ results from the higher ratio of sky to object in the U band compared with the B band. For the B, R pair, the decrease in the number of matches for faint clusters results primarily from the decreased signal-to-noise ratio of the 098-04 as compared with the IIIa-J emulsion. Were a 127 emulsion used, the R band sensitivity would have been improved.

Another test of the completeness of our blue list comes from the visual inspection of the plates. This shows that about 8% of the images that can be seen on both plates were not detected by the finding routine. Some of these images have a complex structure and their centroids are poorly defined. On the other hand, the

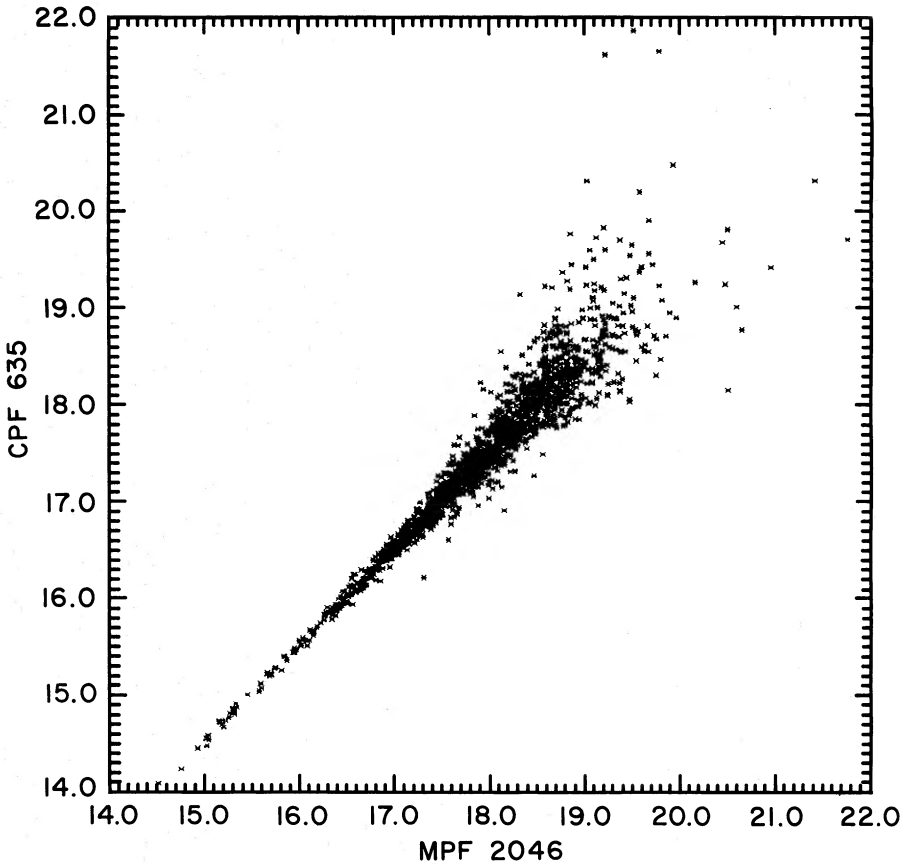

FIG. 6.—A plot of the instrumental magnitudes derived from two B plates (MPF 2046 and CPF 635). For the transformation coefficients from instrumental magnitudes to the B system, refer to the text.

analysis of the images that did not match shows a fairly uniform distribution and no concentration toward the galaxy center. This means that the efficiency of our finding routines is independent of the position on the plate.

In Figure 10 we plot our data for the surface density of clusters brighter than $B=22.5$ as a function of radius. Superposed on this plot are the comparable results of Hanes (1977*a*). The almost exact agreement suggests that, at least to this brightness level, both of our surveys are essentially complete. Also noted are our estimated background counts as well as Hanes's background. Note that the Hanes results were derived not from a region surrounding M87 but rather from the average of several other "galaxy-free" fields in the Virgo cluster.

TABLE 6

ERRORS IN MAGNITUDE AS A FUNCTION OF CLUSTER APPARENT BRIGHTNESS

Magnitude (U,B,R)	σ_U (mag)	σ_B (mag)	σ_R (mag)
19	0.02	0.02	0.06
20	0.03	0.03	0.15
21	0.08	0.05	0.37
22	0.19	0.07	0.94

f) *Halo Colors as a Function of Galactocentric Distance*

To obtain the run of galaxy surface brightness and color with radius, we adopted the reduction procedures first described by Strom and Strom (1978). We list in Table 10 the values of $\mu(U)$ and $\mu(R)$ as a function of $r=(ab)^{\frac{1}{2}}$ where a and b are the dimensions of the semimajor and semiminor axes. The ratio of these quantities as a function of b is given in Table 11. Note that the effective sampling aperture used in our reductions corresponds to 30″. In Table 10 we also list values of the color, $(U-R)$ as a function of r (along with an estimate of the error in this quantity). We expect an error no larger than ± 0.10 mag in the transformation between the instrumental and true U and R systems.

As a further check on the observed color gradient, we obtained U and R profiles from photoelectric scans of

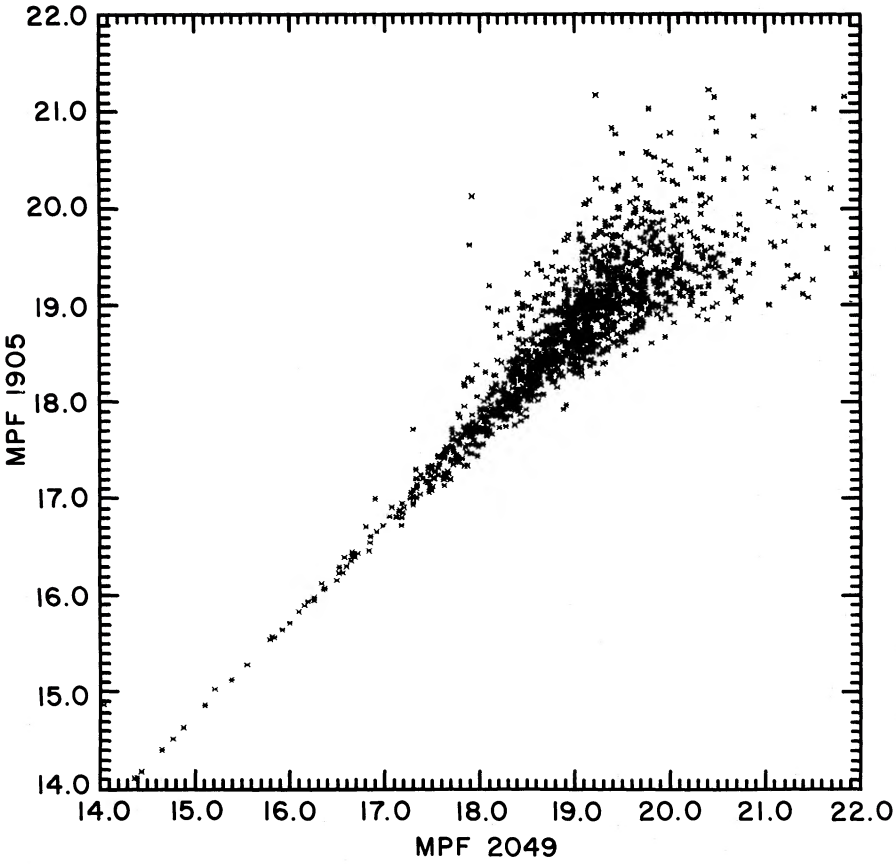

FIG. 7.—Same as Fig. 5, except for the *U* plates (MPF 2049 and MPF 1905).

TABLE 7

MEAN COLOR ERRORS AS A FUNCTION OF B MAGNITUDE[a]

B	σ_{U-B} (mag)	σ_{U-R} (mag)	σ_{B-R} (mag)
19	0.03	0.03	0.02
20	0.04	0.05	0.05
21	0.09	0.14	0.12
22	0.20	0.35	0.30
23	0.45	0.85	0.77

[a]Adopting $\langle(U-B)\rangle \approx 0.1$, $\langle(U-R)\rangle \approx 1.6$, $\langle(B-R)\rangle \approx 1.5$ as typical cluster colors.

TABLE 8

MAGNITUDE ERRORS AS A FUNCTION OF THE DISTANCE TO THE CENTER OF THE GALAXY FOR $U=B=22.5$ AND $R=21.5$

$\langle r \rangle$ (arcmin)	σ_U (mag)	σ_B (mag)	σ_R (mag)
2.3	0.31	0.14	0.78
4.1	0.30	0.11	0.60
6.0	0.30	0.11	0.57
8.3	0.29	0.11	0.53

the galaxy with the FAST-SCAN technique described by Strom *et al.* (1977). In Figure 11, we compare the photoelectric and photographic color-radius relations; note that these relations have been arbitrarily normalized at $r=120''$ after shifting the curves by $\Delta(U-R)=0.10$ mag. We regard the agreement as satisfactory. We also compare (Fig. 12) the $(U-R)$ color-radius relation with that deduced from de Vaucouleurs's (1969) observations of $(U-V)$ in the M87 halo. We transformed these colors to the $(U-R)$ system by using an equation (§ V*a*) derived from unpublished *UBVR* observations of a selection of galactic globular clusters by the authors. The agreement between our $(U-R)$ colors and those of de Vaucouleurs is satisfactory for $r<300''$; at larger radii, the disagreement is significant. Because we lack further observations, we are unable to discuss the relative merits of these data.

IV. ANALYSIS

a) The Run of Cluster Color as a Function of Galactocentric Distance

In Table 12 we list the mean colors and the errors in the mean for all clusters brighter than $B=23.0$, $U=23.0$,

TABLE 9

BACKGROUND COUNTS AND COLORS[a]

B Range	N	(U-B) Range	N	(U-R) Range	N	(B-R) Range	N
19.0→19.5....	1	-1.0 →-0.75....	0	0.0 →0.25....	0	0.0 →0.25....	0
19.5→20.0....	5	-0.75→-0.50....	5	0.25→0.50....	1	0.25→0.50....	1
20.0→20.5....	4	-0.50→-0.25....	16	0.50→0.75....	6	0.50→0.75....	4
20.5→21.0....	6	-0.25→ 0.0.....	13	0.75→1.00....	5	0.75→1.00....	6
21.0→21.5....	4	0.0 → 0.25....	18	1.00→1.25....	7	1.00→1.25....	8
21.5→22.0....	15	0.25→ 0.50....	8	1.25→1.50....	7	1.25→1.50....	8
22.0→22.5....	18	0.50→ 0.75....	2	1.50→1.75....	6	1.50→1.75....	6
22.5→23.0....	25	0.75→ 1.00....	0	1.75→2.00....	4	1.75→2.00....	3
23.0→23.5....	26			2.00→2.25....	0		
23.5→24.0....	22			2.25→2.50....	1		
				2.50→2.75....	1		
				2.75→3.00....	1		

[a]Note that these counts refer to an area of 43.0 arcmin^2, sampled at a mean distance from the galaxy center of 18!7.

and $R=22.0$ as a function of galactocentric distance r. It is important to realize that the mean colors have been corrected for the contribution of background objects by using the data presented in Table 9. Their expected numbers at each radius are explicitly listed in Table 12.

We conclude from this table that the *clusters located at larger galactocentric distance tend to be bluer.*

We plot in Figure 12 the run of mean cluster colors as a function of log r. Superposed on this plot are the relationships between color and radius derived for the smooth halo component in M87. The colors used are derived from de Vaucouleurs's (1969) observations as well as our own (see the discussion in the previous section). We conclude that the *color gradients in the halo and in the globular cluster system are identical to within the errors of observation.* However, there appears to be a shift of $\Delta(U-R)=0.50$, $\Delta(U-B)=0.30$, and $\Delta(B-R)=0.20$ between the cluster colors and those of the halo. We believe (see § III*b*) that the errors in our zero-point determination are not large enough to account for the above differences. We note again that the color zero points derived from surface photometry of the M87 halo

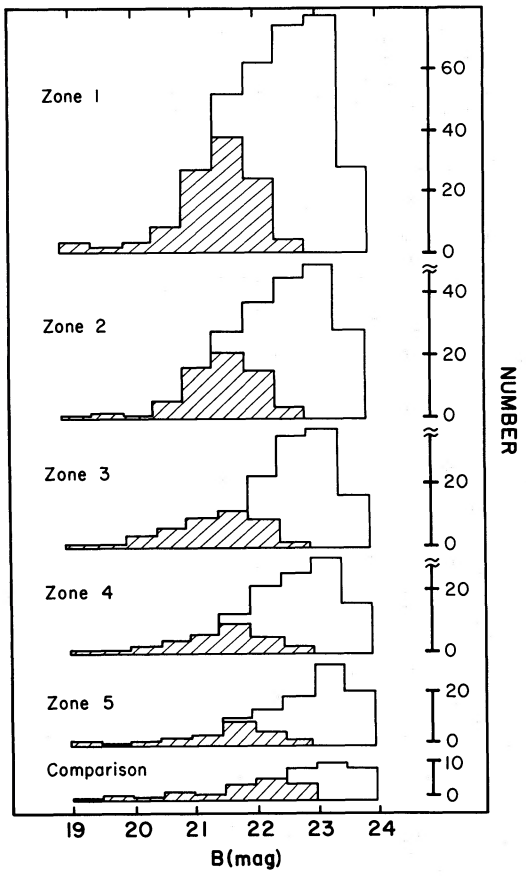

FIG. 9.—The frequency distribution in five annular zones (see Table 12) of globular clusters found from matching the stellar objects found on (*a*) two *B* plates and (*b*) our best *U*, *B*, and *R* plates (crosshatched areas). Note that the ordinates have been normalized such that the area in each zone is assumed equal to that in Zone 1 (see Table 12).

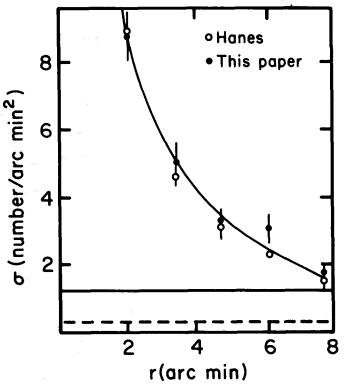

FIG. 10.—The table surface density σ (number arcmin^{-2}) of globular clusters ($B\leq 22.5$ mag) as a function of radius. Superposed on this plot are the results derived by Hanes. The *solid line* represents the background count level adopted in this study; the *dashed line* is the background estimated by Hanes.

TABLE 10

PHOTOGRAPHIC SURFACE PHOTOMETRY OF M87

r (arcsec)	μ(U) (mag arcsec^{-2})	μ(R) (mag arcsec^{-2})	(U − R) (mag)
30.....	21.05	18.54	2.51±0.02
45.....	21.67	19.29	2.38±0.02
60.....	22.17	19.84	2.33±0.02
75.....	22.53	20.27	2.26±0.02
90.....	22.82	20.61	2.21±0.03
120.....	23.40	21.25	2.15±0.03
150.....	23.96	21.86	2.10±0.04
300.....	25.27	23.21	2.06±0.05
600.....	26.57	24.58	1.99±0.10

NOTE: The estimated external error in the transformation to the U and R systems is expected to be less than 0.10 mag.

provide a *differential* measure of cluster and halo colors. Hence, we must seriously entertain the notion that *at comparable radial distance the globular cluster system is everywhere significantly bluer in the mean than is the integrated halo light.* In view of the recent results of Frogel, Persson, and Cohen (1980), suggesting a possible systematic difference between galaxy and globular cluster colors, we repeat that it would be of considerable importance to invest additional effort directly toward providing a precise calibration of the color systems. The data presented in § III*b* are sufficiently detailed, we believe, to permit such work.

TABLE 11

ELLIPTICITY AS A FUNCTION OF *r* FOR M87

r (arcsec)	*b*/*a* (mag)
30.....	0.95
45.....	0.93
60.....	0.90
75.....	0.88
90.....	0.86
120.....	0.82
300.....	0.77[a]

[a]Value assumed for $r \geq 300''$.

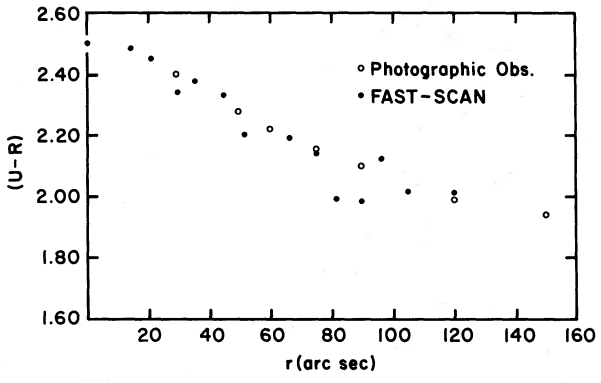

FIG. 11.—A comparison of the $(U-R)$, radius relations derived from FAST-SCAN photoelectric measurements (*filled circles*) with the relations derived from photographic photometry.

b) *Color-Luminosity Relationship for M87 Globulars*

In Table 13 we present the mean cluster colors as a function of luminosity for all clusters within $1'.39 \leq r \leq 2'.78$. *We find no evidence for a systematic trend of cluster color with luminosity.*

c) *Projected Cluster Surface Density as a Function of r*

In Figure 13 we present σ, the number of clusters per square arcmin at $B_{\rm lim} \approx 22.5$ mag as a function of galactocentric distance. We also superpose on this plot the *R* surface brightness profile normalized to match the cluster curve at $r = 2'.5$. We conclude that the projected cluster surface density follows the halo surface brightness distribution over the range of $r(1'.5 < r < 9'.0)$ studied here.

We note, however, that at larger radii ($r \gtrsim 20'$) it appears that the M87 cluster system may be more extended than the halo light and, therefore, has a shallower density gradient (Harris and Smith 1976; HR). Our data do not permit comment regarding this conclusion, since our background counts have been made at a mean radius $r \sim 18'.7$.

d) *Cluster Luminosity Function*

We present in Figure 14 a histogram depicting the frequency distribution of cluster luminosities. Superposed on this histogram is the distribution obtained by Hanes; the scale of the Hanes luminosity function has been normalized to the total number of clusters in our sample in the range $19.5 \leq B \leq 22.5$ mag. The agreement between the two samples is gratifying.

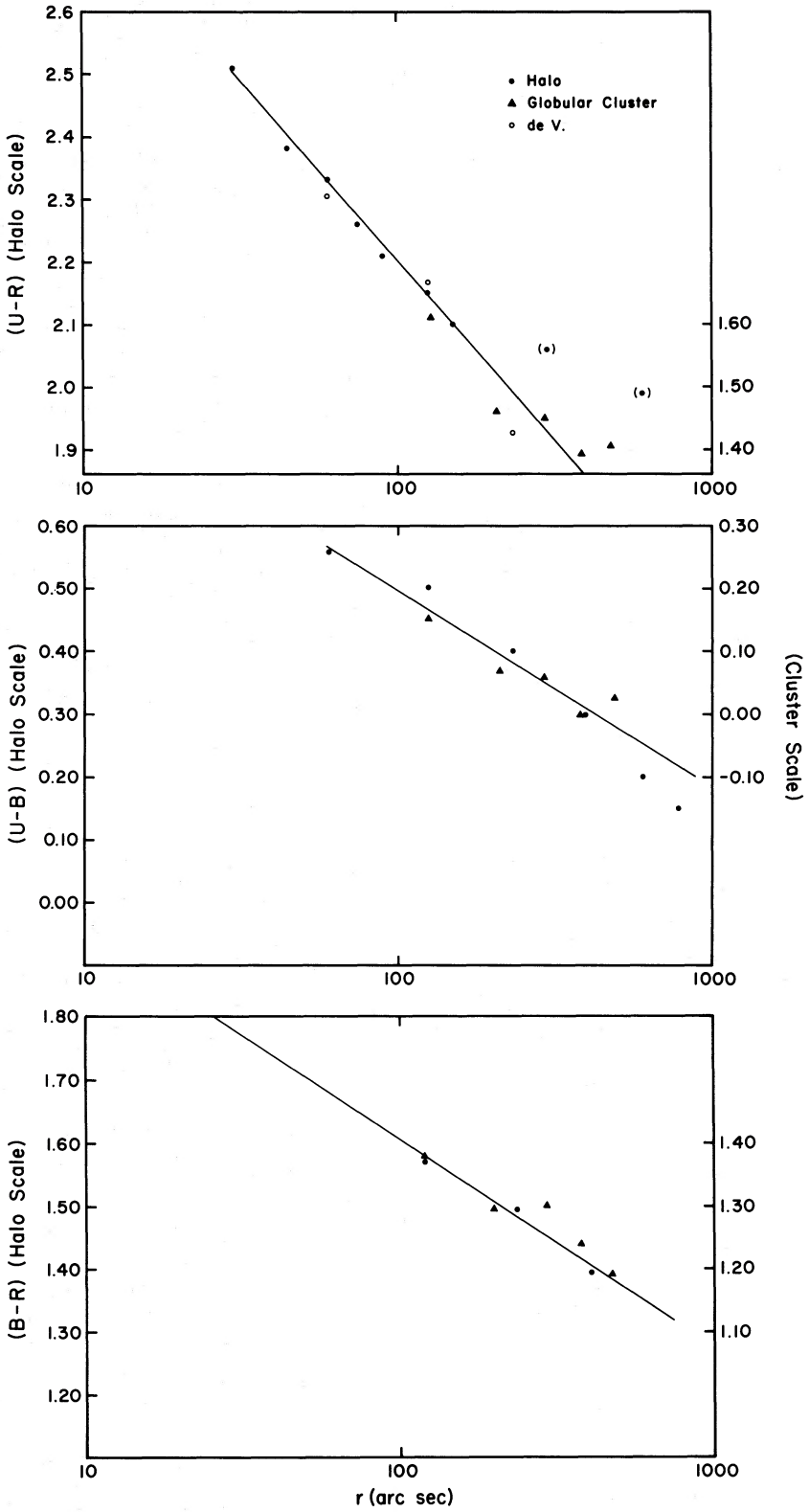

FIG. 12.—Plots of the mean $(U-B)$, $(B-R)$, and $(U-R)$ colors for the M87 globular clusters against galactocentric distance. Superposed on these plots are the relations between M87 halo color and radius derived from our measurements $[(U-R)]$ and those of de Vaucouleurs (*open circles*). Note that the color scale for the globulars appears on the right-hand side of each panel, while the scale for the halo colors appears on the left.

TABLE 12

GLOBULAR CLUSTER COLORS AS A FUNCTION OF RADIUS

	Zone 1	Zone 2	Zone 3	Zone 4	Zone 5	Comparison Field
Radius range (arcmin)..	1.39-2.78	2.78-4.17	4.17-5.56	5.56-6.95	6.95-9.83	
Mean radius (arcmin)...	2.05	3.43	4.87	6.25	7.88	18.7
Area (arcmin^2).....	18.3	30.3	42.5	54.6	41.7	43.0
$(\overline{U-R})_{observed}$.....	1.61	1.46	1.45	1.39	1.41	1.32
σ_{U-R}.....	±0.05	±0.04	±0.05	±0.05	±0.08	±0.09
$N_{objects}$.....	97	106	92	109	44	41
N_{field}.....	17	29	41	52	40	41
$(\overline{U-R})_{corrected}$.....	1.66	1.50	1.52	1.42	--	--
$(\overline{U-B})_{observed}$.....	0.15	0.07	0.06	0.00	0.03	-0.06
σ_{U-B}.....	±0.02	±0.02	±0.03	±0.03	±0.05	±0.05
$N_{objects}$.....	137	154	133	168	66	62
N_{field}.....	25	41	58	75	57	59
$(\overline{U-B})_{corrected}$.....	0.19	0.10	0.12	0.02	--	--
$(\overline{B-R})_{observed}$.....	1.37	1.29	1.30	1.24	1.19	1.21
σ_{B-R}.....	±0.03	±0.03	±0.03	±0.04	±0.05	±0.06
$N_{objects}$.....	97	101	89	102	43	36
N_{field}.....	17	29	41	52	40	37
$(\overline{B-R})_{corrected}$.....	1.40	1.32	1.36	1.26	--	--

NOTE: $(U-R)_f = 1.36$; $(U-B)_f = -0.02$; $(B-R)_f = 1.22$.

We also plot (Fig. 15) the derived luminosity functions (corrected for foreground and normalized to Zone 1) as a function of galactocentric distance.

From Hanes (1977*b*), we adopted a mean apparent magnitude $B=23.41$ and computed a mean dispersion $\sigma=1.26$. The normal curve corresponding to these parameters is shown in Figure 15. By comparing the observed luminosity functions in each radial zone with the derived normal curve, we conclude that there is no significant systematic variation of luminosity function with radius.

V. DISCUSSION

a) Cluster Colors

The existence of a gradient both in the mean color of the clusters and in the smooth M87 halo, *combined* with our conclusion that mean color is independent of luminosity, permits us to conclude that *M87 was likely not assembled from preexisting globular clusters.* One might have imagined that a galaxy-wide abundance gradient of the observed sense could have been produced had the more massive globular clusters been

TABLE 13

MEAN COLORS FOR DIFFERENT BLUE MAGNITUDE RANGES

Color Index	*B* Range 20.5–21.5	*N*	*B* Range 21.5–22.5	*N*
$\langle(U-B)\rangle$ ...	0.14±0.07	29	0.13±0.03	84
$\langle(U-R)\rangle$ ...	1.51±0.07	25	1.54±0.06	61
$\langle(B-R)\rangle$ ...	1.39±0.06	31	1.34±0.05	58

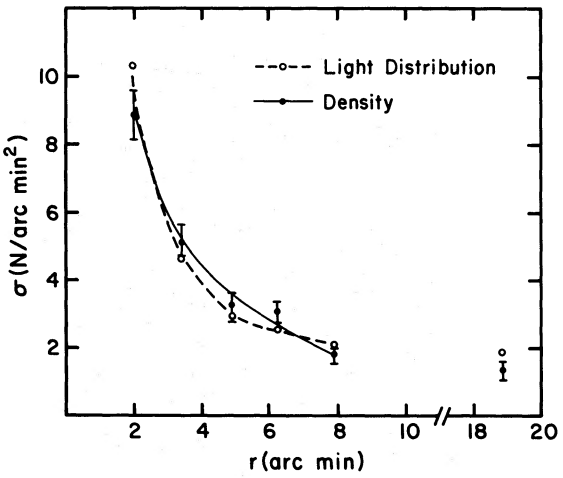

FIG. 13.—A plot of the projected surface density of clusters, N(r) for $B<22.5$, as a function of galactocentric distance. Superposed on this plot is the observed *R*-light surface brightness distribution, normalized to match N(r) at $r=2'.5$.

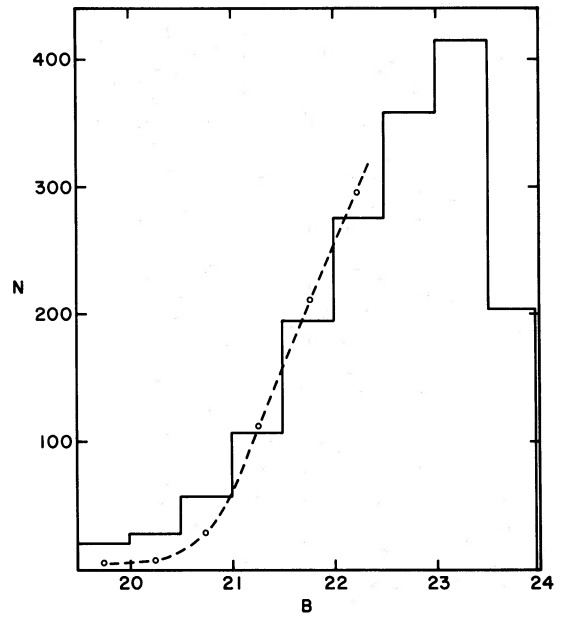

FIG. 14.—The frequency distribution N(B) of M87 globular clusters as a function of B. Superposed on this plot is the luminosity function observed by Hanes.

systematically more metal-rich. Then relaxation would have produced a galaxy in which the heavy, metal-rich clusters were confined to the central regions. We must conclude, instead, that a single process or series of processes systematically enriched both the halo stars and the galaxy during the galaxy formation epoch.

But we have also found a systematic color difference between the M87 globulars and the smooth halo background. If real, this is difficult to explain: It might conceivably arise from a difference in (a) the initial mass function, (b) formation epochs, (c) place of origin, or (d) the mean composition of the globular clusters and halo stars. We can look at these possibilities in turn.

From the computations presented by Aaronson *et al.* (1978), a change from 0 to 4 in the slope s of an initial mass function of the form

$$\frac{d\phi(M)}{dM} = cM^{-s}$$

changes ($U-B$), for example, by only +0.10. This value is too small by 0.20 mag to account for the observed difference in ($U-B$) between the clusters and the halo stars. However, we cannot increase ($U-B$) for the halo beyond this value, since $s>4$ appears ruled out by the infrared CO first overtone-band observations reported by Aaronson *et al.* (1978).

It is difficult to imagine that possibility (b) is correct, since it presupposes that two ostensibly similar dynamical subsystems (the clusters and the halo) have radically different ages. To explain the observed difference in halo and cluster $U-B$ colors requires an age difference of $>7\times10^9$ years (Aaronson *et al.* 1978).

It has been proposed (van den Bergh 1977; HR) that the M87 cluster system may owe its origin in part to clusters, tidally stripped from other Virgo galaxies, falling into the potential well of M87 (possibility [c]). However, halo stars as well as clusters should be stripped during tidal interactions. Hence, it is difficult to see why the smooth halo-star background and the cluster system should exhibit color differences unless such differences were already present in the stripped parent galaxies.

Regarding possibility (d), it is difficult to understand why globular clusters should undergo different enrichment histories from the halo stars *if the spatial distributions (and presumably the dynamical histories of the subsystems) are identical.* In fact, it is more likely that, if

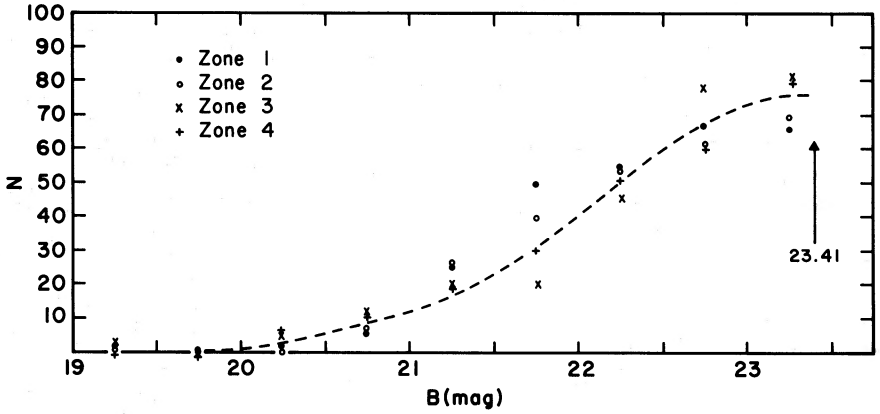

FIG. 15.—A plot of the M87 globular cluster luminosity function derived for five annular zones located at different galactocentric distances. The luminosity functions in each zone have been corrected for contributions of foreground stars and normalized to have the same total number of objects as found in Zone 1. A normal curve with $B=23.4$ mag and $\sigma=1.26$ mag has been superposed on this plot. We find no evidence for a significant radial difference in the observed luminosity function.

formed from the same primordial material, the globular clusters could be more metal-rich than the nearby halo stars since some clusters might retain processed gas and become self-enriched. But now, suppose that the globular clusters do represent a more spatially distended population than do the halo stars (cf. HR). It might then be supposed that the globular cluster system was formed earlier than the halo stars and therefore exhibits a significantly lower heavy element enrichment.

Certain differences in halo and cluster properties within our own Galaxy have been implicitly apparent for many years. For example, examination of the H-R diagram in Baade's window (Arp 1965; Butler, Carbon, and Kraft 1976) clearly shows that the majority of giant stars near the galactic center appear to have intrinsic colors redder by 0.2–0.3 mag in $(B-V)$ than the giants in the most metal-rich globular clusters.

Whitford's (1978) study of the spectral energy distribution of a selection of patches in Baade's window permits a quantitative check on the difference between globular cluster and halo star colors in the Milky Way. From his measured G band and Mg b band strengths and Faber's (1973) relations between these index strengths and galaxian color, we can predict values of $(U-V)_0$ for Baade's window (see Strom *et al.* 1978) of 1.39 and 1.38. Alternatively, from Whitford's monochromatic color index 3785–4250, we predict $(U-V)_0=1.41$. We adopt, therefore, a value of $(U-V)_0=1.39$ for the bulge. From an average of globular cluster colors for systems located within 1.5 kpc of the galactic center, we obtain $\langle(U-V)\rangle_0^{\text{clusters}}=1.01$. Hence, the difference in $(U-V)$ colors between the bulge and the globular clusters is 0.38 mag. In M87 the observed mean difference in $(U-R)$ is 0.50 mag which translates to a $(U-V)$ difference of 0.40 mag. Thus, *the difference in halo and cluster mean colors is remarkably similar in the Milky Way and in M87.* In short, the combined implications from our data considerably strengthen the possibility that the globular cluster and halo stars represent two distinct subsystems characterized by different chemical and possibly dynamical histories. Note that $\Delta(U-V)=0.4$ corresponds to a difference in [Fe/H] of $\sim$0.6 dex (Aaronson *et al.* 1978; Strom *et al.* 1976).

Our data also permit a discussion of the likelihood that M87 was formed in several "merger" events. Let us assume that disk systems are the "universal" galaxy form and that E galaxies result from multiple mergers of such galaxies. Let us further postulate that an abundance gradient is produced during the collapse of the disk system. When two or more disk galaxies merge, the abundance gradients initially present in each globular cluster system will become obscured as a consequence of orbital mixing in the merged galaxy. Hence, the abundance gradient in the halo of a galaxy such as M87 (the presumed product of multiple mergers) should be smaller than that characteristic of the halo of a disk galaxy similar to our own.

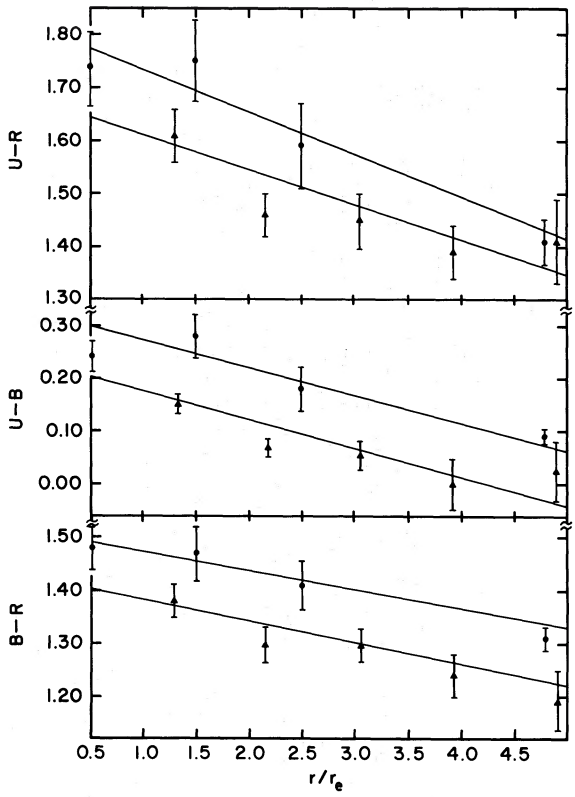

FIG. 16.—A plot of the globular cluster mean colors against the scale-free radius parameter r/r_e. Superposed are the color-radius relations for the Milky Way globular cluster system.

In Figure 16 we plot the mean globular cluster colors derived for the M87 system (see Table 12) against r/r_e. Here r_e is the de Vaucouleurs effective radius (de Vaucouleurs 1953), which, for M87, is $r_e=96''$ (de Vaucouleurs and Nieto 1978). Superposed on this plot are the color-radius relations for the Milky Way globular clusters (Table 14; data from HR). The published colors have been transformed to the $(U-R)$ and $(B-R)$ system using relationships between $(U-R)$ and $(B-R)$, $(U-V)$ and $(B-V)$ derived from unpublished observations of galactic globular clusters by the authors, viz.,

$$(U-R)=1.27(U-V)+0.46,$$

$$(B-R)=1.58(B-V)+0.28.$$

Similar transformations can be derived from Kron and Mayall's (1960) observations, if proper adjustment is made to the Johnson system. Note that we adopted a value $r_e=3$ kpc (HR; de Vaucouleurs 1977) for our Galaxy in order to normalize the radial scale.

TABLE 14

PROPERTIES OF THE MILKY WAY GLOBULAR CLUSTER SYSTEM

r/re	Δr (kpc)	$(U-B)$ σ	N	$U-R$ σ	$B-R$ σ
0.5	0→3	0.24±0.15	24	1.74±0.32	1.48±0.19
1.5	3→6	0.28±0.19	25	1.75±0.38	1.47±0.23
2.5	6→9	0.18±0.15	21	1.59±0.36	1.41±0.21
4.8	9→20	0.09±0.07	26	1.41±0.19	1.31±0.11

The scaled color gradients in each cluster system are identical in M87 and in our Galaxy to within the observational errors; the zero points differ by less than 0.10 mag. Note that part of the displacement between the two relations could result from uncertainties in the values of r_e for M87 and the Milky Way. *There is no evidence that the abundance gradient in M87 is relatively shallower than in the Milky Way.*

It is possible to estimate the change in abundance gradients expected from the merger of two galaxies similar to the Milky Way. From White's (1978) *n*-body simulations of galaxy mergers, we chose to examine model H, for which he publishes changes in binding energy ΔE for test particles (stars) in the merger of two initially identical "galaxies" as a function of binding energy E. By assuming (a) that $|\Delta E/E| \sim |\Delta r/r|$, (b) that the *initial* color gradient is that observed in the Milky Way $\Delta(U-B)/\Delta \log r \sim 0.27$, and (c) that the projected surface density of clusters follows a $1/r^2$ law, we predict $\Delta(U-B)/\Delta \log r = 0.20$ in the merged model. In other words, the slope is reduced by ~25% in a single merger. This contrasts with White's (1980) estimate of a 21% change based on somewhat different models. We can (with some confidence) rule out a change of 25% from the comparisons shown in Figure 16. Note that ~10 galaxies similar to the Milky Way would have to merge to produce a system comparable to M87, thereby reducing the initial color gradient even more. It is, therefore, difficult to believe that M87 was formed by mergers of galaxies similar to our Milky Way. However, we note that the effects of any metal production in merger events have been ignored. Moreover, the assumption that r_e provides an appropriate scaling parameter is also somewhat uncertain. Given the possible zero-point errors, the color-radius relations for the M87 and galactic globulars could well be identical.

As a further check on the merger hypothesis, we note that in merged galaxies an increase in color dispersion at a given radius is expected. To examine this possibility, we have selected M87 clusters in the magnitude range $20.5 < B < 21.5$ mag; examination of Table 7 and Figure 9 suggests this range as providing the best compromise between the number of clusters and the expected internal errors in color determination.

In Table 15 we list the following information: (a) the observed dispersion in each of the colors, (b) the number of clusters in the sample, (c) the dispersion corrected for the observed color dispersion in the comparison field, and (d) the color dispersion predicted from (1) the observed color dispersion at equivalent r/r_e for the Milky Way system and (2) the expected internal color dispersion (interpolated from Table 7). Also noted is the fraction of stellar-like objects predicted to be globular clusters in each zone.

We conclude from examination of the results for Zones 1, 2, and 3 that the observed color dispersions in M87 are not significantly different from those predicted from the Milky Way system. In Zones 4 and 5, the large number of expected foreground stars precludes an accurate estimate of color dispersions. Relatively small differences (within the expected sampling errors) in the adopted dispersions for the comparison field can produce large excursions in the deduced cluster color dispersions. Hence, a comparison of the M87 system with the Milky Way at values of r/r_e, where the Milky Way cluster dispersion drops significantly, is precluded at this time. Observations of foreground counts over a much larger area, devoid of contaminating M87 clusters, will be necessary. Until then, no definitive test of the merger hypothesis based on color dispersion will be possible.

At present we can only say that in the inner regions ($r/r_e \lesssim 3$) the Milky Way Galaxy and M87 exhibit remarkably similar abundance ranges.

b) Cluster Luminosity Distribution

The fact that the luminosity function appears to be distance independent in the range $1.4 < r < 9'$ suggests that distance determinations, based on the form of cluster luminosity functions, are unlikely to be seriously affected by systematic depletion of clusters of a particular luminosity range (for example, by tidal destruction).

VI. CONCLUSIONS

The basic results of this contribution can be summarized as follows:

1. The mean colors of the M87 globular clusters become bluer with increasing galactocentric distance

TABLE 15

COLOR DISPERSIONS AS A FUNCTION OF RADIUS

		Zone 1	Zone 2	Zone 3	Zones 4 and 5
obs.	$\sigma(U-R)$.....	0.37	0.50	0.46	0.60
	N_{obj}.....	25	34	37	49
corr.	$\sigma(U-R)$.....	0.32	0.48	0.37	0.67:
pred.	$\sigma(U-R)$.....	0.42	0.41	0.35	0.26
obs.	$\sigma(U-B)$.....	0.19	0.27	0.23	0.28
	N_{obj}.....	28	34	38	49
corr.	$\sigma(U-B)$.....	0.15	0.26	0.12	0.22:
pred.	$\sigma(U-B)$.....	0.22	0.21	0.16	0.13
obs.	$\sigma(B-R)$.....	0.29	0.28	0.27	0.40
	N_{obj}.....	25	34	36	45
corr.	$\sigma(B-R)$.....	0.27	0.22	0.09	0.42:
pred.	$\sigma(B-R)$.....	0.27	0.26	0.24	0.19
	r/r_e.....	1.28	2.14	3.04	4.42
	N_{cl}/N_{obj}.....	0.82	0.71	0.54	0.36

NOTE: For the comparison field $\sigma(U-R) = 0.55$ (39 objects), $\sigma(U-B) = 0.32$ (62 objects), $\sigma(B-R) = 0.39$ (39 objects).

over the range $1.5<r<9'$ ($9<r<54$ kpc if the distance to M87 is 20 Mpc).

2. The color gradient of the halo stars and of the globular cluster system is identical to within the errors of observation. However, the mean colors of the globular clusters are bluer by 0.50, 0.30, and 0.20 in $(U-R)$, $(U-B)$, and $(B-R)$, respectively, when compared with the smooth halo-star background.

3. There appears to be no evidence of a systematic variation of color with luminosity. Lacking a relationship between mass and chemical composition for the clusters, it is impossible to explain an abundance gradient in the halo if galaxy formation occurred in this manner. Hence, we conclude that M87 was not likely to have been produced from gravitational assembly of previously formed clusters.

4. The gradient in the mean color of the M87 globulars is *not* less steep than that characterizing the galactic globular clusters. From this result, we conclude that M87 was probably not formed as a result of multiple mergers of disk galaxies similar to the Milky Way. Furthermore, the observed dispersion in cluster colors is no larger in M87 as compared with the Milky Way. This conclusion also argues against the likelihood of mergers as the process by which M87 was formed.

5. The difference in color between the clusters and the smooth halo component suggests that the chemical enrichment history of the two subsystems may be quite different. If we accept Harris and Racine's suggestion that the globular cluster system is more distended than the smooth halo component, then it seems reasonable to presume that the globular clusters were formed prior to the halo stars. The globular clusters might, therefore, be viewed as a link between the "Population II" halo stars and the unseen matter thought to extend beyond the visible boundaries of galaxies.

6. The luminosity function found for the M87 cluster is similar to that observed previously by Hanes (1977*a*) and is thus consistent with that found for other Virgo and Local Group galaxies.

7. There is no systematic trend in cluster luminosity function with galactocentric distance over the range $1.5<r<9'$. Hence, the use of globular cluster luminosity functions to derive distances appears, to first order, immune to differential tidal disruption effects.

8. The projected cluster surface density follows the galaxy light distribution over the range $2<r<9'$.

We thank Dr. Laird Thompson for his assistance in obtaining the Palomar Schmidt material employed in this survey. The Director of the Hale Observatories is also thanked for his generosity in granting Schmidt time. The assistance at the telescope of Messrs. H. Halbedel and D. Tody and Ms. Barbara Schaeffer of KPNO is gratefully acknowledged. W. Rice, W. Romanishin, and E. Jensen also contributed their time during the early phases of this investigation, and we thank them. Discussions with Dr. Paul Schechter were a source of considerable stimulation and encouragement for which we are most grateful. We also thank Dr. A. E. Whitford who contributed useful critical remarks regarding the galactic

bulge. Finally, we thank the members of the Wyoming Infrared Observatory and the University of Wyoming Physics and Astronomy Program for providing the ambience that made completion of this effort possible. We are grateful for their hospitality, their good humor, and their professional stimulation. J. C. Forte was supported by a fellowship from the Consejo Nacional de Investigaciones Cientificas y Técnicas, Republica Argentina.

REFERENCES

Aaronson, M., Cohen, J. G., Mould, J., and Malkan, M. 1978, *Ap. J.*, **223**, 824.
Arp, H. 1965, *Ap. J.*, **141**, 43.
Butler, D., Carbon, D., and Kraft, R. P. 1976, *Ap. J.*, **210**, 120.
de Vaucouleurs, G. 1953, *M.N.R.A.S.*, **113**, 134.
_____. 1969, *Ap. Letters*, **4**, 17.
_____. 1977, *A.J.*, **82**, 456.
de Vaucouleurs, G., and Nieto, J.-L. 1978, *Ap. J.*, **220**, 449.
Faber, S. M. 1973, *Ap. J.*, **179**, 731.
Frogel, J., Persson, S. E., and Cohen, J. G. 1980, *Ap. J.*, **240**, 785.
Hanes, D. A. 1971, Ms.C. thesis, University of Toronto.
_____. 1977*a*, *M.N.R.A.S.*, **179**, 331.
_____. 1977*b*, *M.N.R.A.S.*, **180**, 309.
Harris, W. E., and Racine, R. 1979, *Ann. Rev. Astr. Ap.*, **17**, 241 (HR).
Harris, W. E., and Smith, M. G. 1976, *Ap. J.*, **207**, 1036.
_____. 1981, *Ap. J.*, in press.
Johnson, H. L. 1966, *Ann. Rev. Astr. Ap.*, **4**, 193.
Kron, G. E., and Mayall, N. U. 1960, *A.J.*, **65**, 581.
Schweizer, F. 1976, *Ap. J. Suppl.*, **31**, 313.
Strom, K. M., and Strom, S. E. 1978, *A.J.*, **83**, 73.
Strom, K. M., Strom, S. E., Jensen, E. B., Moller, J., Thompson, L. A., and Thuan, T. X. 1977, *Ap. J.*, **212**, 335.
Strom, K. M., Strom, S. E., Wells, D. C., and Romanishin, W. 1978, *Ap. J.*, **220**, 62.
Strom, S. E., Strom, K. M., Goad, J. W., Vrba, F. J., and Rice, W. 1976, *Ap. J.*, **204**, 684.
van den Bergh, S. 1977, *Vistas Astr.*, **21**, 71.
Wells, D. C. 1979, in *Proc. SPIE Symposium, Instrumentation in Astronomy III*, **172**, 418.
White, S. D. M. 1978, *M.N.R.A.S.*, **184**, 185.
_____. 1980, *M.N.R.A.S.*, **191**, 1P.
Whitford, A. E. 1978, *Ap. J.*, **226**, 777.

J. C. Forte, K. M. Strom, S. E. Strom, and D. C. Wells: Kitt Peak National Observatory, P.O. Box 26732, Tucson, AZ 85726

W. E. Harris: Department of Physics, McMaster University, 1280 Main Street, W., Hamilton, ON L8S 4M1, Canada

Malcolm G. Smith: Royal Observatory, Blackford Hill, Edinburgh EH9 3HJ, Scotland

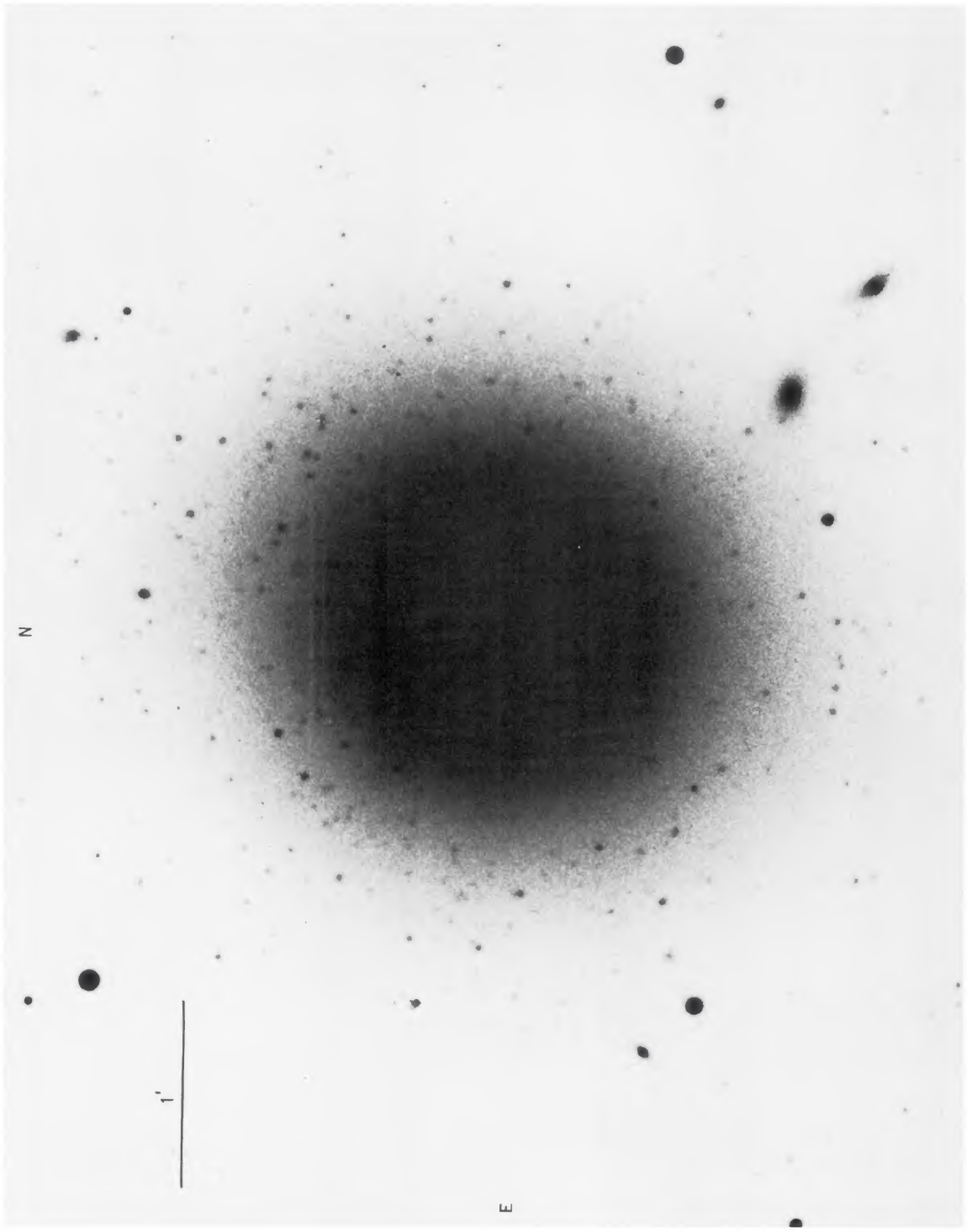

FIG. 1. — A reproduction of the central region of the Mayall 4 m plate MPF 2046 (IIIa-J+GG-385). This figure illustrates the crowding of cluster images near the galaxy center as well as the significant contribution of background light from the smooth halo component.

STROM *et al.* (*see* page 417)

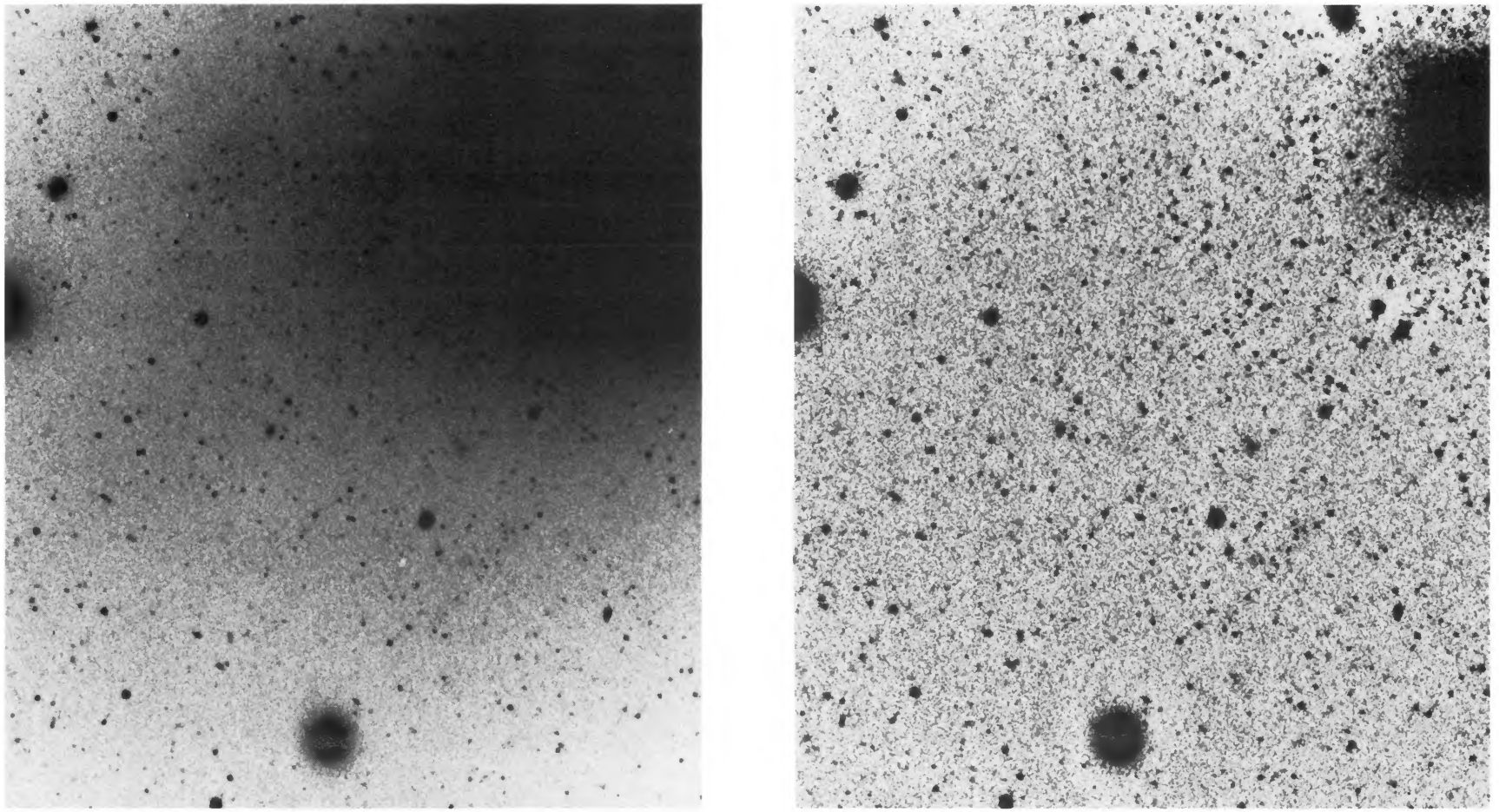

FIG. 2.—The left-hand photograph illustrates the appearance of the central region of M87 before subtraction of galaxy light. In the right-hand image the galaxy contribution has been removed by using the prescription set forth in the text.

STROM *et al.* (*see* page 418)

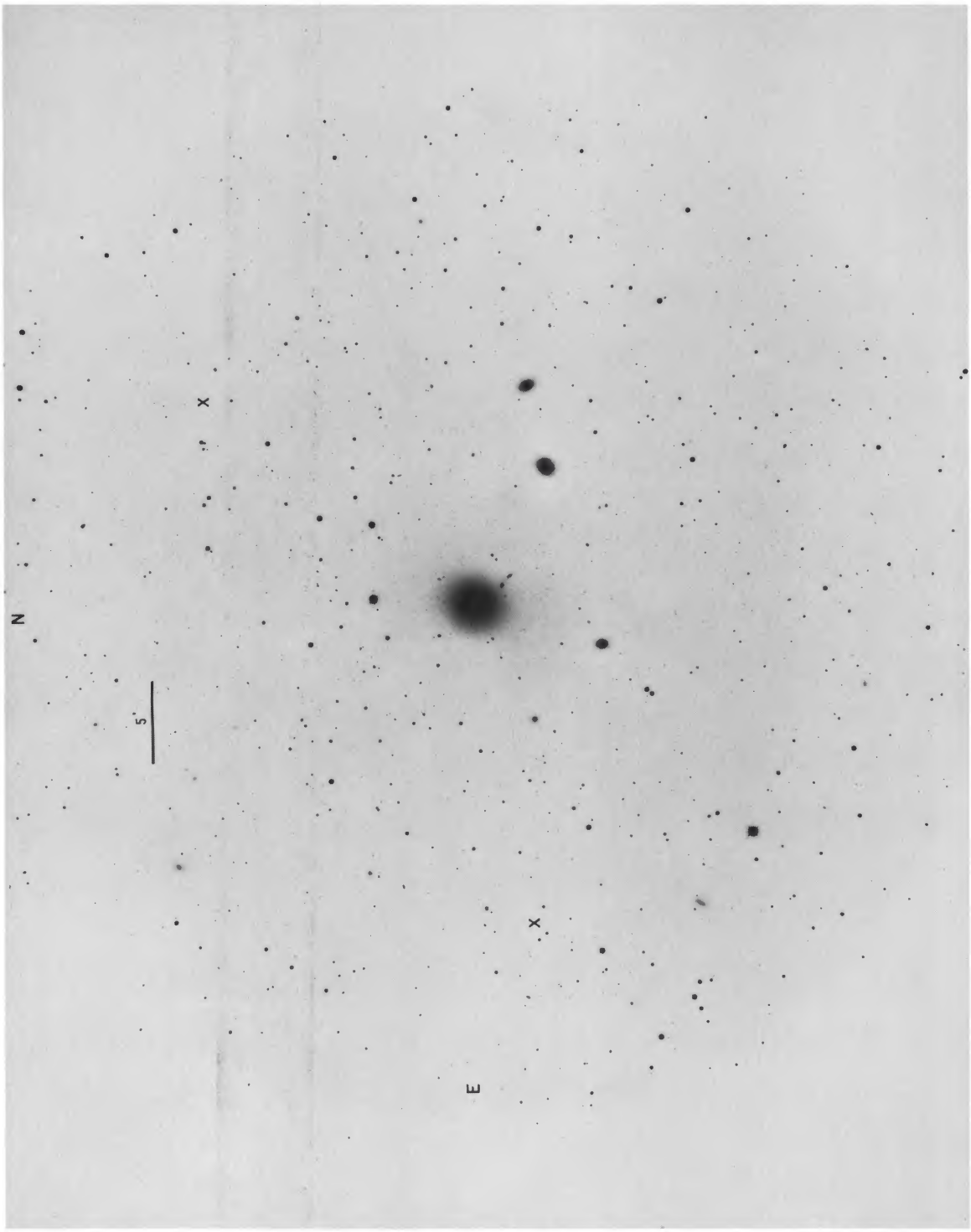

FIG. 8.—A reproduction of the *B* plate (MPF 2046) of M87. The location of the center of each of the two comparison fields is indicated by a cross. The area of each field is 21.5 arcmin^2, and the average distance from the galaxy center is 18.7.

STROM *et al.* (*see* page 442)